

Copyright Warning & Restrictions

The copyright law of the United States (Title 17, United States Code) governs the making of photocopies or other reproductions of copyrighted material.

Under certain conditions specified in the law, libraries and archives are authorized to furnish a photocopy or other reproduction. One of these specified conditions is that the photocopy or reproduction is not to be “used for any purpose other than private study, scholarship, or research.” If a user makes a request for, or later uses, a photocopy or reproduction for purposes in excess of “fair use” that user may be liable for copyright infringement,

This institution reserves the right to refuse to accept a copying order if, in its judgment, fulfillment of the order would involve violation of copyright law.

Please Note: The author retains the copyright while the New Jersey Institute of Technology reserves the right to distribute this thesis or dissertation

Printing note: If you do not wish to print this page, then select “Pages from: first page # to: last page #” on the print dialog screen

The Van Houten library has removed some of the personal information and all signatures from the approval page and biographical sketches of theses and dissertations in order to protect the identity of NJIT graduates and faculty.

ABSTRACT

BIOREMEDIATION OF PETROLEUM HYDROCARBONS IN COASTAL SEDIMENTS

**by
Charbel Abou Khalil**

The biodegradation of dispersed crude oil in the ocean is relatively rapid (a half-life of a few weeks). However, it is often much slower on shorelines, usually attributed to low moisture content, nutrient limitation, and higher oil concentrations in beaches than in dispersed plumes. Another factor may be the increased salinity of the upper intertidal and supratidal zones since these parts of the beach are potentially subject to prolonged evaporation and only intermittent inundation. Therefore, two laboratory experiments are conducted to investigate whether such an increase in porewater salinity results in additional inhibitory effects on oil biodegradation in seashores.

In the first experiment, oil biodegradation is investigated in seawater at different salinities by evaporating sampled seawater to a concentrated brine and then adding it to fresh seawater to generate high salinity microcosms. Artificially weathered Hibernia crude oil is added, and biodegradation is followed for 76 days. Results show that the biodegradation of hydrocarbons is substantially inhibited at high salinities, whereby the half-life slows down by 20-fold when increasing the salinity from 30 to 160 g/L. Genera of well-known aerobic hydrocarbonoclastic bacteria are only identified at 30 g/L salt in the presence of oil, and only a few halophilic hydrocarbon-degrading microorganisms show a slight enrichment at higher salt concentrations.

In the second experiment, oil biodegradation is investigated in coastal sediments. Lightly weathered Hibernia crude oil is added to beach sand at 1 or 10 mL/kg, and fresh

seawater, at salinities of 30, 90, and 160 g/L, is added to 20% saturation. The sand mixtures are placed in glass cylinders, with and without the addition of nutrients. All microcosms are analyzed every 30 days for a total incubation period of 180 days. Results show that the biodegradation of oil is slower at higher salinities, where the half-life increases from 40 days at 30 g/L salt to 58 and 76 days at 90 and 160 g/L salt, respectively, and adding fertilizers somewhat enhances oil biodegradation. Increasing oil concentration in the sand, from 1 to 10 mL/kg, slows the half-life by about 10-fold. Interestingly, the biodegradation of aromatic hydrocarbons is much slower at higher salinities, while that of alkanes is not considerably affected. The relative abundance and diversity of genera vary significantly with the increase in porewater salinity, whereby halophilic hydrocarbon-degrading microorganisms, particularly the ones of the *Marinobacter* genus, are the most abundant only under hypersaline conditions. Enzymes pertaining to hydrocarbon biodegradation pathways are noticeably less abundant at high salinities, specifically for those pertaining to the degradation pathways of aromatics.

Both experiments indicated that high porewater salinity in the upper parts of sandy beaches could significantly slow down the microbial degradation of crude oil, specifically that of the aromatic fraction. Consequently, occasional irrigation with seawater (i.e., to decrease the salinity) with fertilization could be a suitable bioremediation strategy for the upper parts of contaminated beaches. However, given that the high oil concentration in sandy beaches also plays a major role in the persistence of petroleum hydrocarbons on contaminated shorelines, chemically dispersing the spilled oil at sea and preventing it from reaching the coast is probably the most suitable option for its optimal removal from marine and coastal ecosystems.

**BIOREMEDIATION OF PETROLEUM HYDROCARBONS
IN COASTAL SEDIMENTS**

**by
Charbel Abou Khalil**

**A Dissertation
Submitted to the Faculty of
New Jersey Institute of Technology
in Partial Fulfillment of the Requirements for the Degree of
Doctor of Philosophy in Environmental Engineering**

John A. Reif, Jr. Department of Civil and Environmental Engineering

December 2022

Copyright © 2022 by Charbel Abou Khalil

ALL RIGHTS RESERVED

APPROVAL PAGE

**BIOREMEDIATION OF PETROLEUM HYDROCARBONS
IN COASTAL SEDIMENTS**

Charbel Abou Khalil

Dr. Michel C. Boufadel, Dissertation Advisor Date
Distinguished Professor of Civil and Environmental Engineering, NJIT

Dr. Taha F. Marhaba, Committee Member Date
Professor and Chair of Civil and Environmental Engineering, NJIT

Dr. William H. Pennock, Committee Member Date
Assistant Professor of Civil and Environmental Engineering, NJIT

Dr. Ashish D. Borgaonkar, Committee Member Date
Assistant Professor of School of Applied Engineering and Technology, NJIT

Dr. Roger C. Prince, Committee Member Date
Retired, Biologist Expert at ExxonMobil in Clinton, NJ

BIOGRAPHICAL SKETCH

Author: Charbel Abou Khalil
Degree: Doctor of Philosophy
Date: December 2022

Undergraduate and Graduate Education:

- Doctor of Philosophy in Environmental Engineering, New Jersey Institute of Technology, Newark, NJ, 2022
- Master of Science in Civil Engineering, Notre Dame University-Louaize, Lebanon, 2018
- Bachelor of Engineering in Civil Engineering, Notre Dame University-Louaize, Lebanon, 2016

Major: Environmental Engineering

Journal Publications:

Abou-Khalil, C., Sarkar, D., Braykaa, P., and Boufadel, M.C. Mobilization of Per and Polyfluoroalkyl Substances (PFAS) in Soils: A Review. *Current Pollution Reports* (Accepted 10/10/2022).

Abou-Khalil, C., Prince, R. C., Greer, C. W., Lee, K., and Boufadel, M. C. Microbial Analysis of Oil-impacted Hypersaline Coastal Sediments. *Under Review*.

Abou-Khalil, C., Ji, W., Prince, R. C., and Boufadel, M. C. Field Fluorometers for Assessing Oil Dispersion at Sea. *Under Review*.

Abou-Khalil, C., Prince, R. C., Greer, C. W., Lee, K., and Boufadel, M. C. (2022). Bioremediation of Petroleum Hydrocarbons in the Upper Parts of Sandy Beaches. *Environmental Science & Technology* (Accepted 05/17/2022).

Abou Khalil, C., Eraky, M. T., and Ghanimeh, S. (2021). Localized Mixing of Anaerobic Plug Flow Reactors. *Water Research*, 204, 117588.

- Abou Khalil, C.,** Prince, R. C., Greer, C. W., Lee, K., and Boufadel, M. C. (2021). Hydrocarbon Biodegradation in the Upper and Supratidal Seashores. *Journal of Hazardous Material*, 416, 125919.
- Abou Khalil, C.,** Prince, V. L., Prince, R. C., Greer, C. W., Lee, K., Zhang, B., and Boufadel, M. C. (2021). Occurrence and Biodegradation of Hydrocarbons at High Salinities. *Science of the Total Environment*, 762, 143165.
- Jayalakshamma, M. P., **Abou Khalil, C.,** and Boufadel, M. C. Fate and Transport of Secondary Microplastics in Aquatic Ecosystems. *Under Preparation*.
- Ji, W., **Abou Khalil, C.,** Lee, K., and Boufadel, M. C. Post-Formation of Oil Particle Aggregates: Breakup and Biodegradation. *Under Preparation*.
- Geng, X., **Abou Khalil, C.,** Prince, R. C., Lee, K., An, C., and Boufadel, M. C. (2021). Hypersaline Pore Water in Gulf of Mexico Beaches Prevented Efficient Biodegradation of *Deepwater Horizon* Beached Oil. *Environmental Science & Technology*, 55(20), 13792-13801.
- Ghanimeh, S., **Abou Khalil, C.,** Stoecklein, D., Kommasojula, A., and Ganapathysubramanian, B. (2020). Flow Sculpting Enabled Anaerobic Digester for Energy Recovery from Low-solid Content Waste. *Renewable Energy*, 154, 841-848.
- Ji, W., **Abou Khalil, C.,** Boufadel, M. C., Coelho, G., Daskiran, C., Robinson, B., King, T., Lee, K., and Galus, M. (2022). Impact of Mixing and Resting Times on The Droplet Size Distribution and The Petroleum Hydrocarbons' Concentration in Water-accommodated Fractions (WAFs). *Chemosphere*, 296, 133087.
- Ji, W., **Abou Khalil, C.,** Jayalakshamma, M. P., Zhao, L., and Boufadel, M. C. (2020). Behavior of Surfactants and Surfactant Blends in Soils During Remediation: A Review. *Environmental Challenges*, 100007.
- Ghanimeh, S., **Abou Khalil, C.,** Mosleh, C. B., and Habchi, C. (2018). Optimized Anaerobic-aerobic Sequential System for the Treatment of Food Waste and Wastewater. *Waste Management*, 71, 767-774.
- Ghanimeh, S., **Abou Khalil, C.,** Mosca Angelucci, D., and Tomei, M. C. (2019). Anaerobic-aerobic Sequential Treatment: Temperature Optimization and Cost Implications. *Journal of the Air & Waste Management Association*, 69(10), 1170-1181.
- Ghanimeh, S., **Abou Khalil, C.,** and Ibrahim, E. (2018). Anaerobic Digestion of Food Waste with Aerobic Post-treatment: Effect of Fruit and Vegetable Content. *Waste Management & Research*, 36(10), 965-974.

- Iskander, L., **Abou Khalil, C.**, and Boufadel, M. C. (2021). Fate of Crude Oil in the Environment and Remediation of Oil Spills. *STEM Fellowship Journal*, 8(1), 1-7.
- Ji, W., Jayalakshamma, M. P., **Abou Khalil, C.**, Zhao, L., and Boufadel, M. C. (2020). Removal of Hydrocarbon from Soils Possessing Macro-heterogeneities Using Electrokinetics and Surfactants. *Chemical Engineering Journal Advances*, 100030.
- Jayalakshamma, M. P., Ji, W., **Abou Khalil, C.**, Marhaba, T. F., and Boufadel, M. C. (2020). Removal of Hydrocarbons from Soil Possessing Macro-heterogeneity using Electrokinetics and Surfactants. *Environmental Challenges*, 10071.
- Boufadel, M. C., Ji, W., Jayalakshamma, M. P., **Abou Khalil, C.**, Abrams, S., Zhao, L., and Wang, A. (2020). Nonaqueous Phase Liquid Removal by Postconventional Techniques. *Journal of Environmental Engineering*, 147(3), 03120011.

Presentations and Conference Proceedings:

- Abou Khalil, C.**, Fortin, N., Prince, R. C., Greer, C. W., Lee, K., and Boufadel, M. C. Bioremediation of Petroleum Hydrocarbons in Oiled Shorelines. Accepted for presentation at the *International Oil Spill Science Conference 2022*, in Halifax, Canada, October 04-07, 2022.
- Abou Khalil, C.**, Arida, C., Ghnatios, C., and Ghanimeh, S. Low Tech Anaerobic Digestion with Innovative Mixing Scheme. In proceedings of the *World Congress of the International Solid Waste Association (ISWA)*, Euskalduna Conference Centre and Concert Hall in Bilbao, Spain, from 7-9 October 2019.
- Abou Khalil, C.**, Ghanimeh, S., and Aoun, M. Sustainability of Small-Scale Waste Treatment Units for Refugee Camps. In proceedings of the *Air and Waste Management Association - A&WMA's 112th Annual Conference & Exhibition*, in Québec City, Québec, Canada, 25-28 June 2019.
- Abou Khalil, C.**, Hajj, C., Khalil, K., Nassar, J. B., and Ghanimeh, S. Benefits and Cost Implications of Anaerobic-aerobic Sequential Treatment of Waste in Developing Countries: The Case of Lebanon. In proceedings of the *Air and Waste Management Association - A&WMA's 112th Annual Conference & Exhibition*, in Québec City, Québec, Canada, 25-28 June 2019.
- Abou Khalil, C.**, Arida, A., El Khoury, E., and Ghanimeh, S. Analysis of Temperature Variation Between Dumpsites and their Surroundings Using Thermal Infrared Remote Sensing. In proceedings of the *World Congress of the International Solid Waste Association (ISWA)*, in Kuala Lumpur, Malaysia, October 22-24, 2018.

- Abou Khalil, C.,** Korbane, K., Salem, K., Kabbany, C., and Ghanimeh, S. Options for the Management of Healthcare Waste in Developing Countries. In proceedings of the *Air and Waste Management Association - A&WMA's 111th Annual Conference & Exhibition*, in Hartford, USA, June 25-28, 2018.
- Abou Khalil, C.,** El Khoury, E., Saba, D., Korbane, K., El Beaino, G., Adam, N., and Khoury, N. Ground Water Exploration in Tarshich-Lebanon Using Audio Magnetotelluric (AMT). In proceedings of the *44th International Conference for Hydrogeologists*, in Dubrovnik, Croatia, September 25-29, 2017.
- Abou Khalil, C.,** El Khoury, E., and Ibrahim, E. Correction of Landsat 8 TIRS Acquisitions Using Split-Window Algorithms for Analyzing Names Landfill, Lebanon. In proceedings of the *4th International Conference on Sensors and Networks SENSET2017*, in Beirut, Lebanon, September 12-14, 2017.
- Abou Khalil, C.,** Ghanimeh, S., and Medawar, Y. Ammonia Inhibition and Recovery Potential in Anaerobic Digesters: A Review. In proceedings of the *Air and Waste Management Association - A&WMA's 110th Annual Conference & Exhibition*, in Pittsburgh, USA, June 5-8, 2017.
- Abou Khalil, C.,** Salha, T., and Ghanimeh S. Anaerobic-Aerobic Sequential System: The Case of a Fruit and Vegetable Market. In proceedings of the *World Congress of the International Solid Waste Association (ISWA)*, in Serbia, September 19-21, 2016.
- Abou Khalil, C.,** Ibrahim, L., Ibrahim, E., and Ghanimeh S. Clean energy Generation through Psychrophilic Anaerobic Digestion of Food Waste and Landscaping Waste. In proceedings of the *International Conference on Renewable Energies for Developing Countries (REDEC)*, IEEE, in Zouk Mosbeh, Lebanon, July 13-14, 2016.
- El Khoury, E., **Abou Khalil, C.,** and Ibrahim, E. Deriving Surface Temperature of Naameh Landfill and its Surroundings Using Landsat 8 OLI and TIRS Acquisition. In proceedings of the *38th Asian Conference on Remote Sensing (ACRS)*, in New Delhi, India, October 22-28, 2017.
- Ji, W., **Abou Khalil, C.,** Boufadel, M. C., Coelho, G., Daskiran, C., Robinson, B., King, T., Lee, K., Galus, M. Impact of Mixing and Resting Times on The Droplet Size Distribution Oil WAFs. Accepted for presentation at the *International Oil Spill Science Conference 2022*, in Halifax, Canada, October 04-07, 2022.
- Jabagi, E., Chibani, G., **Abou Khalil, C.,** Bou Mosleh, C., and Ghanimeh S. Anaerobic-Aerobic Sequential System: Improved Treatability and Methane Potential of Waste. In proceedings of the *6th International Symposium on Energy from Biomass and Waste*, in Venice, Italy, November 14-17, 2016.

*I Would Like to Dedicate my Dissertation Work to my Beloved
Uncle Antoine E. Abou Khalil (1943 - 2019)*

ACKNOWLEDGMENT

About three years ago, I was applying for several Ph.D. programs in environmental engineering in the United States. I was accepted by a few research groups, and I am very glad that I chose the Center of Natural Resources (CNR) at NJIT. Now, although I am excited that I have successfully completed the program, I am slightly upset that I am leaving the CNR, which was my home since Fall 2019.

First and foremost, I would like to show my sincere gratitude to Prof. Michel C. Boufadel who pushed me to achieve the best outcomes and supplied me with all the possible means and resources which substantially increased my productivity. During the second week of my program, Dr. Boufadel introduced me to Dr. Roger C. Prince, who further guided me in my research projects as a technical advisor. Dr. Prince is an expert biologist with more than 40 years of experience in the bioremediation of oil-contaminated environments. Therefore, there is no need to point out that I was extremely lucky. Dr. Prince helped me when needed, even on weekends, in addition to providing good insights on how to conduct research, publish papers, and present meaningful data. It was sincerely an honor working with him.

I would also like to show my gratefulness for the assistance provided by Dr. Charles W. Greer and Dr. Nathalie Fortin who conducted the microbial analyses pertaining to this work. In addition, I want to thank Dr. Taha F. Marhaba, Dr. William H. Pennock, and Dr. Ashish D. Borgaonkar for being so considerate and part of my dissertation committee. I highly appreciate their time, effort, and all of their constructive and critical suggestions and comments.

Furthermore, I would like to express my gratitude to the John A. Reif, Jr. Department of Civil and Environmental Engineering for financially supporting me. In addition, I would like to acknowledge the Canada's Oceans Protection Plan under the Multi-Partner Research Initiative of the Department of Fisheries and Oceans for funding my research.

Moreover, I would like to thank my peers in the CNR who helped me during challenging times: Dr. Wen Ji, Dr. Firas Gerges, Dr. Cosane Daskiran, Dr. Xiaolong Geng, Ms. Meghana Parameswarappa Jayalakshamma, Ms. Ruixue Liu, Mr. Anirban Dhulia, and Mrs. Pamela Braykaa, among others. Also, I want to thank the staff of the Department of Civil and Environmental Engineering, notably, Ms. Sylvana Brito, who provided technical support when needed.

Lastly, I would like to thank my family for their encouragement. It would have been extremely arduous without their emotional support. Particularly, I would like to acknowledge my brother, Dr. Charles Abou Khalil; my sister, Mrs. Yasmine Abou Khalil; and my sister-in-law, Dr. Rita Abou Khalil, whom I spent time with during the holidays.

TABLE OF CONTENTS

Chapter	Page
1 INTRODUCTION.....	1
1.1 General Overview.....	1
1.2 Research Objectives.....	4
2 BIODEGRADATION OF HYDROCARBONS AT HIGH SALINITIES.....	7
2.1 Overview.....	7
2.2 Ionic Composition of Hypersaline Environments.....	8
2.3 Hydrocarbons in Permanent Hypersaline Ecosystems.....	11
2.3.1 Salt Lakes	11
2.3.2 Hypersaline Coastal Lagoons	13
2.3.3 Salterns and Salt Pans	14
2.3.4 Deep-sea Brine Pools	15
2.3.5 Oil Reservoirs	16
2.3.6 Salt Cavern Oil Storage	17
2.3.7 Anaerobic Arctic Springs	18
2.4 Hydrocarbons in Transient Hypersaline Ecosystems	18
2.4.1 Supratidal Zones	18
2.4.2 Brine Channels in Ice	20
2.4.3 Hypersaline Frozen Soils	21
2.4.4 Brine and Oil Spills	22
2.4.5 Oil Well Blowouts	23

TABLE OF CONTENTS
(Continued)

Chapter	Page
2.5 Microbiology of Hydrocarbon Biodegradation at High Salinities	24
3 BIODEGRADATION OF CRUDE OIL IN HYPERSALINE SEAWATER	29
3.1 Objectives of the Experiment	29
3.2 Materials and Methods	29
3.2.1 Seawater Evaporation and Sampling	29
3.2.2 Experimental Setup	32
3.2.3 Extraction and GC-MS Analysis	33
3.2.4 Filtration of Microcosms	34
3.2.5 Metataxonomics	34
3.3 Results	37
3.3.1 Sterile Control Experiment	37
3.3.2 Biodegradation of Hydrocarbons	38
3.3.3 Microbial Populations in Microcosms	43
3.4 Discussion	58
4 MICROBIAL ACTIVITY IN VADOSE ZONES	61
4.1 Overview	61
4.2 Characteristics and Challenges	62
4.2.1 Microbial Density and Diversity	62
4.2.2 Biofilms	62
4.2.3 Microbial Motility and Retainment	64

TABLE OF CONTENTS
(Continued)

Chapter	Page
4.2.4 Film Thickness and Microbial Immersion	67
4.2.5 Viscosity	70
4.2.6 Solid-water and Air-water Interfaces	70
4.2.7 Nutrients and Desiccation	71
4.2.8 Pressure	72
4.3 Conclusion	72
5 BIOREMEDIATION OF HYDROCARBONS IN SANDY BEACHES	73
5.1 Objectives of the Experiment	73
5.2 Materials and Methods	74
5.2.1 Seawater Sampling, Evaporation, and Analysis	74
5.2.2 Preparing the Saline Blends	75
5.2.3 Sand Sampling and Analysis	76
5.2.4 Experimental Setup	77
5.2.5 Oil Extraction and GC-MS Analysis	82
5.2.6 Preparation and Sampling for Microbial Analyses	82
5.2.7 Metataxonomics and Metagenomics	84
5.3 Oil Chemistry Analysis	86
5.3.1 Sterile Control Experiment	86
5.3.2 Biodegradation of Hydrocarbons	87
5.4 Microbial Analysis	95

TABLE OF CONTENTS
(Continued)

5.4.1 Metataxonomic Analysis	95
5.4.2 Metagenomic Analysis	103
5.5 Discussion	106
6 CONCLUSIONS AND RECOMMENDATIONS	109
REFERENCES	110

LIST OF TABLES

Table	Page
1.1 Summary of Half-lives of GC-detectable Hydrocarbons from Oil Biodegradation Experiments that Attempted to Mimic Environmental Conditions During Oil Spills	3
2.1 Approximate Ionic Composition of Representative Saline Water Bodies Around the Globe	10
2.2 Named Aliphatic and Aromatic Hydrocarbon-Degraders from Hypersaline Conditions	25
3.1 Apparent First-order Rate Constant and Half-life of Measurable Analytes at Different Salinities	41
3.2 Table of the Dominant 100 Bacterial Amplicon Sequence Variants Identified in Microcosms at Different Salinities in the Absence of Oil	52
3.3 Table of the Dominant 100 Bacterial Amplicon Sequence Variants Identified in Microcosms at Different Salinities in the Presence of Oil	55
5.1 Properties of Seawater and Concentrated Brine	75
5.2 Properties of Sand	77
5.3 Sand Mixtures	80

LIST OF FIGURES

Figure	Page
1.1 Four sampling wells for oil, nutrients, and salinity analysis (December 2010 and January 2011) of the supratidal zone of the beach at Bon Scour National Wildlife Refuge, Alabama (87.825° W, 30.241° N) that was contaminated by the <i>Deepwater Horizon</i> blowout	5
2.1 GC-MS profiles of crude oil remaining after 60 days of incubation. Chromatograms normalized to hopane	13
2.2 GC-MS profiles of a partially evaporated (12%) Atlantic Canada crude oil, incubated for 76 days, at salinities that might be encountered in a supra-tidal zone of an oiled shoreline. % loss is due to biodegradation, calculated from abiotic controls. Chromatograms normalized to hopane	20
3.1 Pictures taken during the experiment of the (a) seawater being gently evaporated in a glass tank, (b) concentrated brine being mixed at 100 rpm using a magnetic stirrer, and (c) microcosms of batches 1 to 4	30
3.2 Salinity variation during the evaporation of seawater. Expected salinity was deduced from the volume of seawater remaining and the initial salinity. The actual salinity was determined by measuring the total dissolved solid content	31
3.3 Flowchart of the experimental design. Note that the oil chemistry analysis was conducted at each incubation period, while the Metataxonomic analysis was conducted at the end of the experiment (76 days)	33
3.4 GC-MS profiles of crude oil remaining after 8 and 76 days of incubation under sterile conditions: % loss represents abiotic removal, and chromatograms are normalized to hopane. P and F represent Pristane and Phytane, respectively	37
3.5 GC-MS profiles of crude oil remaining after 8 and 76 days of incubation: % loss represents both biodegradation and evaporation, and chromatograms are normalized to hopane. P and F represent Pristane and Phytane, respectively	38
3.6 The % remaining of the GC-detectable hydrocarbons, derived from the sterile and live data to solely show the effect of biodegradation. Note that there are three measurements at every incubation period and salinity since the microcosms were prepared in triplicates	39

LIST OF FIGURES
(Continued)

Figure	Page
3.7 Apparent first-order rate constants at different salinities of measurable alkanes from carbon number 16 (n-hexadecane) to carbon number 30 (n-triacontane)	42
3.8 Apparent first-order rate constants at different salinities of measurable PAHs: Parent and alkylated naphthalenes (N), fluorenes (F), phenanthrenes (P), dibenzothiophenes (D), benz[a]anthracene (Baa), and chrysenes (Chr), with C1-N indicating the sum of all methyl naphthalenes, C2-N indicating the sum of all dimethyl and ethyl naphthalenes, etc.	42
3.9 Bacterial alpha diversity in microcosms (a) at different salinities and (b) in the absence (No Oil) and presence of oil	44
3.10 Alpha diversity (Shannon) with and without oil, with respect to salinity and incubation period	45
3.11 Most abundant genera at T = 0; (a) abundance calculated from the 30 g/L salt microcosms and the seawater to concentrated brine ratios, and (b) actual observed abundance	46
3.12 PCoA analysis of the total microbial community in microcosms with 30, 90, or 160 g/L salt (a) in the presence and absence of oil, and (b) with respect to the incubation period	49
3.13 Taxonomic profiles of the 20 most abundant genera identified in the microcosms with 30, 90 or 160 g/L salt at the beginning of the experiment and after 8, 16, 38, and 76 days of incubation, in the presence (bottom panels) and absence of oil (top panels). Note that the total contribution of these most abundant genera was lower in the 30 g/l microcosms, indicating the greater diversity in those incubations	50
3.14 The average concentration of a short-chain (n-C18) and a long-chain (n-C30) alkane vs. the relative abundance of the <i>Alcanivorax</i> genus in the oiled and non-oiled microcosms with respect to time at a salinity of (a) 30 g/L, (b) 90 g/L, and (c) 160 g/L. Note that, in the oiled and non-oiled microcosms at 30 g/L salt, the abundance of <i>Alcanivorax</i> increased at t = 8 days, and then increased again only in the oiled microcosms after t = 16 days	51
3.15 Venn diagram of the dominant 100 bacterial amplicon sequence variants of Table 3.2	54

**LIST OF FIGURES
(Continued)**

Figure	Page
3.16 Venn diagram of the dominant 100 bacterial amplicon sequence variants of Table 3.3	57
4.1 The life cycle of a soil biofilm consists of four phases: attachment, colonization, maturation, and dispersal. At maturation, the biofilm structure and composition are relatively stable. However, with the depletion of nutrients or external disturbances, the cells within can respond quickly by releasing enzymes capable of dispersing the biofilm and triggering the scattering of cells. During biofilm dispersal, cells can detach from the biofilm matrix, colonize another site and start a new biofilm cycle	63
4.2 Different types of bacteria with respect to flagellar arrangement and abundance. Some don't have any and are classified as atrichous, while others are covered with flagella and are called peritrichous. Trichous comes from a Greek word which means "hairy" or "hair"	65
4.3 The different propulsive structures of a bacterium	67
4.4 (a) An illustration of microbes inhabiting soil pore spaces concentrating in corners and crevices where water is comparatively abundant; (b) potential for nutrient flux interception due to diffusion limitation and microbial consumption (arrows indicate nutrient flux); (c) definition sketch for the size of aquatic habitat in a corner bounded by liquid-vapor interface and a spherical or cylindrical fully-immersed microbe behind the interface; and (d) calculated maximal radius of fully-immersed microbe in a cylindrical capillary, and in corners with different angles for a range of matric potential values. Note that (d) does not represent the immersion in thin films	69
4.5 Comparison of theoretical effective film thickness on smooth and rough surfaces as a function of matric potential, based on measurements from Tuff rock surface obtained by Wan and Tokunaga (1997)	70
5.1 Particle size distribution curve of the sand	76

LIST OF FIGURES
(Continued)

Figure	Page
5.2 Initial concentration of the GC-detectable (a) alkanes and (b) aromatics in the Hibernia oil that was used in this experiment. Alkanes that were analyzed are from carbon number 16 (n-hexadecane) to carbon number 34 (n-tetratriacontane). Pr and Ph represents pristane and phytane, respectively. Aromatics represent parent and alkylated naphthalenes (N), fluorenes (F), phenanthrenes (P), dibenzothiophenes (D), benz[a]anthracene (baa), and chrysenes (Chr), with C1-N indicating the sum of all methyl naphthalenes, C2-N indicating the sum of all dimethyl and ethyl naphthalenes, etc.	79
5.3 Flowchart of the experimental design	81
5.4 Sand column microcosms and seawater bottle (positive control). Note that there was a total of 42 columns and 24 bottles	81
5.5 GC-MS profiles of crude oil remaining after 30, 90, and 180 days of incubation under sterile conditions: %loss represents abiotic removal, and chromatograms are normalized to hopane	87
5.6 GC-MS profiles of crude oil remaining after 30, 90, and 180 days of incubation with and without the addition of nutrients: % loss represents total removal, and chromatograms are normalized to hopane	89
5.7 The %remaining of the GC-detectable hydrocarbons with (a) indigenous nutrients and (b) additional nutrients, due to the effect of biodegradation. Data from the sterile control and seawater flasks is also provided for comparison. Half-life of dispersed oil in seawater was 18.5 days. Half-lives in microcosms that underwent natural attenuation were 40.2, 58.1, and 76.5 days at 30, 90, and 160 g/L salt. Half-lives in microcosms that underwent biostimulation were 34.4, 43.2, and 49.1 days at 30, 90, and 160 g/L salt	90
5.8 The % decrease in apparent first-order rate constants (k) at different salinities of GC-detectable hydrocarbons in seawater (dispersed plumes) and sand (with and without additional nutrients). *Data for dispersed plumes was taken from Chapter 3	91

LIST OF FIGURES
(Continued)

Figure	Page
5.9 Apparent first-order rate constants (k) at different salinities of (a, b) measurable alkanes from carbon number 16 (n-hexadecane) to carbon number 34 (n-tetratriacontane), (c, d) and parent and alkylated naphthalenes (N), fluorenes (F), phenanthrenes (P), dibenzothiophenes (D), benz[a]anthracene (Baa), and chrysenes (Chr), with C1-N indicating the sum of all methyl naphthalenes, C2-N indicating the sum of all dimethyl and ethyl naphthalenes, etc. (a) and (c) are for microcosms that underwent natural attenuation, and (b) and (d) are for the microcosms that underwent biostimulation. Apparent k for naphthalene (N) could be higher since it was not detected at any incubation period	93
5.10 GC-MS profiles of crude oil remaining after 180 days for the seawater microcosms (positive control), and the oiled sand columns at a concentration of 1 and 10 mL/kg, with and without nutrients, at a salinity of 30 g/L. Chromatograms are normalized to hopane	94
5.11 Taxonomy of the 20 most abundant genera identified in fresh seawater and concentrated brine at the beginning of the experiment. The color coding in the stacked graphs follows the same sequence as the colors in the legend from bottom to top. The sequences are essentially 'equivalent taxonomic units' identified to the genus, but based on the database used, some are identified to the order (**)	96
5.12 Taxonomy of the 20 most abundant genera identified in dry beach sand and in beach sand infiltrated with the live blends (20% saturation) at different salinities at the beginning of the experiment (T = 0). The color coding in the stacked graphs follows the same sequence as the colors in the legend from bottom to top. The sequences are essentially 'equivalent taxonomic units' identified to the genus, but based on the database used, some are identified to the family (*) or order (**). Note: It has been proposed to move <i>Planococcaceae</i> into <i>Caryophanaceae</i> (Gupta and Patel, 2020).....	96
5.13 Bacterial alpha diversity in the seawater bottles and sand column microcosms at different salinities	98
5.14 Beta diversity of the total microbial community in the seawater bottles and sand column microcosms with respect to salinity and incubation period	99

LIST OF FIGURES
(Continued)

Figure	Page
5.15 Taxonomy of the 20 most abundant genera identified in the seawater microcosms (i.e., dispersed plume). The color coding in the stacked graphs follows the same sequence as the colors in the legend from bottom to top. The sequences are essentially 'equivalent taxonomic units' identified to the genus, but based on the database used, some are identified to the order (**)	99
5.16 Taxonomy of the 20 most abundant genera identified in the sand microcosms with/without oil and with/without additional nutrients at different salinities and incubation periods. The color coding in the stacked graphs follows the same sequence as the colors in the legend from bottom to top. The sequences are essentially 'equivalent taxonomic units' identified to the genus, but based on the database used, some are identified to the family (*) or order (**). Note: It has been proposed to move <i>Planococcaceae</i> into <i>Caryophanaceae</i> (Gupta and Patel, 2020)	102
5.17 Taxonomy of the 20 most abundant genera identified in the sand microcosms at different oil concentrations with/without additional nutrients after 180 days of incubation. The color coding in the stacked graphs follows the same sequence as the colors in the legend from bottom to top. The sequences are essentially 'equivalent taxonomic units' identified to the genus, but based on the database used, some are identified to the family (*) or order (**). Note: It has been proposed to move <i>Planococcaceae</i> into <i>Caryophanaceae</i> (Gupta and Patel, 2020)	103
5.18 Enzymatic pathways for the degradation of alkanes (in green) and aromatics (in blue) of the initial conditions (fresh seawater, dry sand, concentrated brine), oiled seawater bottles, and the sand columns (with/without oil, with/without additional nutrients) at different oil concentrations and incubation periods. Note that RPKM = Reads Per Kilobase Million and that disp., Ind. Nut., and add. Nut. stands for Dispersed, Indigenous Nutrients, and Additional Nutrients, respectively	105

CHAPTER 1

INTRODUCTION

1.1 General Overview

Crude oil and natural gas seeps in the ocean have probably been emitting petrogenic hydrocarbons for millions of years, fostering the evolution of microorganisms that can readily degrade this rich source of potential metabolic energy (Hazen et al., 2016). Consequently, the half-life of dispersed crude oil in the ocean is relatively short (Table 1.1), varying from one to three weeks (Prince et al., 2013; Wang et al., 2016; Prince et al., 2017; Brakstad et al., 2018), even under high pressures (Prince et al., 2016b) and sub-zero temperatures (McFarlin et al., 2014; Garneau et al., 2016). The biodegradation of stranded oil on shorelines, however, is often much slower (Bragg et al., 1994; Bociu et al., 2019), which could be attributed to the much higher oil concentrations on contaminated shorelines (Geng et al., 2021) than in dispersed plumes.

High salinities could be another impediment to the biodegradation of petroleum hydrocarbons in sandy beaches, specifically in the upper parts of shorelines which are prone to prolonged periods of evaporation and may be inundated only during spring tides (upper intertidal zone) or storm events (supratidal zone). Therefore, the salinity can drastically increase (by up to eight-fold) in the upper intertidal (Geng et al., 2016a) and supratidal (Geng & Boufadel, 2017) zones. Such hypersaline conditions might inhibit the indigenous marine hydrocarbon degraders. Although limited, literature is available on the biodegradation of hydrocarbons in coastal hypersaline settings by halophilic hydrocarbon degraders, at salinities ranging from 40 g/L up to 320 g/L (Bertrand et al., 1990; Díaz et

al., 2002; Abed et al., 2006; Al-Mailem et al., 2010). However, data obtained using isolated strains from permanent hypersaline ecosystems might not represent the natural *in-situ* oil biodegradation in transient hypersaline environments such as contaminated shorelines. Therefore, further investigations should be carried out to better understand the effect of salinity on the hydrocarbonoclastic activity in the upper parts of sandy beaches since several catastrophic marine oil spills have contaminated such coastal systems in the past, such as during the Gulf War (Fowler et al., 1993), the spills from the *Exxon Valdez* (Taylor & Reimer, 2008), *Erika* (Jézéquel & Poncet, 2011), and *Haven* (Martinelli et al., 1995) tankers, and the blowouts of the Ixtoc-1 (Radović et al., 2020) and *Deepwater Horizon* (Boufadel et al., 2011; Michel et al., 2013) wells.

The low moisture content in the upper parts of sandy beaches is another challenge that might limit the hydrocarbonoclastic activity, whereby the water saturation within the sand's voids ranges from 5 to 40% (Geng et al., 2021), resulting in a volumetric moisture content ranging from 0.2 to 15%, depending on the sand's porosity. The availability of nutrients is another key factor that should be considered in oiled beaches since it can significantly limit the biodegradation of hydrocarbons. Many have investigated the bioremediation of oiled beaches when adding fertilizers to the contaminated intertidal zones (i.e., biostimulation), which improved the biodegradation of hydrocarbons (Prince, 1993; Bragg et al., 1994; Prince & Bragg, 1997; Prince et al., 2003; Becker et al., 2016). However, the concentration of nutrients in the upper intertidal and supratidal zones is intrinsically relatively high because they are concentrated along with the salinity by evaporation (Geng et al., 2021), and hence, might not be as limiting relative to the intertidal zone.

Table 1.1 Summary of Half-lives of GC-detectable Hydrocarbons from Oil Biodegradation Experiments that Attempted to Mimic Environmental Conditions During Oil Spills

Oil Type	Concentration of Oil (ppm)	Seawater inoculum	Half-life (days)	Temp. (°C)	Dispersant, DOR*	Reference
Alaska North Slope crude oil	2.5	NJ, USA	14	8	None	Prince et al. (2013)
			11	8	Corexit 9500, 1:20	
			7	21	Corexit 9500, 1:20	Prince and Butler (2014)
			7	20	Corexit 9500, 1:15	Prince et al. (2016a)
		7	20	Slickgone NS, 1:20		
		7	20	Finasol OSR52,1:20		
		Barrow, AK, USA	36	-1	None	
			37	-1	Corexit 9500, 1:20	
Macondo crude oil	2	Trondheims Fjord, Norway	26	5	Corexit 9500, 1:15	Brakstad et al. (2015)
		Gulf of Mexico, USA	11	5	Corexit 9500, 1:15	Wang et al. (2016)
European crude oil	3	Logy Bay, Canada	13	5	Corexit 9500, 1:100	Prince et al. (2016b)
	2.5	NJ, USA	10	21	Corexit 9500, 1:100	Prince et al. (2017)
Bintulu crude oil	100	Penang, Malaysia	28	26	None	Zahed et al. (2010)
			15	26	Corexit 9500, 1:20	

*Note: DOR = Dispersant to Oil Ratio

1.2 Research Objectives

The research's overall objective is to suggest alternative solutions to oil-spill responders and decision-makers for remediating oil-contaminated shorelines by thoroughly investigating the effect of salinity, moisture content, oil concentration, and nutrient limitation on the microbial degradation of petroleum hydrocarbons in sandy beaches. Consequently, two experiments are conducted, whereby the first is carried out using oiled natural inoculum (seawater) at different salinities (Chapter 3), while in the second experiment, oil biodegradation is investigated using sand columns prepared by mixing beach sand with natural seawater at different salinities, with and without additional nutrients, while achieving a moisture content similar to that in supratidal zones and oil concentrations similar to those observed in beaches contaminated by large oil spills (Chapter 5). Such investigations would provide answers to several questions:

(1) Would high salinities substantially decrease the hydrocarbonoclastic activity of the indigenous coastal microorganisms?

The seawater has a salinity ranging from 30 to 35 g/L, and hence, the marine's indigenous microorganisms are either halophilic (i.e., thrive at high salinities) or halotolerant (i.e., can live in saline ecosystems, but salinity is not required for survival). Hypersaline conditions (i.e., salinity > 35 g/L), however, might inhibit most of the marine's hydrocarbon-degrading microorganisms. Nonetheless, previous studies (Bertrand et al., 1990; Díaz et al., 2002; Abed et al., 2006; Al-Mailem et al., 2010) have isolated extreme halophiles from coastal ecosystems that can degrade hydrocarbons under hypersaline conditions, and hence, it is suspected that the hydrocarbonoclastic activity in seawater would slow down, but not necessarily halt, at salinities three to six-fold higher than that of seawater (Figure 1.1).

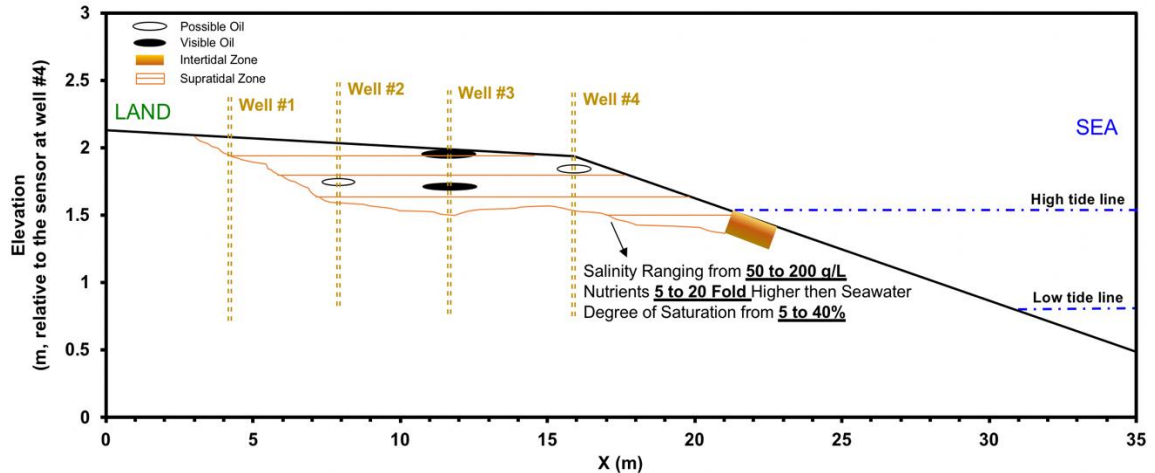


Figure 1.1 Four sampling wells for oil, nutrients, and salinity analysis (December 2010 and January 2011) of the supratidal zone of the beach at Bon Scour National Wildlife Refuge, Alabama (87.825° W, 30.241° N) that was contaminated by the *Deepwater Horizon* blowout.

Source: (Boufadel et al., 2011; Geng & Boufadel, 2014, 2015; Geng et al., 2016b)

(2) *Would high oil concentration on shorelines affect the half-life of petroleum hydrocarbons?*

Although the half-life of dispersed crude oil in the ocean is short, varying from one to three weeks (Prince et al., 2013; Wang et al., 2016; Prince et al., 2017; Brakstad et al., 2018), that of undispersed crude oil slicks is relatively much longer (Prince et al., 2017). The same concept can be applied to beached oil where the effective oil concentration (average of thousands of ppm depending on the moisture content and oil concentration) is particularly high relative to dispersed plumes (few ppm).

(3) *Does low moisture content in coastal sediments substantially alter the petroleum hydrocarbon's biodegradation rate?*

Since upper shorelines are prone to evaporation and infrequent inundation, they would inevitably be subject to dryness (Figure 1.1). The biodegradation of petroleum hydrocarbons occurs at the oil-water interface, and thus, lack of moisture might negatively impact the hydrocarbonoclastic activity. Nonetheless, it is unlikely that such transient hypersaline settings would become completely dry, and having a low moisture content

would more likely sustain the microbial activity in coastal sediments. Thus, we hypothesize that at a low degree of saturation (~20%), extreme hypersaline conditions and high oil concentration would be the main contributors to increasing the petroleum hydrocarbons' half-life in such ecosystems.

(4) *Would hypersaline conditions enrich rare organisms in seawater or slow most of the microbial community's activity?*

Since the marine microbial species thrive at low salinities (i.e., seawater), most of them would probably perish when subject to extreme hypersaline conditions. Nonetheless, hydrocarbon-degraders of different genera found in seawater, such as *Marinobacter*, *Thalassospira*, and *Alcanivorax*, were found to degrade hydrocarbons at high salinities (Gauthier et al., 1992; Berlendis et al., 2010; Dastgheib et al., 2012; Hassan et al., 2012; Al-Mailem et al., 2013; Fang et al., 2016; Zhou et al., 2016; Wang et al., 2018). Therefore, we assume that halophilic and extreme halotolerant hydrocarbon-degrading microorganisms present in seawater would become the most relatively abundant at high salinities.

(5) *Does fertilizing oil-contaminated beaches significantly enhance the microbial degradation of petroleum hydrocarbons?*

Generally, the biodegradation of crude oil in contaminated beaches is limited by the low availability of nutrients. Several studies investigated the bioremediation of oiled beaches when adding fertilizers to the intertidal zones (biostimulation), which significantly improved the biodegradation of hydrocarbons (Prince, 1993; Bragg et al., 1994; Prince & Bragg, 1997; Prince et al., 2003; Becker et al., 2016). Therefore, it is expected that supplying additional nutrients would enhance the hydrocarbonoclastic activity.

CHAPTER 2

BIODEGRADATION OF HYDROCARBONS AT HIGH SALINITIES

2.1 Overview

About one-third of the world's economy runs on the combustion of crude oil and its products, consuming about 5.1 billion tons per year worldwide (USEIA, 2019): inevitably some gets spilled during production, transportation, and use. While spilled hydrocarbons are subject to a diversity of weathering processes (e.g., evaporation, dissolution, photooxidation, and emulsification), only combustion and biodegradation remove significant quantities of hydrocarbons from the environment. The microbiology and biochemistry of hydrocarbon biodegradation, both aerobic and anaerobic, are well-studied (Ladino-Orjuela et al., 2016; Prince & Walters, 2016; Rabus et al., 2016; Ławniczak et al., 2020), but little is known about hypersaline environments. Ward and Brock (1978) studied biodegradation in Utah's Great Salt Lake and found that high salt was inhibitory, and although subsequent work has shown that this is not strictly true (Sei & Fathepure, 2009), it does seem that hydrocarbon biodegradation is slowed at high salt concentrations.

Generally, hypersaline environments are defined as having a salinity concentration above that of seawater (3 – 3.5%), and there are many where waters approach saturation. Numerous surface hypersaline settings have a close association with natural oil seeps, oil industries, or anthropogenic activities, so it is vital to have a toolkit for efficiently remediating such sites in the event of a significant spill. Physical removal of spilled oil is obviously the best first response, but if this is impossible, or if moving equipment at a spill site leads to further damage, it may be best to rely on natural processes to remove the

contaminants. Consequently, biodegradation is likely the most important natural process that will remove hydrocarbons, and if better understood might be amenable to stimulation.

Several reviews have discussed the biodegradation of organic pollutants, including hydrocarbons, by halophilic or halotolerant microbes in highly saline settings (Le Borgne et al., 2008; Timmis et al., 2010; Sorokin et al., 2012; Fathepure, 2014; Edbeib et al., 2016; Oren, 2019). Note that petroleum is not the only source of hydrocarbons in the environment; other sources include biogenic and pyrogenic processes, which can be discriminated by the intrinsic chemistry of the hydrocarbons (Wang et al., 2014). In this chapter, an overview of permanent (Section 2.3) and transient (Section 2.4) hypersaline environments that might be exposed to hydrocarbon contamination is provided, along with a discussion of what is known about hydrocarbon biodegradation by the resident halophilic and halotolerant microorganisms. In addition, the microbiology of hydrocarbon biodegradation at high salinities, and why it is slow in such ecosystems, is addressed (Section 2.5).

2.2 Ionic Composition of Hypersaline Environments

Generally, hypersaline ecosystems are divided into two categories based on their association with seawater. Thalassohaline environments have an ionic composition (although not concentration) similar to that of seawater and are thought to arise from the evaporation of recent or historic seawaters. For instance, intertidal and supratidal zones of tidally influenced beaches are thalassohaline, since seawater evaporates between inundations, resulting in a substantial increase in salinity (Geng & Boufadel, 2015). Other examples include sabkhas (i.e., salt flats), which are subject to episodic seawater flooding and evaporation, leading to the accumulation of salts (Al-Mailem et al., 2013). Similarly,

coastal hypersaline water bodies are often thalossohaline, since they originate from seawater and are frequently recharged by the ocean. The Garabogazköl (Kara-bogaz-gol) lagoon in Turkmenistan (11,265 km²) is one example; it is intermittently replenished by the Caspian Sea, and evaporation leads to a salinity reaching up to 35% (Kosarev et al., 2013). Some inland salt lakes, such as the Great Salt Lake in Utah, have an ionic composition similar to that of the ocean, and hence, are also considered thalossohaline (Yoon, 2016). The second category of hypersaline settings is designated as athalassohaline, where the ionic composition differs from that of seawater. For instance, the Dead Sea is athalassohaline; it results from evaporated river water (River Jordan), and, unlike the Great Salt Lake, divalent cations dominate the cationic content (Nissenbaum, 1975; Yoon, 2016). Table 2.1 provides the ionic composition of the ocean and some perennially hypersaline water bodies around the globe.

Table 2.1 Approximate Ionic Composition of Representative Saline Water Bodies Around the Globe

Saline Body, Country	Salinity (%)	Approximate Percentage of Ions (Mol, %)							Reference
		Na ⁺	K ⁺	Ca ²⁺	Mg ²⁺	SO ₄ ²⁻	Cl ⁻	Other	
Ocean	3.5	43.1	0.9	0.3	1.8	2.6	50.7	0.6	Marine Science (2008)
Lake Urmia, Iran	8 – 28	44.1	0.3	0.4	3.2	1.7	49.8	0.5	Alipour (2006)
Great Salt Lake, USA	10 – > 30	44.5	1.3	0.2	3.6	2.1	48.2	0.1	Ward and Brock (1978); Yoon (2016)
Lake Tuz, Turkey	32.4	43.0	1.2	0.2	5.8	1.9	47.9	0.8	Camur and Mutlu (1996); Kilic and Kilic (2010)
Lake Bagaejinor, Mongolia	30	34.2	0.4	0.0	2.3	16.3	45.7	1.1	Grant et al. (2011)
Mono Lake, USA	8.1	49.9	2.8	0.0	0.1	16.2	30.1	0.9	Johannesson et al. (1994); Pecoraino et al. (2015)
Lake Chagann, Mongolia	18	50.9	0.4	0.0	0.0	16.9	29.4	2.4	Grant et al. (2011)
Lake Erliannor, Mongolia	20 – 25	20.8	0.7	0.1	11.0	13.2	53.2	1.0	Grant et al. (2011)
Lake Ejinor, Mongolia	11.1	21.3	0.9	0.0	16.4	10.1	50.9	0.4	Grant et al. (2011)
Dead Sea, Israel and Jordan	33.7	15.2	1.8	3.6	18.3	0.1	60.4	0.6	Nissenbaum (1975); Yoon (2016)
Don Juan Pond, Antarctica	38.2	4.1	0.1	29.4	0.8	0.0	65.6	0.0	Cameron et al. (1972)

2.3 Hydrocarbons in Permanent Hypersaline Ecosystems

2.3.1 Salt Lakes

Many hypersaline lakes are subject to hydrocarbon contamination from natural sources. For instance, the Dead Sea (considered to be the lowest point on earth), with a salinity of 34.2%, contains biogenic hydrocarbons from the halophilic algae that grow therein (Oldenburg et al., 2000), and is exposed to petroleum contamination from seeps of asphalt and heavy oils in the lake's basin (Rullkötter et al., 1985; Gvirtzman & Stanislavsky, 2000; Sokol et al., 2014). Although previous studies found genera (*Haloarcula* and *Halobacterium*) in the Dead Sea that might be capable of degrading hydrocarbons (Hase et al., 1980; Oren, 1983; Oren et al., 1990; Baliga et al., 2004), there are no published reports (i.e., till the year of 2022) of hydrocarbon biodegradation in waters or sediments of this hypersaline lake. However, hypersaline aquifers near the Dead Sea are home to anaerobic methane consumers (Avrahamov et al., 2014). Utah's Great Salt Lake, with salinities ranging from 10% to > 30%, has oil seepage at Rozel Point (Sinninghe Damsté et al., 1987). The dramatic range of salinity in this lake was triggered in the 1960s by the replacement of a wooden railroad trestle with an almost complete berm, dividing the lake into North and South Arms, and essentially isolating the North Arm from freshwater input of the melting snow in the Wasatch Mountain Range; it has become close to saturation with salt, although this will decline in the future since water exchange between the Arms is now being encouraged (Null & Wurtsbaugh, 2020). Other examples of hypersaline lakes likely exposed to hydrocarbon seeps include Lake Tuz in Turkey (Aydemir, 2008), Little Manitou Lake in Canada (Quijada & Stewart, 2008), and Chott El-Djerid Lake in Tunisia (Neifar et al., 2019), with salinities of 32%, 18%, and up to 35%, respectively.

Ward and Brock (1978) analyzed the biodegradation potential of the Great Salt Lake and noted that the rates of hydrocarbon degradation decreased as the salinity increased from 3.3 to 28.4%. In a later study, Sei and Fathepure (2009) used an enrichment culture obtained from the Great Salt Lake at Rozel Point that is capable of degrading benzene or toluene as the sole carbon source over a broad range of salinities (14 to 29%). The Great Salt Lake contains a diverse community of potential hydrocarbon-degrading microbes (Tazi et al., 2014), and they have a broad appetite for hydrocarbons, at least at the moderate salinities of the South Arm. Figure 2.1 displays GC-MS profiles of crude oil in hypersaline water samples from the Great Salt Lake incubated with 5 ppm of an artificially weathered light crude oil (20% loss by evaporation) for 60 days (Prince & Prince, 2022). The samples were taken from the South Arm (Great Salt Lake Marina, 40.735° N, 112.212° W) and North Arm (Spiral Jetty, 41.438° N, 112.669° W) and it is clear that biodegradation was much more extensive in the South Arm (16% salt) than in the North Arm (34% salt).

Interestingly, hydrocarbon-degrading halophiles are found in hypersaline water bodies with no known hydrocarbon contamination history. For instance, Tapilatu et al. (2010) isolated alkane-degrading halophilic archaea related to *Haloarcula* and *Haloferax* from a pristine hypersaline pond in Camargue, France, that consumed heptadecane at a salinity of 22.5%. In addition, aerobic methane consumption is likely widespread in hypersaline lakes since it has been found in lakes in Crimea with up to 33% salinity (Sokolov & Trotsenko, 1995; Heyer et al., 2005) and Mono Lake (Table 2.1) in California (Lin et al., 2005). The apparent exception is the remarkable saline Don Juan Pool in the Wright Dry Valley of Antarctica (Cameron et al., 1972), perhaps the most saline water on

the planet (> 38% solids). Although a potentially hydrocarbon-degrading *Achromobacter* was isolated (Cameron et al., 1972), subsequent visitors determined it was a ‘metabolically dormant’ environment (Samarkin et al., 2010).

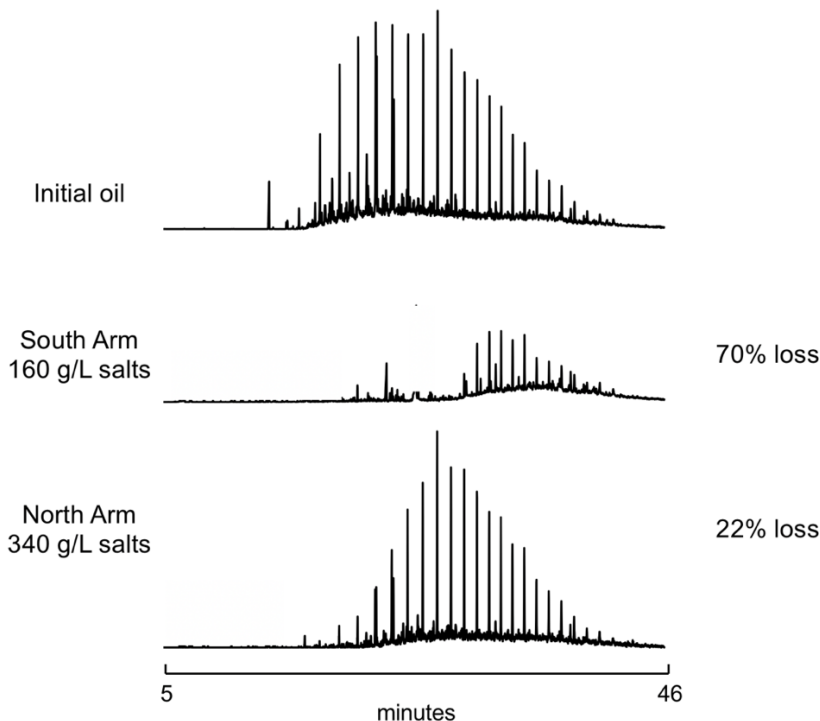


Figure 2.1 GC-MS profiles of crude oil remaining after 60 days of incubation. Chromatograms normalized to hopane.

Source: (Prince & Prince, 2022)

2.3.2 Hypersaline Coastal Lagoons

Hypersaline coastal lagoons are shallow and periodically recharged by seawater. Such coastal water bodies might be susceptible to hydrocarbon contamination since coastal seas serve as receptors of natural and anthropogenic organic matter. A considerable portion of the production and transportation of crude oil occurs in the marine environment, leading to some spillage into the ocean (Eckle et al., 2012), despite the efforts of the industry and regulators. In addition, catastrophic accidents can occur, leading to the discharge of thousands of tons of crude oil into the marine environment, and in many cases, forcing the

oil to be stranded on the coast. The Garabogazköl Aylagy (Black Strait Lake) in Turkmenistan (salinity 35%), is potentially vulnerable to oil contamination since its recharging source, the Caspian Sea, is subject to crude oil pollution due to seeps (Ivanov et al., 2020) and petroleum exploration and production (Effimoff, 2000; Tolosa et al., 2004; Miller et al., 2019). The Caspian Sea is estimated to have potential oil reserves of 16 – 32 billion barrels and is bordered by nations with huge terrestrial oil and natural gas reserves (Effimoff, 2000; Tolosa et al., 2004). In addition, several other slightly hypersaline coastal lagoons (salinity of 3.7 – 5%) have detectable hydrocarbons. For example, the Laguna Madre system, a long, shallow lagoon along the western coast of the Gulf of Mexico in Texas, is the largest hypersaline coastal basin in the United States. It is exposed to trace levels of biogenic, petrogenic, and pyrogenic hydrocarbons, with notable anthropogenic input (Sharma et al., 1997). Another example of a slightly hypersaline coastal lagoon known to be contaminated with low levels of hydrocarbons, mainly pyrogenic, is the Mar Menor lagoon in the Iberian Peninsula, south-east of Murcia, Spain (León et al., 2013). The microbial diversity of this mildly saline lagoon (5% salt) is dominated by bacteria (Ghai et al., 2012), and it is expected that hydrocarbon degradation is very likely in such environments.

2.3.3 Salterns and Salt Pans

Generally, salterns and salt pans describe man-made installations for making salt. They usually consist of evaporation and crystallization ponds that are initially fed by seawater, and have a salinity that varies from seawater values (around 3%) up to saturation (35%). Consequently, such hypersaline ecosystems are analogs to coastal lagoons and are similarly susceptible to oil pollution. One potential example is the saltworks of Sfax in Tunisia,

which consists of interconnected shallow (0.2 – 0.7 m) ponds separated from the sea by a red silt artificial seawall, with salinities of 4 to 35%. Hydrocarbon extraction and analysis from the Sfax coastal region showed that the natural hypersaline ponds outside the saltern are contaminated by petrogenic aliphatic and aromatic hydrocarbons (Zaghden et al., 2007; Zaghden et al., 2014). Hydrocarbons present in such hypersaline ecosystems can be biodegraded by indigenous hydrocarbon-degrading halophiles. For instance, Erdoğan et al. (2013) analyzed archaeal isolates from brine from the Çamaltı Saltern in Turkey that could use naphthalene, phenanthrene, and pyrene as sole carbon and energy sources. They were identified to be *Halobacterium*, *Halorubrum*, *Haloarcula*, and *Haloferax* species (Table 2.2). The same genera are present in salterns around the world (Asker & Ohta, 2002; Lizama et al., 2002; Pašić et al., 2007; Manikandan et al., 2009).

2.3.4 Deep-sea Brine Pools

Perhaps surprisingly, stable hypersaline brine pools with a salinity three to eight times that of seawater can be formed in the deep sea by the dissolution of salt during seafloor tectonic activity. Substantial anoxic hypersaline brine ‘pools’ are found on the floor of the Red Sea, the Mediterranean Sea, and the Gulf of Mexico. The Red Sea Rift is a spreading center between two tectonic plates (the African plate and the Arabian plate), leading to the formation of several anoxic deep-sea brine pools with salinity reaching 26% (Antunes et al., 2011; Duarte et al., 2020). These brine pools are enriched with light hydrocarbons from natural seepage (Faber et al., 1998; Gordon et al., 2010; Schmidt et al., 2015). The Gulf of Mexico also contains a brine pool (Orca basin) at a depth of 2,300 m with a salinity reaching up to 32%; it has biogenic hydrocarbons (Wiesenburg et al., 1985). More complex petrogenic hydrocarbons may be in other pools in the vicinity because the Gulf of Mexico

has many hydrocarbon seeps with thermogenic hydrocarbon gases (Sassen et al., 1999; MacDonald et al., 2010; Wankel et al., 2010). Anaerobic methane oxidation has been detected at a saline seep (salinity four-fold higher than seawater) in the Green Canyon in the Gulf of Mexico (Lloyd et al., 2006), and at a similar site (salinity eight-fold higher than seawater) at the Mercator mud volcano in the Gulf of Cadiz, Spain (Maignien et al., 2013).

2.3.5 Oil Reservoirs

Oil and gas in natural reservoirs typically sit on water that can range from fresh to > 30% salt (Birkle et al., 2009; Fakhru'l-Razi et al., 2009). The presence of microorganisms in oil reservoirs was recognized long ago (Bastin et al., 1926), and there is evidence that some microbes may have survived from the initial deposition of the reservoir (Gales et al., 2016). Nevertheless, the reality of their effective *in-situ* activity remains both extensive and elusive (Ollivier et al., 2014). Biodegradation of crude oil in reservoirs is common and can lead to a devaluation of the oil since biodegradation decreases the aliphatic and light aromatic content, thereby increasing the oil's density, sulfur content, acidity, and viscosity (Connan, 1984). Heavily degraded reservoirs, such as the Athabasca tar sands in Alberta, Canada, and the Orinoco oil belt in Venezuela are enormous examples of residues from extensive biodegradation (Connan, 1984). Early work assumed that such biodegradation was aerobic, which implied enormous flows of meteoric water over the millions of years available (the average age of commercially important crude oils is about 100 million years (Tissot & Welte, 1984)), but scientific evidence supports the theory that anaerobic degradation may have also contributed to the process (Aitken et al., 2004; Jones et al., 2008; Wang et al., 2011; Gao et al., 2019; Liu et al., 2020). For example, the Gullfaks field in the Norwegian North Sea contains oils that have undergone mild anaerobic

biodegradation (Vieth & Wilkes, 2006). Temperature seems to be the major controlling factor for biodegradation, with no growth yet detected above 82°C (Pannekens et al., 2019). Some cooler reservoirs show no signs of biodegradation, and this is attributed to periods in the past at far higher temperatures – paleo-sterilization or paleo-pasteurization (Wilhelms et al., 2001; Larter et al., 2003; Röling et al., 2003). Larter et al. (2006) state that salinity has a second-order effect on slowing biodegradation at higher salt concentrations; Gao et al. (2019), Wang et al. (2011), and Liu et al. (2020) studied biodegradation in brackish reservoirs (1 – 8% salt), not hypersaline ones.

2.3.6 Salt Cavern Oil Storage

Salt caverns are “crafted” by dissolving enormous cavities in salt lenses (Lux, 2009). Storage of hydrocarbons in such caverns started in the early 1950s (Avery Island, USA) and is now used worldwide (Wang et al., 2018). The US Strategic Petroleum Reserve stores up to 714 million barrels of oil in four locations in the southern US (Office of Fossil Fuels, 2020). These are salt caverns, but unlined rock caverns have also been used where such geological features are unavailable (Roffey, 1989).

Oil storage caverns might appear to be the equivalent of natural oil reservoirs, but they are radically different. Salt and rock caverns are gigantic tanks that would be empty if not for the stored oil or gas; oil reservoirs are porous rocks, with no obvious large spaces, under great pressure from overlying rock. However, the basic physics that oil will float on any water remains true, and storage cavern operators take pains to minimize water in the system. Nonetheless, microbes are generally present (Yoshida et al., 2005), and biological degradation of oil in salt caverns has been found in a few cases, spoiling jet fuel with biomass, pressurizing tanks with biogenic methane, or causing corrosion with biologically

generated H₂S (Roffey, 1989). Biodegradation in salt caverns can be both aerobic and anaerobic (Roffey, 1989; Bock et al., 1994), and halophilic oil-degrading genera, such as *Marinobacter*, have been observed in such ecosystems (Bordenave et al., 2013).

Oil biodegradation is not the only microbiological issue in storage tanks – microbial growth on other substrates, such as small volatile fatty acids (acetate, propionate, etc.) can potentially lead to the production of H₂S, which is both toxic and corrosive (Ibrahim et al., 2018; Jia et al., 2019). These problems can sometimes be eliminated with the judicious use of biocides (Raczkowski et al., 2004; Johnson et al., 2017; Jia et al., 2019).

2.3.7 Anaerobic Arctic Springs

The only known terrestrial methane seep in an otherwise frozen environment is a Canadian hypersaline anaerobic Arctic spring (17 – 25% salt) called the Lost Hammer Spring, located in the central west region of Axel Heiberg Island. The spring contains small alkanes (methane to butane), but no anaerobic oxidation of methane could be detected. Nevertheless, the site's microbial inhabitants show clear similarities to those of other cold environments around the world, and the authors believe it will be important to assess anaerobic ethane and butane oxidation in the future, since this plays a significant role in both carbon and sulfur cycling, which often occurs under sulfate-reducing conditions (Niederberger et al., 2010; Lamarche-Gagnon et al., 2015).

2.4 Hydrocarbons in Transient Hypersaline Ecosystems

2.4.1 Supratidal Zones

Supra-tidal zones are above the routine tidal zone, typically only inundated during storms at spring tides. As the seawater evaporates, it leaves a hypersaline residue, controlled by the hydrological, geological, and climatic conditions of the region. A good example is the

Arabian Gulf coast (a semi-arid region) of Saudi Arabia, which is subject to significant seasonal changes in temperature and salinity as well as daily cycles of dehydration and replenishment by tides, resulting in moderate (3 – 4%, 25°C) to extreme (16%, 50°C) salinity variations on a daily basis (Abed et al., 2006). The upper intertidal zone of temperate zones may become similarly hypersaline at low tide (Geng et al., 2016a).

Oil spills can contaminate shorelines if natural physical processes or responders fail to disperse the oil at sea (Prince, 2015). If it occurs, most of the residual oil is deposited in the upper intertidal zone, but storms and spring tides can push it into supratidal zones. This happened after the Gulf War (Fowler et al., 1993), the spills from the *Exxon Valdez* (Taylor & Reimer, 2008), *Erika* (Jézéquel & Poncet, 2011), and *Haven* (Martinelli et al., 1995) tankers, and the *Deepwater Horizon* blowout (Michel et al., 2013).

With exposure to hypersaline excursions, marine organisms within the supratidal zone may well face transiently inhibitory conditions. Abed et al. (2006) found that the mineralization of hexadecane and phenanthrene by microbial mats from the Persian Gulf side of Saudi Arabia was slowed substantially when the salinity increased from 3.5 (seawater) to 16%. A similar effect is seen in Figure 2.2, where fresh seawater was added to evaporated brine to mimic what might happen when seawater impinges on a supratidal zone that has dried out for some time. Clearly, biodegradation is substantially slowed, but not prevented, at a salinity more than five-fold that of seawater. The calculated half-lives were about 10 and 293 days at salinities of 30 and 160 g/L, respectively.

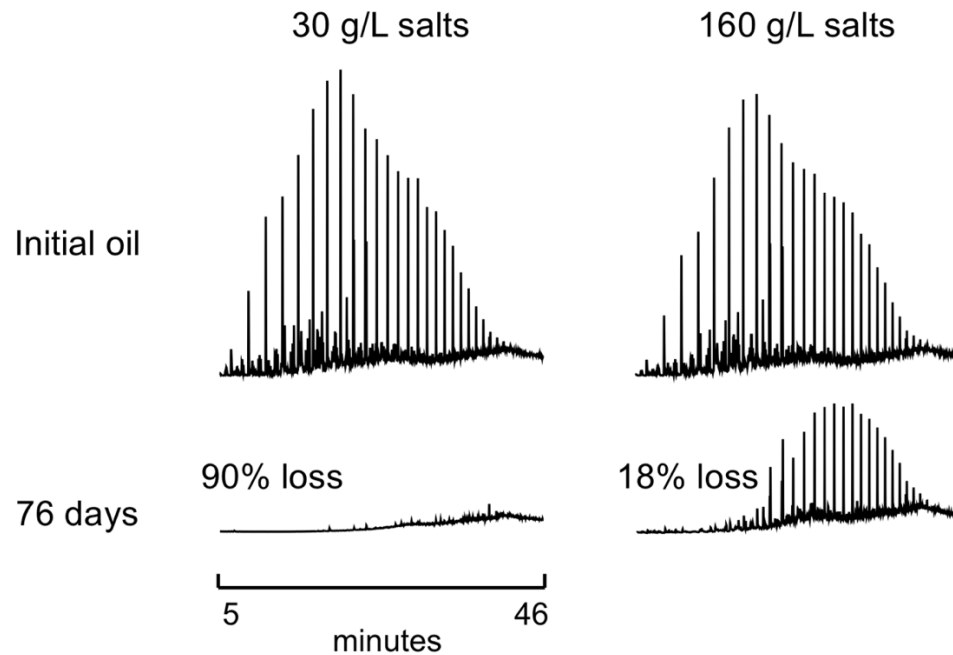


Figure 2.2 GC-MS profiles of a partially evaporated (12%) Atlantic Canada crude oil, incubated for 76 days, at salinities that might be encountered in a supratidal zone of an oiled shoreline. % loss is due to biodegradation, calculated from abiotic controls. Chromatograms normalized to hopane.

Source: (Abou Khalil et al., 2021b)

2.4.2 Brine Channels in Ice

Seawater separates in polar regions as it freezes, with the salt excluded as brine channels within the ice (Krembs et al., 2000). These brine channels typically contain thriving communities of algae and the organisms that graze on them (Arrigo et al., 2010), with examples of growth at temperatures as low as -13°C (Murray et al., 2012). As the Arctic Ocean becomes more amenable to transportation and oil exploration (Lasserre, 2014; Meier et al., 2014), it also becomes more vulnerable to marine accidents, mandating well-thought-out oil-spill response plans (Knol & Arbo, 2014; Garneau et al., 2016; Lewis & Prince, 2018). Spilled crude oil might become encapsulated in the sea ice as it forms, trapping it within the ice (Oggier et al., 2020). Fortunately, the brine pouches and channels are inhabited by microbial species, some of which degrade hydrocarbons (Ballesterro &

Magdol, 2011; Garneau et al., 2016; Brakstad et al., 2017). This phenomenon also occurs in lakes; strains of *Rhodobacter*, *Pseudomonas*, *Psychrobacter* and *Leifsonia* were isolated from brine lenses in three Antarctic lakes of the Northern Victoria Land, some of which were hydrocarbon-degraders (Rizzo et al., 2020). Biodegradation of oil occurs readily at -1 to -2°C (McFarlin et al., 2014; Garneau et al., 2016), although the process may be limited by the low availability of nutrients in such environments, and the low temperatures which increase crude oil's viscosity (Gleitz et al., 1995; Mohn & Stewart, 2000; Ballesterro & Magdol, 2011).

2.4.3 Hypersaline Frozen Soils

Transiently hypersaline soils are formed wherever soils freeze, generating hypersaline damp patches, which may themselves freeze if temperatures get low enough (Levy et al., 2012). Hydrocarbon and salt-contaminated soils frequently co-exist at drilling waste disposal sites and abandoned flare pits in cold regions around the globe; often the salt comes from the brine associated with the oil (Arocena & Rutherford, 2005), but all soils contain soluble components that are excluded as the water freezes. Numerous former and current Canadian Armed Forces sites in the Arctic have soil contaminated by Arctic diesel fuel (Whyte et al., 1999; Eriksson et al., 2001; Bell et al., 2013). The soils thaw for 1 to 2 months/year, and even in the summer, daily temperature fluctuations lead to alternating freezing and thawing of surface soils. Similarly, Antarctic soils are subject to hydrocarbon pollution and frequent freezing and thawing (Aislabie et al., 2004; Aislabie et al., 2006; Schafer et al., 2009). Hydrocarbons are degraded in Arctic Tundra soil above 0°C , and the process may be enhanced by daily freezing and thawing. Biodegradation is usually enhanced by adding nutrients such as nitrogen and phosphorus (Mohn & Stewart, 2000;

Eriksson et al., 2001), and there is some evidence that bioaugmentation may be effective (Mohn & Stewart, 2000; Abdulrasheed et al., 2020). Little work has appreciated the transient increase in salinity that occurs as soil moisture freezes, but it is clear that the organisms doing the effective degradation must at least tolerate such conditions. Chang et al. (2018) isolated halotolerant strains of diesel-degrading *Dietzia* from two oil-impacted sub-Arctic sites in Canada which tolerate up to 12.5% NaCl.

2.4.4 Brine and Oil Spills

Reservoir waters are entrained during oil extraction (Igunnu & Chen, 2014), and crude oil and natural gas production are often accompanied by large volumes of hypersaline water, predominantly as production nears its end. This water, known as produced water, contains a complex mixture of small volatile acids, dissolved aromatics, primarily BTEX (Benzene, Toluene, Ethylbenzene, and Xylenes) and Naphthalenes (i.e., parent and alkylated Naphthalene), along with some suspended oil droplets containing less soluble hydrocarbons (Birkle et al., 2009; Piubeli et al., 2012). Conventional initial treatment involves centrifugation and reinjection of the water into the subsurface, but some water remains entrained in the produced oil and eventually gets to processing stations or refineries. Treatment then relies primarily on the removal of suspended solids (grit, sand, large inorganic compounds, and some organic compounds) using physicochemical methods, followed by biological wastewater treatment systems to remove dissolved organics with indigenous halophilic hydrocarbon-degraders (Piubeli et al., 2012; Castillo-Carvajal et al., 2014; Igunnu & Chen, 2014). The brines in oil reservoirs are typically rich in divalent cations (Mg^{2+} and Ca^{2+}), and include inorganic nutrients (N and P) required for microbial growth (Bhupathiraju et al., 1993; Morrow et al., 1998). Bioaugmentation using

aromatic degrading halotolerant microbes isolated from hypersaline settings has been investigated (Bonfá et al., 2011). Amended systems reduced the chemical oxygen demand of hypersaline crude oil reservoir produced waters significantly beyond that achieved using standard hydrogen peroxide treatment alone. If hypersaline-produced water is accidentally discharged into the environment without prior treatment, it results in salt and hydrocarbon contamination of soil, and perhaps surface and groundwater (Halvorson & Lang, 1989; Leskiw et al., 2012). Conventional wisdom has been that the salt is more of an issue than the oil since the latter will degrade reasonably rapidly with mild biostimulation (National Research Council, 1993) while the salts will remain until they leach away. Displacing monovalent cations with divalent ones, such as Ca^{2+} in the form of gypsum ($\text{CaSO}_4 \cdot 2\text{H}_2\text{O}$), is one approach (Dornbusch et al., 2020), and adding organic matter such as hay can minimize gypsum requirements (Sublette et al., 2007), apparently by improving soil quality and porosity, facilitating salt leaching.

2.4.5 Oil Well Blowouts

Accidental oil well blowouts are fortunately rare events, but the largest spill in the US was likely the 1910 Lakeview Gusher in Kern County, California, from the Midway-Sunset field. The blowout produced an estimated 8.25 million barrels of oil over 544 days of uncontrolled flow (Sims & Frailing, 1950), but little sign of the spill remains. Occasionally such incidents occur in saline conditions; for example, Kuh-e-namak (mountain of salt), near Qom, Iran, has been polluted by hydrocarbons for nearly six decades due to the blowout of a crude oil well in the Alborz oil field in the 1960s (Jaafari, 1963). Despite a slow rate of natural biodegradation by extreme halophiles inhabiting the mountain's hypersaline soil, only a trace of contamination remains today (Hosseini et al., 2017).

2.5 Microbiology of Hydrocarbon Biodegradation at High Salinities

The biodegradation of crude oil and refined products in the sea (3 – 3.5% salinity) is well studied (Hazen et al., 2016; Prince et al., 2016b; Prince et al., 2017), but less is known about hydrocarbon fate at significantly higher salinities. The numerous environments where high salinity ecosystems are continuously or frequently exposed to hydrocarbons were described in Sections 2.3 and 2.4, and it is obvious that biodegradation must be contributing to the natural cleansing of such settings. Methane was included because, although it is not likely to be a direct anthropogenic contaminant, it is the simplest hydrocarbon, and methane monooxygenases are notoriously promiscuous (Hazen, 2018) and may contribute to the initial metabolism of other hydrocarbons. As previously discussed, methane has often been detected in hypersaline environments (Sokolov & Trotsenko, 1995; Heyer et al., 2005; Lin et al., 2005; Avrahamov et al., 2014). Furthermore, there has been insightful work on the use of halophilic organisms in treating hypersaline waste streams contaminated by hydrocarbons, such as produced water, which clearly work well (Bonfá et al., 2011; Fathepure, 2014; Jamal & Pugazhendi, 2018).

Table 2.2 lists described halophilic genera shown to biodegrade a range of aliphatic and aromatic hydrocarbons under high salinities. They are clustered in a few taxonomic classes, and all the bacteria have close relatives that grow in seawater on hydrocarbons. In contrast, the listed archaea are obligate hyper-halophiles, with few growing below 2 M (11.6% salt), while most prefer above 3 M NaCl (16.6% salt) (Vauclare et al., 2020), and they have relatives able to degrade a range of other substrates. All these isolates grow aerobically on hydrocarbons, and the identity of anaerobic halophilic hydrocarbon degraders remains unclear.

Table 2.2 Named Aliphatic and Aromatic Hydrocarbon-Degraders from Hypersaline Conditions (Continued)

Genus	Salinity (%)	Substrate	Reference
Kingdom Bacteria			
Order Corynebacteriales			
<i>Dietzia</i>	> 17	Diesel	Riis et al. (2003)
	15	Crude Oil	Borzenkov et al. (2006)
	0 – 12	Crude Oil	Chen et al. (2020)
<i>Gordonia</i>	15	Crude Oil	Borzenkov et al. (2006)
<i>Rhodococcus</i>	15	Crude Oil	Borzenkov et al. (2006)
	7.5	Hexadecane	de Carvalho (2012)
	6 – 9	Phenanthrene	Plotnikova et al. (2011)
Order Micrococcales			
<i>Cellulomonas</i>	> 17	Diesel	Riis et al. (2003)
<i>Arthrobacter</i>	6 – 9	Phenanthrene	Plotnikova et al. (2011)
Order Actinopolysporales			
<i>Actinopolyspora</i>	25	Crude Oil	Al-Mueini et al. (2007)
Order Streptomycetales			
<i>Streptomyces</i>	3–30	Crude Oil	Kuznetsov et al. (1992)
Order Bacillales			
<i>Bacillus</i>	> 17	Diesel	Riis et al. (2003)
	10	Crude Oil	Kumar et al. (2007)
	10	Crude Oil	Gudiña et al. (2012)
	6 – 9	Phenanthrene	Plotnikova et al. (2011)
<i>Geobacillus</i>	12	Crude Oil	Chamkha et al. (2008)
<i>Exiguobacterium</i>	0 – 12	Crude Oil	Cao et al. (2020)
Order Oceanospirillales			
<i>Halomonas</i>	> 17	Diesel	Riis et al. (2003)
	10	Crude Oil	Mnif et al. (2009)
	10	Crude Oil	Gargouri et al. (2012)
	20	Crude Oil	Biswas et al. (2015)
	3 – 20	Phenanthrene	Wang et al. (2018)
	10 – 20	Pyrene	Budiyanto et al. (2018)
	0 – 20	Naphthalene	Fang et al. (2016)
	1 – 15	Phenanthrene	Dastgheib et al. (2012)
	2 – 10	Crude Oil	Neifar et al. (2019)
<i>Alcanivorax</i>	3 – 15	Benzene	Hassan et al. (2012)
Order Pseudomonadales			
<i>Pseudomonas</i>	15	Crude Oil	Borzenkov et al. (2006)
	10	Crude Oil	Mnif et al. (2009)
	6 – 9	Phenanthrene	Plotnikova et al. (2011)
	7	BTEX	Hassan and Aly (2018)
Order Rhodospirillales			
<i>Thalassospira</i>	1 – 20	Pyrene	Zhou et al. (2016)
Order Rhizobiales			
<i>Ochrobactrum</i>	4 – 16	Fluorene	Jamal and Pugazhendi (2018)
<i>Mesorhizobium</i>	4 – 16	Fluorene	Jamal and Pugazhendi (2018)
Order Salinisphaerales			
<i>Salinisphaera</i>	10	Dodecane	Antunes et al. (2011)

Table 2.2 (Continued) Named Aliphatic and Aromatic Hydrocarbon-Degraders from Hypersaline Conditions

Order Pseudomonadales			
<i>Acinetobacter</i>	0 – 7	Alkanes	Dahal et al. (2017)
	0 – 12	Crude Oil	Chen et al. (2020)
Order Alteromonadales			
<i>Marinobacter</i>	4.6 – 20	Crude Oil	Gauthier et al. (1992)
	3 – 29	Crude Oil	Al-Mailem et al. (2013)
	3 – 15	BTEX	Berlendis et al. (2010)
	1 – 15	Phenanthrene	Dastgheib et al. (2012)
	3 – 29	Crude Oil	Al-Mailem et al. (2013)
	0 – 20	Naphthalene	Fang et al. (2016)
	3 – 20	Phenanthrene	Wang et al. (2018)
Order Methylococcales			
<i>Methylohalobius</i>	1 – 15	Methane	Heyer et al. (2005)
Order Bacteroidetes			
<i>Salinibacter</i>	31	Crude Oil	Corsellis et al. (2016)
Order Burkholderiales			
<i>Delftia</i>	3 – 30	Diesel	Lenchi et al. (2020)
<i>Achromobacter</i>	4 – 16	Fluorene	Jamal and Pugazhendi (2018)
Order Xanthomonadales			
<i>Stenotrophomonas</i>	4 – 16	Fluorene	Jamal and Pugazhendi (2018)
Kingdom Archaea			
Order Halobacteriales			
<i>Haloarcula</i>	> 20	Crude Oil	Bertrand et al. (1990)
	> 22	Heptadecane and Phenanthrene	Tapilatu et al. (2010)
	20	Mixture of PAHs*	Erdoğan et al. (2013)
<i>Halobacterium</i>	29	Crude Oil	Kulichevskaya et al. (1991)
	> 26	Crude Oil	Al-Mailem et al. (2010)
Order Haloferacales			
<i>Haloferax</i>	> 22	Heptadecane and Phenanthrene	Tapilatu et al. (2010)
	20	Mixture of PAHs*	Bonfá et al. (2011)
	> 26	Crude Oil	Al-Mailem et al. (2010)
<i>Halorubrum</i>	20	Mixture of PAHs*	Erdoğan et al. (2013)
Order Natrilabales			
<i>Natrialba</i>	> 20	Pyrene	Khemili-Talbi et al. (2015)
Kingdom Fungi			
Order Hypocreales			
<i>Fusarium</i>	5 – 10	Crude Oil	Obuekwe et al. (2005)
Order Pleosporales			
<i>Drechslera</i>	5 – 10	Crude Oil	Obuekwe et al. (2005)
Order Micosphaerellales			
<i>Hortaea</i>	10	Phenanthrene	Kristanti et al. (2018)

*Polycyclic Aromatic Hydrocarbon

The early work by Ward and Brock (1978) was perhaps the first to show that high salinity slowed hydrocarbon biodegradation, and Figures 2.1 and 2.2 confirm this effect,

even in environments long exposed to high salt (Utah's Great Salt Lake, Figure 2.1). The experiment of Figure 2.2 used seawater as the inoculum, but even these microbes are occasionally exposed to high salt if they spend any time on the upper-intertidal or supratidal shorelines. Why is biodegradation so slow? Clearly, the nutrient and hydrocarbon concentrations in Figures 2.1 and 2.2 were adequate for faster biodegradation at lower salinity, so it must be linked to the higher salt concentrations. Yet hyper-halophiles growing on other substrates do not necessarily grow slowly at high salinities. For example, *Halobacterium* growing on rich nutrient broth has doubling times of < 4 hours over a range of salinities from 3 – 5 M NaCl (17 – 29%) (Rodriguez-Valera et al., 1983; Chandler & McMeekin, 1989). The Gammaproteobacterium *Halomonas* grows in salinities ranging from 1 – 32.5% (Vreeland, 2015), and requires external organic solutes to maintain its osmotic strength at high salinity, but grows quite rapidly in their presence; doubling every 10 hr at 3.5 M NaCl (19% salt) (Cummings & Gilmour, 1995). The slow rates of hydrocarbon biodegradation under hypersaline conditions thus seem determined by the metabolism of the substrate (potentially including uptake, intracellular transport, and enzyme activities) rather than more global effects of salinity on growth. Arulazhagan and Vasudevan (2011) realized that the addition of yeast extract significantly enhanced the biodegradation of PAHs by an *Ochrobactrum* at a salinity two-fold higher than seawater. On the other hand, it is possible that laboratory strains selected for active growth in the laboratory may only represent a very minor fraction of the active hydrocarbon-degrading hypersaline community, which naturally grows very slowly because there is no competitive pressure for faster growth. There have been attempts to stimulate halophilic biodegradation by adding nutrients, vitamins, or minerals with mild success (Al-Mailem et al., 2013; Al-

Mailem et al., 2014; Al-Mailem et al., 2017), but even the highest rates yet seen above about 10% salt are very slow compared to the rates seen in seawater (Prince et al., 2017).

In some cases, oil biodegradation is not desired, such as in oil reservoirs and oil storage salt caverns. Of course, it is too late to prevent oil biodegradation that has already occurred, but the ability to accurately predict whether a newly discovered oil reservoir likely has suffered extensive biodegradation could potentially save the enormous investment that would be wasted on an uneconomic oil well. Even though new biodegradation of a recently discovered reservoir would be unlikely to change the economic value of the oil, the other effects of biodegradation, such as souring (the production of H₂S) or corrosion, can be very expensive (Ibrahim et al., 2018), and predicting their likelihood would be a valuable tool in understanding the overall economics of a new discovery. As for oil biodegradation in salt caverns, biocides (Johnson et al., 2017; Jia et al., 2019) are the most widely used treatment for inhibition (Raczkowski et al., 2004), but a better understanding of the microbiology responsible might lead to more ecologically-driven responses. For example, nitrate is frequently injected with reservoir injection water to raise the ambient redox potential so that sulfate-reducing bacteria cannot thrive (Dolfing & Hubert, 2017) and similar approaches might help preserve oil in storage.

CHAPTER 3

BIODEGRADATION OF CRUDE OIL IN HYPERSALINE SEAWATER

3.1 Objectives of the Experiment

As discussed in Chapter 2, several studies have clearly shown that hydrocarbon biodegradation can occur in hypersaline coastal ecosystems. However, most of the data were obtained using isolated strains which might not represent the natural *in-situ* oil biodegradation in contaminated shorelines by the indigenous seawater microorganisms. Therefore, to understand the impact of salinity on the hydrocarbonoclastic activity in such transient hypersaline settings, oil biodegradation was investigated using a natural inoculum (seawater) at different salinities. Other features in supratidal and upper intertidal zones, such as the degree of saturation and oil thickness, were not investigated in this experiment. In addition, the effect of high salinities on hydrocarbon evaporation due to “salting out” – reduction in aqueous solubility of neutral solutes in the presence of dissolved ions (Oh et al., 2013) – was analyzed using sterile experiments to dissociate between biotic and abiotic hydrocarbon removal. Furthermore, a metataxonomic analysis was conducted to see whether the high salinity conditions enriched rare organisms in the seawater or negatively impacted the indigenous microbial community’s activity.

3.2 Material and Methods

3.2.1 Seawater Sampling and Evaporation

Seawater (100 L, salinity = 28.5 g/L) was collected from the Manasquan Inlet, New Jersey, USA (40.1021° N – 74.0332° W) and promptly placed in a 150 L rectangular glass tank. For gentle mixing, aeration was performed by submerging a perforated Tygon tube

connected to an aerator (Figure 3.1-a). A space heater was used to increase the surrounding temperature up to 25 – 28°C, encouraging slow evaporation.



3.1 Pictures taken during the experiment of the (a) seawater being gently evaporated in a glass tank, (b) concentrated brine being mixed at 100 rpm using a magnetic stirrer, and (c) seawater and sterile microcosms.

After 40 days, the seawater had lost approximately 90% of its volume, and solids were observed at the bottom of the tank, explaining why the measured salinity was lower than the expected salinity during the last two weeks of evaporation (Figure 3.2). The concentrated brine and the settled solids were placed in a 20 L glass jar and mixed for 24 hours using a magnetic stirrer at 100 rpm (Figure 3.1-b). The concentrated brine was then left stagnant for one hour to allow the settling of non-dissolved solids.

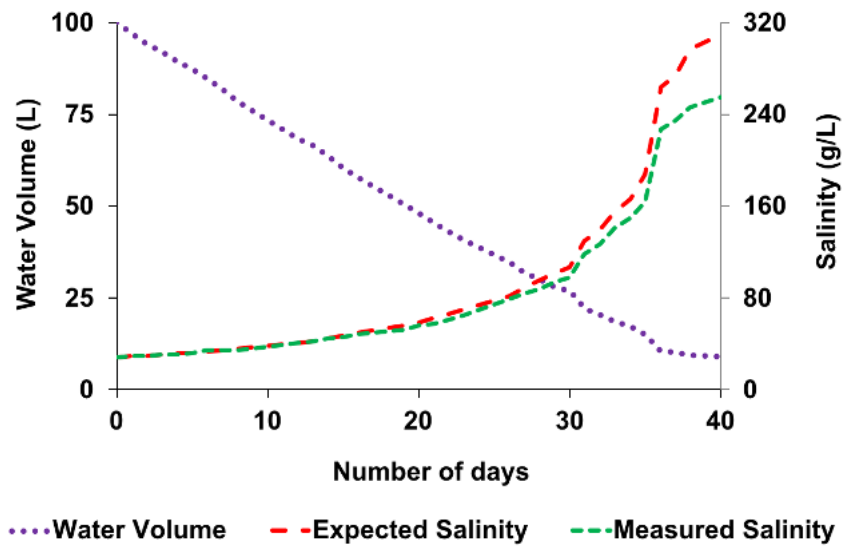


Figure 3.2 Salinity variation during the evaporation of seawater. Expected salinity was deduced from the volume of seawater remaining and the initial salinity. The actual salinity was determined by measuring the total dissolved solid content.

Salinity was measured by determining the total dissolved solid content using standard method 2540D (APHA et al., 2017), pH was measured using a pH meter (Aqua Shock, Sper Scientific, 850056), and nutrients were measured through spectrophotometry (ultra-vis spectrophotometer, Cole-Parmer, 4802) using Low Range Hach reagents (HACH Company, Loveland, Colorado). The concentrated brine had a salinity of 255 g/L (Figure 3.2), a pH of 8.2, and a nutrient concentration of 19.2 mg/L N for $\text{NO}_3^- + \text{NO}_2^-$ and 4.1 mg/L P for PO_3^{4-} . Concomitantly, a batch of fresh seawater (salinity = 29.2 g/L, pH = 7.8,

$\text{NO}_3^- + \text{NO}_2^- = 1.2 \text{ N mg/L}$, $\text{PO}_3^{4-} = 0.3 \text{ P mg/L}$) was collected from the same location, and then promptly used with the concentrated brine to set-up the microcosms.

3.2.2 Experimental Setup

Three seawater blends (live blends) were prepared by mixing concentrated brine with the fresh seawater to increase the salinity up to 30, 90, and 160 g/L. The seawater to concentrated brine ratios were about 99:1, 73:27, and 42:58 for the 30, 90, and 160 g/L blends, respectively. The microcosms were prepared in 250 mL capped but not sealed flasks (GL 45 Media Bottle, Blue Polypropylene Cap) filled with the live blends up to 200 mL. These microcosms were prepared in two identical series; one (Batch 1) was used to analyze the oil and the other (Batch 2) for conducting the microbial analyses. Concomitantly, a sterile control experiment (Batch 3), which used three artificial saline mixtures made by mixing Milli-Q water with sea salt (Pentair Aquatic Eco-Systems INC IS160) to achieve the same salinities (30, 90, and 160 g/L), was poisoned with mercuric chloride (50 mg/L) to halt any microbial activity and obtain sterile blends. Hibernia crude oil, which is a light oil (gravity of 34.1° API, sulfur content of 0.56 wt %) obtained from the Hibernia sandstone formation (ExxonMobil, 2018), was artificially weathered in a hood for 24 hours (12% loss by weight) to mimic the condition of stranded oil on beaches. The live and sterile microcosms (Batches 1, 2, and 3) were contaminated with the artificially weathered oil at a concentration of 50 $\mu\text{L/L}$ using a positive displacement pipette and then shaken vigorously for one minute to generate small oil droplets. An additional set of microcosms (Batch 4) was prepared using the live blends, but without adding oil to compare the abundance and diversity of the indigenous seawater microbial communities with and without petroleum hydrocarbons. The experimental flasks of all four batches were

prepared in triplicates and harvested at 0, 8, 16, 38, and 76 days. The microcosms were placed in a room (Figure 3.1-c) with an average temperature of 20°C, which corresponds to the average annual temperature of many beaches, such as the ones that were contaminated by the Macondo oil from the *Deepwater Horizon* blowout (Geng & Boufadel, 2017). Figure 3.3 provides a flowchart of the experimental design.

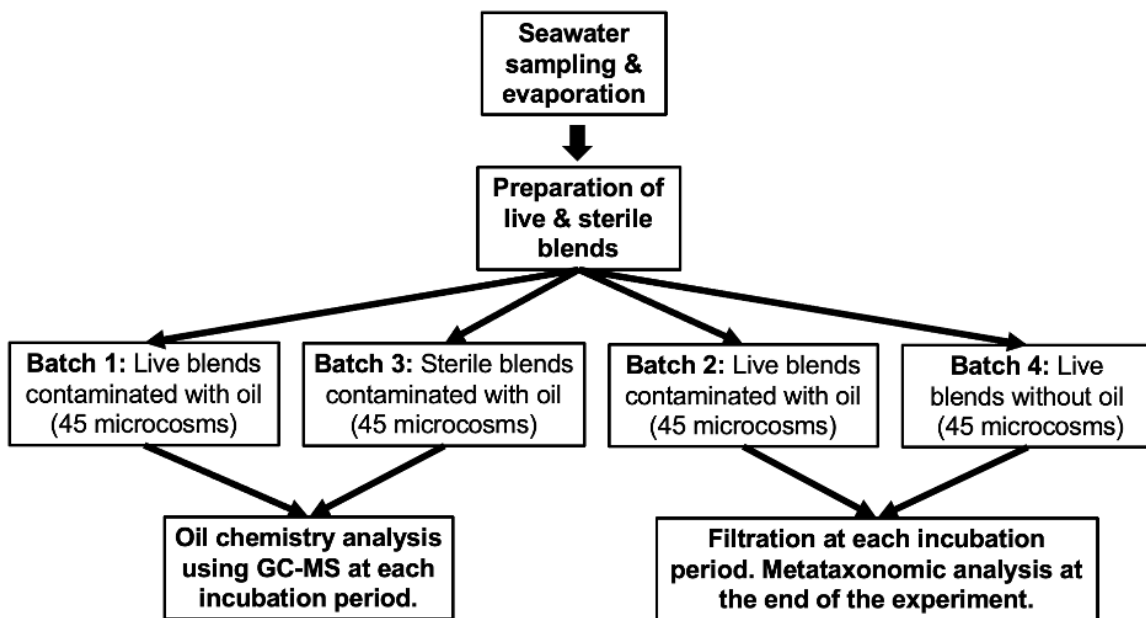


Figure 3.3 Flowchart of the experimental design. Note that the oil chemistry analysis was conducted at each incubation period, while the Metataxonomic analysis was conducted at the end of the experiment (76 days).

3.2.3 Extraction and GC-MS Analysis

After each incubation period, the dissolved oxygen concentration in microcosms of batches 1 and 3 was measured (CHEMets visual kit, K-7512), then the oil was extracted (three times) with methylene chloride. After extraction, the samples were dried by adding anhydrous sodium sulfate and finally evaporated (under a gentle nitrogen purge) to approximately 350 μ L, with care not to evaporate to dryness. Subsequently, GC-MS (Gas Chromatography-Mass Spectrometry, Model# 5973N, Benchtop GC having a 30 m X 0.25

mm ID film column db-5ms, Millipore Sigma) was used to analyze the extracted oil, along with appropriate standard samples (10 µL of the artificially weathered Hibernia oil per mL of methylene chloride) before and after each run. Hydrocarbon removal was assessed using hopane as a conserved internal standard (Prince et al., 1994).

3.2.4 Filtration of Microcosms

The contents of microcosms of batches 2 and 4 were filtered onto 0.2 µm polyethersulfone hydrophilic filters (Fisher Scientific, Ottawa, ON), using a Gast Vacuum pump (Fisher Model#: 0211-V45F-G8CX), and autoclaved filtration units. After filtration, the filters were immediately inserted into 15 mL sterile screw-cap tubes and stored in a freezer at -20°C. The filtration units were rinsed between individual filtrations with sterile artificial seawater and then sterile water using autoclavable squeeze bottles. At the end of the experimental period (76 days), the samples were shipped overnight in a cooler with dry ice to McGill University to conduct the microbial diversity analyses.

3.2.5 Metataxonomics

DNA Extraction and Purification. Nucleic acids were recovered using a modified version of the hexadecyl trimethyl ammonium bromide method described in Oh et al. (2013). DNA samples were treated with RNase If (New England Biolabs, Whitby, ON), purified using a 1:1 volume ratio of magnetic beads from the Macherey-Nagel NucleoMag NGS Clean-up and Size Select kit (D-MARK Biosciences, Toronto, ON), then quantified using the Quant-iT PicoGreen assay from Fisher Scientific Ltd. (Edmonton, AB).

Preparation of 16S rRNA Gene Amplicon Libraries and Sequencing. The 16S 515F-Y/926R primer pair covering the V4 and V5 hyper-variable regions of the 16S rRNA gene was used to characterize the microbial composition and diversity in each sample. These

primers, which can detect both archaea and bacteria, are as follows: 515F-Y (5'GTGYCAGCMGCCGCGGTAA-3') and 926R (5'-CCGYCAATTYMTTTRAGTTT-3'). The 16S rRNA gene amplicon libraries for sequencing were prepared according to Illumina's "16S Metagenomic Sequencing Library Preparation" guide (Part # 15044223 Rev. B). Amplification of the DNA was performed with the Kapa HiFi HS Ready Mix polymerase (Roche, Laval, QC) as follows: reactions were performed in 25 μ L volumes containing 12.5 μ L of Ready Mix buffer and enzyme (0.3 mM of each dNTP, 2.5 mM MgCl₂, 0.5 U of Kapa HiFi HS polymerase), 5–25 ng of DNA, 0.6 μ M of each primer, and 0.5 mg/mL of Bovine Serum Albumin (BSA). PCR amplification conditions involved an initial denaturation at 95°C for 3 min, followed by 25 cycles of 30 sec at 95°C, 30 sec at 55°C, and 30 sec at 72°C. The final elongation step was conducted for 5 min at 72°C. PCR products were evaluated by gel electrophoresis on a 2% agarose gel with SYBR Safe (Fisher Scientific, Ottawa, ON) and purified using a 1:0.8 volume ratio of the Macherey-Nagel NucleoMag NGS Clean-up and Size Select kit (D-MARK Biosciences). Index PCR was performed with 5 μ L of purified PCR product, 2 μ M of index primers, and the Kapa HiFi HS Ready Mix polymerase as described above. PCR amplification conditions included an initial denaturation at 95°C for 3 min, followed by eight cycles of 30 sec at 95°C, 30 sec at 55°C, and 30 sec at 72°C. The final elongation step was conducted for 5 min at 72°C. PCR amplicons were purified as described above, then quantified using the Quant-iT PicoGreen assay (Fisher Scientific). Equal amounts of each indexed PCR product were pooled and diluted. Pooled samples were loaded onto an Illumina MiSeq and sequenced using a 500-cycle MiSeq Reagent Kit v2 Illumina (San Diego, CA, USA).

Bioinformatics Analysis of 16S rRNA Gene Amplicon Sequence Data. Sequencing data were analyzed using AmpliconTagger (Oh et al., 2013). Briefly, raw reads were trimmed for sequencing adapters and PhiX spike-in sequences, and the remaining reads were assembled using their common overlapping part with FLASH (Oh et al., 2013). Primer sequences were removed from merged sequences and remaining sequences were filtered for quality; sequences having an average quality (Phred) score lower than 27 or more than 1 undefined base (N) or more than ten bases lower than quality score 15 were discarded. The remaining sequences were processed with DADA2 (v.1.12.1) (Oh et al., 2013) to generate Amplicon Sequence Variants (ASVs). ASV chimeras were removed with DADA2's internal removeBimeraDeNovo (method = 'consensus') method followed by UCHIME reference (Oh et al., 2013). The ASVs having abundances lower than five were discarded and the remaining ASVs were then assigned a taxonomic lineage with the RDP classifier (Oh et al., 2013) using the AmpliconTagger 16S training set ([DOI:10.5281/zenodo.3560150](https://doi.org/10.5281/zenodo.3560150)). The RDP classifier gives a score (0 to 1) to each taxonomic depth of each ASV. Each taxonomic depth having a score ≥ 0.5 was kept to reconstruct the final lineage. Taxonomic lineages were combined with the cluster abundance matrix obtained above to generate a raw ASV table, from which an ASV table containing only bacteria was generated. Five hundred 1,000 read rarefactions were then performed on this ASV table. The average number of reads of each ASV for every sample was then computed to obtain a consensus rarefied ASV table. A multiple sequence alignment was obtained by aligning ASV sequences on a Greengenes core reference alignment using the PyNAST v1.2.2 aligner (Oh et al., 2013). Alignments were filtered to keep only the hypervariable region of the alignment. A phylogenetic tree was built from

that alignment with FastTree v2.1.10 (Oh et al., 2013). Alpha diversity metrics and taxonomic summaries were computed using the QIIME v1.9.1 software suite (Oh et al., 2013) using the consensus rarefied ASV table and phylogenetic tree (i.e., for UniFrac distance matrix generation).

3.3 Results

3.3.1 Sterile Control Experiment

Figure 3.4 shows the GC-MS total ion traces of sterile experiments along with the respective % loss of hydrocarbons. The evaporation rate of hydrocarbons was subtly higher at elevated salinities, presumably due to the “salting out” effect expected from Henry’s Law; at a salinity of 160 g/L, the abiotic loss of hydrocarbons after 76 days was 36% higher than the loss from unamended seawater.

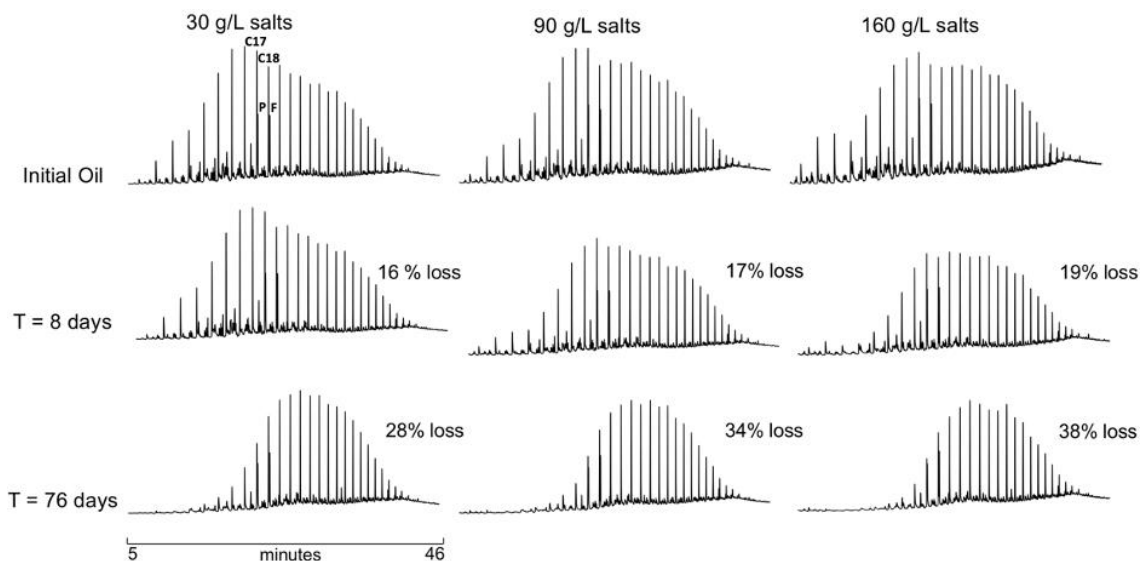


Figure 3.4 GC-MS profiles of crude oil remaining after 8 and 76 days of incubation under sterile conditions: % loss represents abiotic removal, and chromatograms are normalized to hopane. P and F represent Pristane and Phytane, respectively.

3.3.2 Biodegradation of Hydrocarbons

Dissolved oxygen levels were above 5 mg/L during the entire experimental period for all salinities, indicating favorable aerobic conditions where oil biodegradation can be sufficiently supported (Chiang et al., 1989; Michaelsen et al., 1992). Figure 3.5 displays the GC-MS traces of oil remaining in microcosms after 8 and 76 days of incubation. Note that the % loss represents the loss due to both biodegradation and evaporation. Figure 3.6 shows the percentage of oil remaining, due to biodegradation only (deduced from live and sterile data), at different salinities.

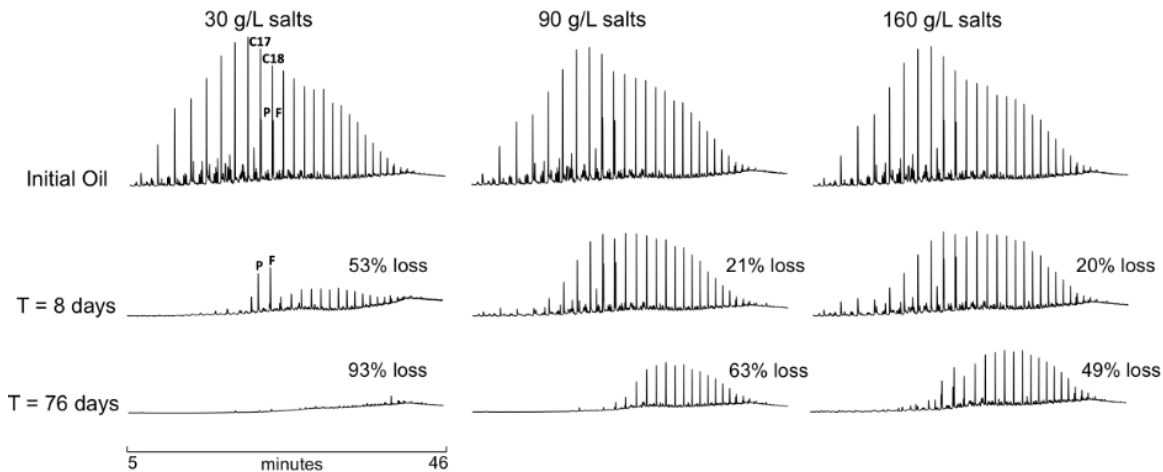


Figure 3.5 GC-MS profiles of crude oil remaining after 8 and 76 days of incubation: % loss represents both biodegradation and evaporation, and chromatograms are normalized to hopane. P and F represent Pristane and Phytane, respectively.

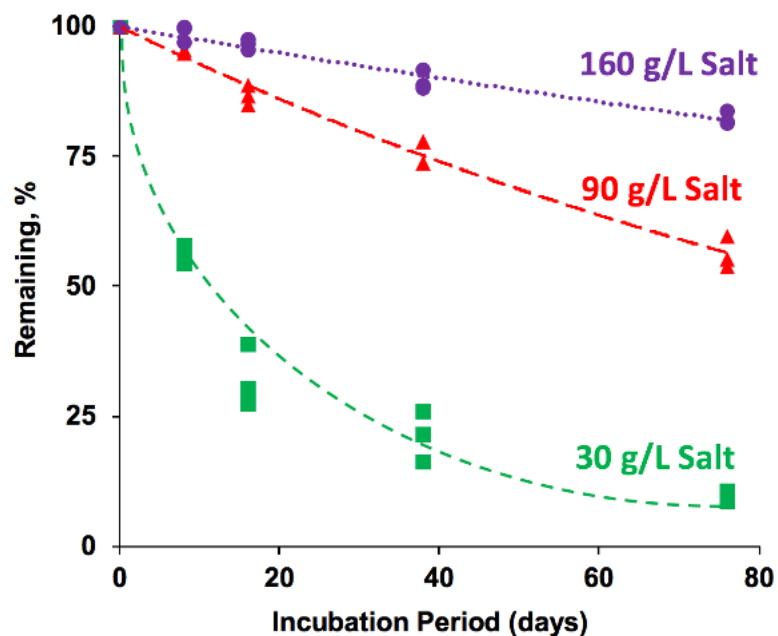


Figure 3.6 The % remaining of the GC-detectable hydrocarbons, derived from the sterile and live data to solely show the effect of biodegradation. Note that there are three measurements at every incubation period and salinity since the microcosms were prepared in triplicates.

As expected, the biodegradation of hydrocarbons (Figures 3.5 to 3.8) was extensive in natural seawater (30 g/L), and most of the alkanes were degraded within 8 days (Prince et al., 2013; Prince et al., 2016b; Wang et al., 2016; Zhuang et al., 2016; Olson et al., 2017; Prince et al., 2017; Brakstad et al., 2018; Ribicic et al., 2018). As anticipated (Pirnik et al., 1974; Prince et al., 2007; Prince et al., 2016b), the biodegradation rate of pristane and phytane (both branched alkanes), which are the two highest peaks at $t = 8$ days in 30 g/L salt, was slower, but they were completely consumed within 38 days (Figure 3.5). This was not the case at salinities three to five-fold higher than seawater, where the branched (pristane and phytane) and large ($> C_{20}$) alkanes were still present even after 76 days.

The biodegradation of phenanthrene (P) and its alkylated congeners (up to those with the equivalent of two methyl substituents, C1-P and C2-P) was almost complete within 38 days at a salinity of 30 g/L (Figure 3.8), which is in agreement with the literature

(Prince et al., 2013; Prince et al., 2016b; Prince et al., 2017). This was not the case at higher salinities, where the phenanthrenes (parent and alkylated) partly remained in the oil, even after 76 days. Partial degradation of benz[*a*]anthracene (Baa) and chrysene (Chr) – the most abundant 4-ring aromatics in crude oil – and chrysene’s alkylated congeners (up to those with the equivalent of two methyl substituents, C1-Chr and C2-Chr) was observed at all three salinities, and again losses were lower as salinity increased (Table 3.1, Figure 3.8).

Table 3.1 displays the apparent first-order rate constant (*k*) and half-life ($t_{1/2}$) of selected analytes at the three salinities, and Figures 3.7 and 3.8 illustrate the apparent first-order rate constants of individual hydrocarbons. Note that Table 3.1 and Figures 3.7 and 3.8 represent only the effect of biodegradation derived from the sterile and live data. Interestingly, the half-life of the alkanes was more affected at high salt than the polycyclic aromatic hydrocarbons (PAHs), especially the large ones such as the alkylated phenanthrenes (C3-P and C4-P) and the four-ring PAHs – Baa + Chr and their alkylated congeners (C1-Chr and C2-Chr). Small alkanes (< C16) could have mostly been lost by evaporation, and thus, are not reported. Alkanes from C16 to C19 were also subject to evaporation (Figure 3.4), but biodegradation was the major contributor to their removal in the active incubations. Similarly, some PAHs such as naphthalenes, fluorenes, phenanthrenes (P and C1-P), and dibenzothiophenes (D and C1-D) showed some evidence of evaporation, especially at high salt, but biodegradation was more important.

Table 3.1 Apparent First-order Rate Constant and Half-life of Measurable Analytes at Different Salinities

Analyte	Initial Concentration (µg/L)	Salinity								
		30 g/L			90 g/L			160 g/L		
		t _{1/2} (d)	k (d ⁻¹)	R ²	t _{1/2} (d)	k (d ⁻¹)	R ²	t _{1/2} (d)	k (d ⁻¹)	R ²
n-16	173.8	3.3	0.209	0.046	18.2	0.038	0.940	21.0	0.033	0.864
n-17	224.3	3.3	0.213	0.103	21.0	0.033	0.937	24.8	0.028	0.878
Pristane	82.5	17.8	0.039	0.983	46.2	0.015	0.926	57.8	0.012	0.857
n-18	129.9	3.7	0.185	0.757	26.7	0.026	0.936	33.0	0.021	0.899
Phytane	90.7	19.3	0.036	0.972	63.0	0.011	0.870	138.6	0.005	0.635
n-19	138.0	3.8	0.184	0.761	33.0	0.021	0.869	38.5	0.018	0.876
n-20	133.3	5.1	0.136	0.890	49.5	0.014	0.819	53.3	0.013	0.860
n-21	109.7	5.3	0.131	0.857	63.0	0.011	0.856	63.0	0.011	0.855
n-22	103.8	5.4	0.129	0.848	69.3	0.010	0.771	77.0	0.009	0.751
n-23	108.2	5.4	0.129	0.840	77.0	0.009	0.621	86.6	0.008	0.670
n-24	104.5	15.4	0.045	0.863	77.0	0.009	0.582	86.6	0.008	0.909
n-25	101.5	18.7	0.037	0.822	77.0	0.009	0.628	99.0	0.007	0.740
n-26	107.5	18.7	0.037	0.793	86.6	0.008	0.514	99.0	0.007	0.633
n-27	107.9	18.2	0.038	0.756	99.0	0.007	0.329	138.6	0.005	0.633
n-28	106.6	19.8	0.035	0.689	99.0	0.007	0.807	138.6	0.005	0.517
n-29	111.3	20.4	0.034	0.660	115.5	0.006	0.765	173.3	0.004	0.645
n-30	87.4	21.7	0.032	0.673	115.5	0.006	0.746	173.3	0.004	0.419
N	0.7	3.3	0.210	0.432	3.4	0.206	0.520	6.7	0.104	0.734
C1-N	10.0	2.4	0.292	0.489	4.7	0.147	0.721	16.9	0.041	0.918
C2-N	28.4	3.1	0.224	0.113	12.4	0.056	0.908	24.8	0.028	0.140
C3-N	32.0	4.3	0.163	0.750	21.0	0.033	0.778	30.1	0.023	0.306
C4-N	18.0	5.4	0.128	0.940	31.5	0.022	0.625	36.5	0.019	0.596
F	5.6	2.5	0.275	0.460	5.2	0.134	0.758	30.1	0.023	0.113
C1-F	9.7	4.7	0.146	0.722	24.8	0.028	0.978	46.2	0.015	0.676
C2-F	12.6	4.7	0.147	0.758	49.5	0.014	0.735	57.8	0.012	0.702
C3-F	8.9	6.9	0.100	0.819	57.8	0.009	0.034	77.0	0.009	0.687
P	10.3	4.7	0.146	0.732	20.4	0.034	0.193	34.7	0.020	0.320
C1-P	26.8	4.3	0.160	0.753	53.3	0.013	0.930	77.0	0.009	0.517
C2-P	26.0	16.1	0.043	0.941	115.5	0.006	0.186	138.6	0.005	0.634
C3-P	16.8	40.8	0.017	0.909	115.5	0.006	0.494	138.6	0.005	0.102
C4-P	10.8	49.5	0.014	0.122	138.6	0.005	0.533	173.3	0.004	0.863
D	7.4	4.5	0.155	0.064	31.5	0.022	0.756	38.5	0.018	0.728
C1-D	12.3	4.7	0.147	0.753	33.0	0.021	0.922	63.0	0.011	0.781
C2-D	14.2	6.7	0.104	0.811	99.0	0.007	0.120	115.5	0.006	0.120
C3-D	11.2	34.7	0.020	0.880	138.6	0.005	0.516	173.3	0.004	0.309
Chr-Baa	2.8	53.3	0.013	0.401	99.0	0.007	0.674	138.6	0.005	0.396
C1-Chr	4.1	57.8	0.012	0.708	99.0	0.007	0.703	115.5	0.006	0.377
C2-Chr	5.8	63.0	0.011	0.577	173.3	0.004	0.513	173.3	0.004	0.726

Note: N = Naphthalene; F = Fluorene; P = Phenanthrene; D = Dibenzothiophene; Chr = Chrysene; Baa = Benz[*a*]anthracene. C-1, C-2 etc. indicate alkylation of the parent aromatics by 1, 2, etc. methyl-equivalents.

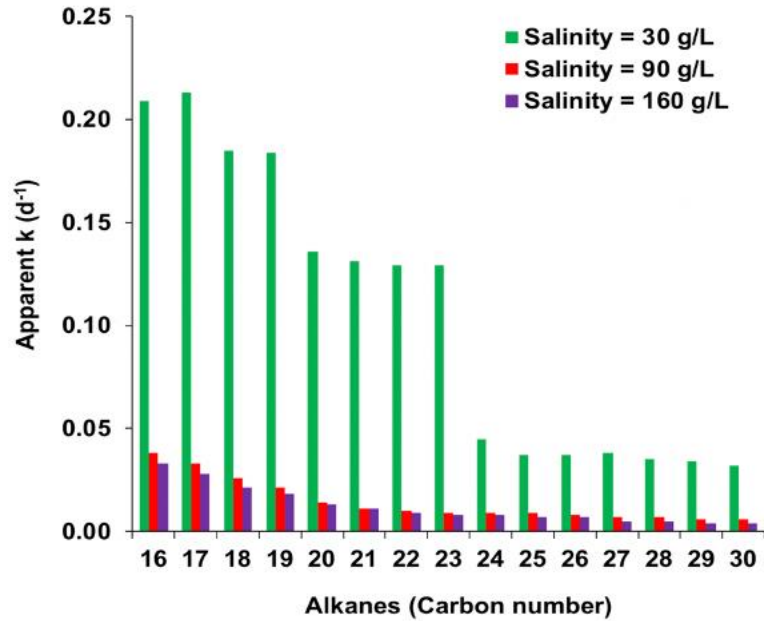


Figure 3.7 Apparent first-order rate constants at different salinities of measurable alkanes from carbon number 16 (n-hexadecane) to carbon number 30 (n-triacontane).

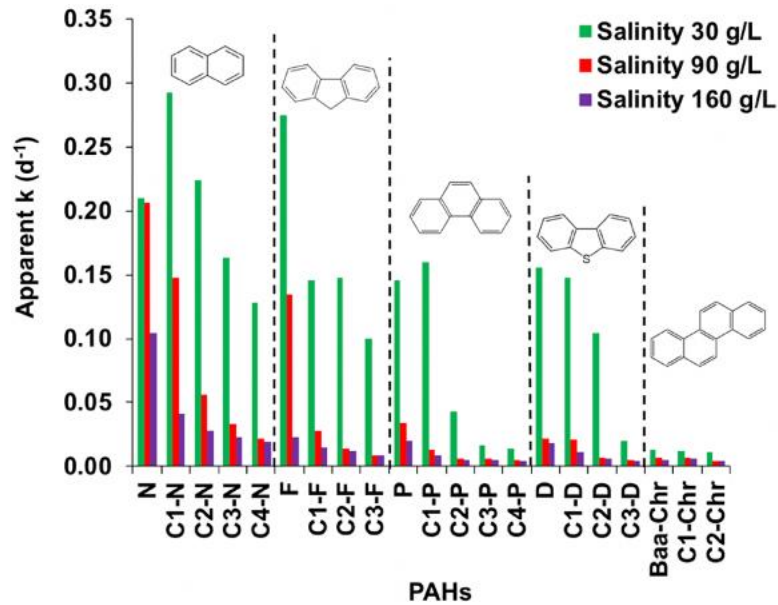


Figure 3.8 Apparent first-order rate constants at different salinities of measurable PAHs: Parent and alkylated naphthalenes (N), fluorenes (F), phenanthrenes (P), dibenzothiophenes (D), benz[a]anthracene (Baa), and chrysenes (Chr), with C1-N indicating the sum of all methyl naphthalenes, C2-N indicating the sum of all dimethyl and ethyl naphthalenes, etc.

3.3.3 Microbial Populations in Microcosms

Microbial diversity decreased as salinity increased and with the presence of oil, although the effect of oil was relatively minor (Figure 3.9). There was little change in the microbial diversity over time, except in the non-oiled 30 g/L salinity microcosms, where the diversity notably increased during the first 16 days of incubation (Figure 3.10). This may have been related to an input of carbon from the concentrated salt inoculum that stimulated the growth of some members of the microbial community, but which were negatively affected by the presence of oil. Principal coordinate analysis (PCoA) of the total ASVs (equivalent to individual organisms) showed that there were three distinct clusters of the microbial communities at $t = 0$ based on the starting salt concentration (Figure 3.11-b). At 30 g/L salt, the communities tended to be more diffuse but remained on the left side of the plot, indicating that the salinity was a larger driver and differences were more based on the presence or absence of oil (Figure 3.11-a) and on the incubation time (Figure 3.11-b). These communities became more closely related at the later incubation times (38 and 76 days). At higher salinities (90 and 160 g/L), the clustering of the microbial communities tended to be much tighter and the separation was more affected by the incubation time than by the presence or absence of oil. These results suggest that, at the later incubation times, the salinity was much more of a driver in the microbial diversity than the presence or absence of oil.

The taxonomic profiles of the 20 most abundant genera identified in the microcosms at all three salinities, with and without oil and at different incubation periods, showed significant differences based on salinity, oil, and incubation time (Figure 3.12). At $t = 0$, extreme halotolerant microorganisms, which were previously observed in

hydrocarbon-contaminated ecosystems (*Marivita* and *Marinobacter* (Prince et al., 2013; Prince et al., 2016b; Prince et al., 2017), dominated the high salinity microcosms (Figure 3.13), indicating that such genera were capable of surviving the extremely hypersaline conditions (255 g/L salt) of the concentrated brine.

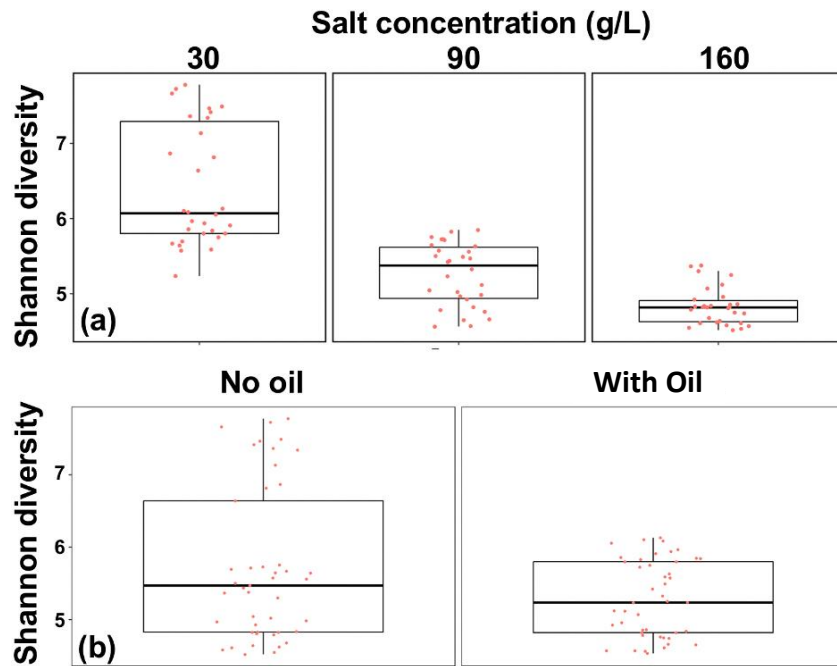


Figure 3.9 Bacterial alpha diversity in microcosms (a) at different salinities and (b) in the absence (No Oil) and presence of oil.

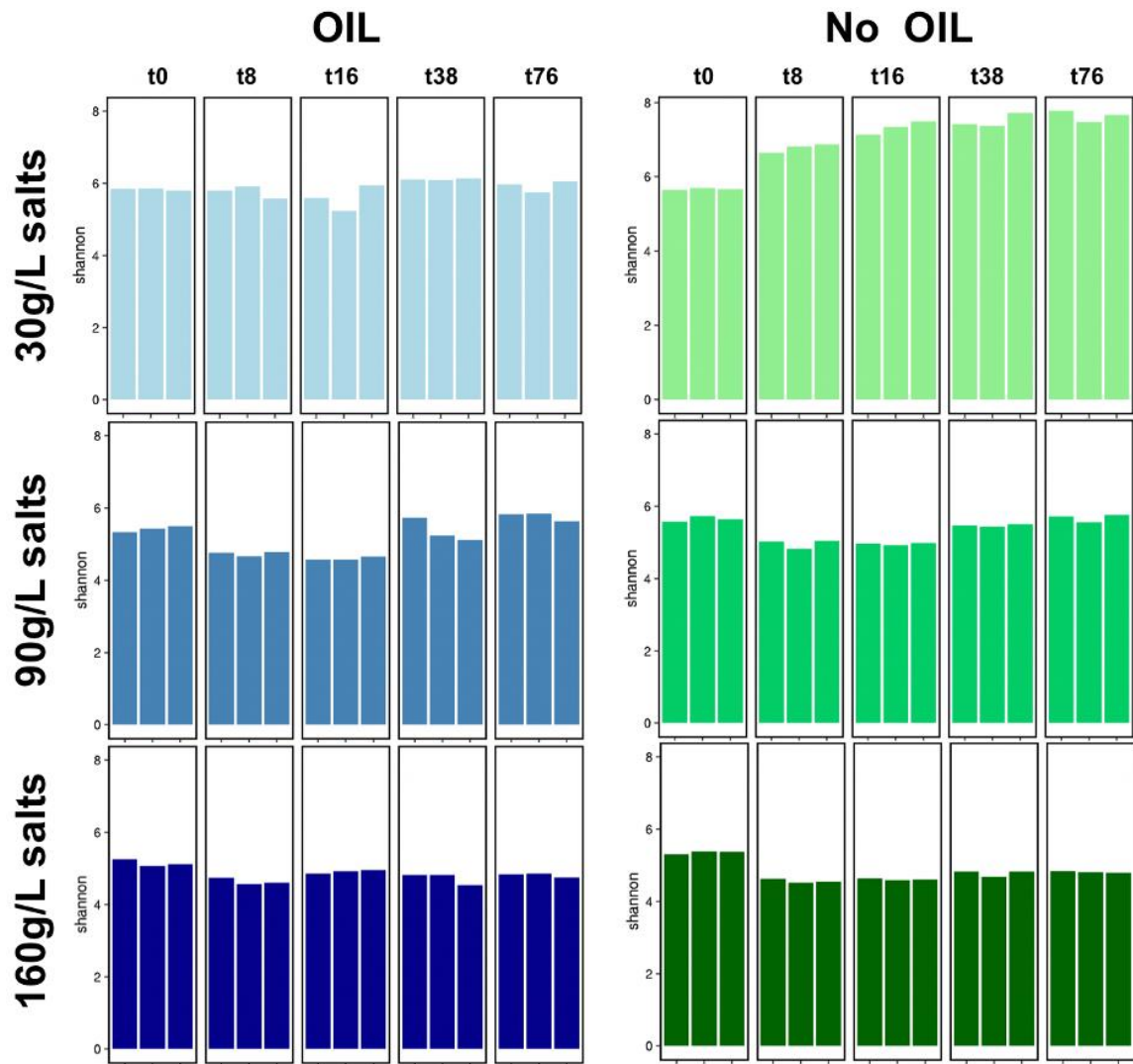


Figure 3.10 Alpha diversity (Shannon) with and without oil, with respect to salinity and incubation period.

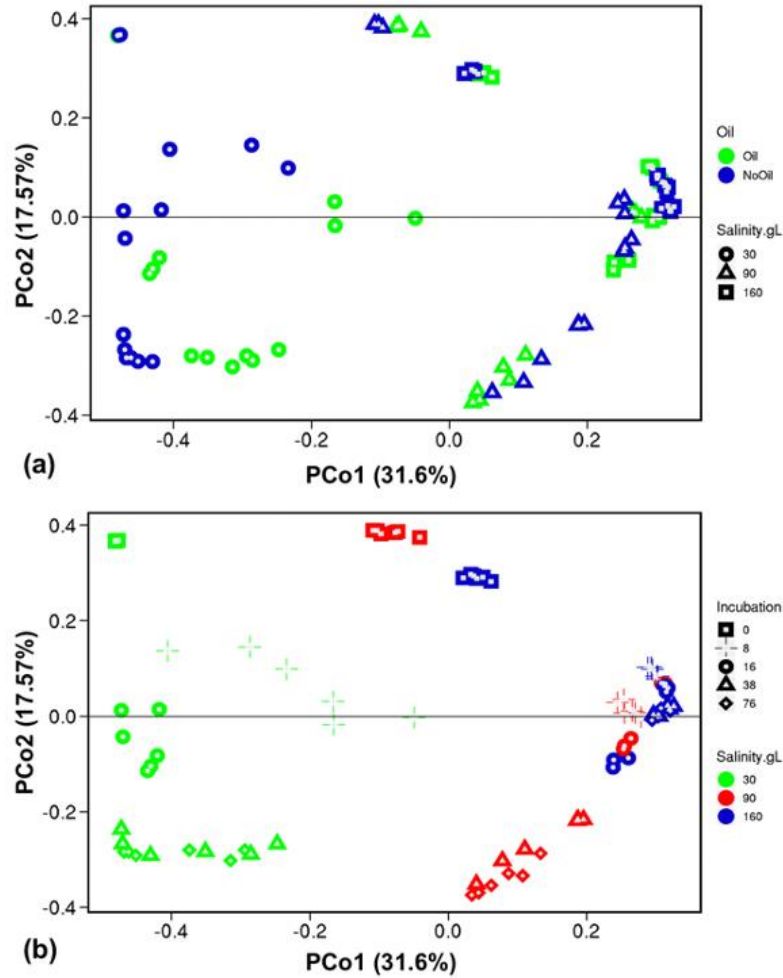


Figure 3.11 PCoA analysis of the total microbial community in microcosms with 30, 90, or 160 g/L salt (a) in the presence and absence of oil, and (b) with respect to the incubation period.

At 30 g/L salt, there was a clear difference in the abundance of different microbial communities between the oiled and non-oiled microcosms. As expected, hydrocarbon degraders (e.g., *Alcanivorax*, with known alkane-degrading species) were more abundant in the presence of oil. The genus *Thalassospira*, which is known as a polycyclic aromatic hydrocarbon-degrader (Zhou et al., 2016), was observed in the presence and absence of oil after 8 days but became more abundant in the oiled samples after 16 and 38 days of incubation. In addition, there was a difference in the abundance of different genera with time, which might indicate that some microorganisms capable of growing on smaller

hydrocarbons (e.g., alkanes shorter than C₂₀) flourished at the beginning, and then became less dominant as the shorter-chain hydrocarbons became scarce. For instance, the abundance of the *Alcanivorax* genus, of which many strains are known to biodegrade long-chain alkanes (Wang & Shao, 2014; SadrAzodi et al., 2019), was relatively low at t = 16 days in the oiled and non-oiled microcosms, and then increased after 16 days only in the oiled microcosms (Figure 3.14-a). In addition, a highly degraded oil in seawater could be indicated by the high abundance of both *Alcanivorax* and *4-Org1-14OR* genera, which are observed after losing more than 75% of petroleum hydrocarbons (t = 38 and 76 days, Figures 3.6 and 3.12). However, it seems that such an indicator is irrelevant under hypersaline conditions (90 and 160 g/L salt) since the *4-Org1-14OR* genus was not among the 20 most abundant genera in the highly saline microcosms (Figure 3.12).

At 90 g/L salt, the microbial distribution between the oil and non-oiled microcosms was somewhat similar. *Marinobacter* was abundant in oiled and unoiled mesocosms, while *Balneola*, associated with hydrocarbon contaminated environments (Fernandes et al., 2020), was absent among the 20 most abundant genera after t = 38 days (Figure 3.12). The genus *Alcanivorax* was detected after 8 days in the presence of oil and remained part of the bacterial community until the end of the experiment. Nonetheless, *Alcanivorax* was not among the 20 most abundant genera in the non-oiled microcosms during the entire experimental period (Figure 3.14-b). ASVs related to *Marinobacter*, *Brumimicrobium*, and *Marivita* were dominant in the first 16 days of incubation in the oiled samples, while after 76 days, other genera (e.g., *Rhodospirillacea* and *Roseovarius*) became more abundant.

At 160 g/L salt, the microbial communities were primarily dominated by the genus *Marinobacter* during the entire experimental period in both oiled and non-oiled samples.

In the oiled microcosms, an increase in abundance of *Thalassospira* was identified after 16 days of incubation, and *Alcanivorax* became part of the 20 most abundant genera after 8 days of incubation. *Alcanivorax* was also present among the 20 most abundant genera in the non-oiled microcosms (Figure 3.14-c). This was not the case for the other salinities (30 and 90 g/L salt), and hence, it cannot be used as an indicator of oil contamination under such hypersaline conditions. In addition, *Brumimicrobium*, previously found in oil-contaminated environments (Wang et al., 2020) and salterns (Wang et al., 2020), appeared at 8 days and lasted until the end of the experiment (76 days), while at 90 g/L salt, it was abundant only at 8 and 16 days and was not among the dominant genera after 38 days.

Analysis of the top 100 ASVs showed that 41% were common to all salt concentrations in the absence of oil (Table 3.2, Figure 3.15), whereas 50% were common to all salt concentrations in the presence of oil (Table 3.3, Figure 3.16), of which several genera are known to be capable of degrading hydrocarbons. Of the 100 ASVs dominant in the absence of oil, 29% were present under hypersaline conditions (90 and 160 g/L salt). The relative numbers were similar in the presence of oil, with 33% present under hypersaline conditions. ASVs associated with the highest salinity (160 g/L) were mainly related to known halophilic bacteria, represented by the *Halobacteriaceae* (Archaea). The Archaea remained present, mainly at higher salt concentrations, and were detected among the dominant 100 taxa but not the dominant 20 taxa. Interestingly, several well-known hydrocarbon degrading genera (*Cycloclasticus*, *Oleibacter*, and *Thalassolituus*) were only identified at the 30 g/L salt concentration in the presence of oil; they were not present without oil or at higher salinities (Figures 3.15 and 3.16, Tables 3.2 and 3.3).

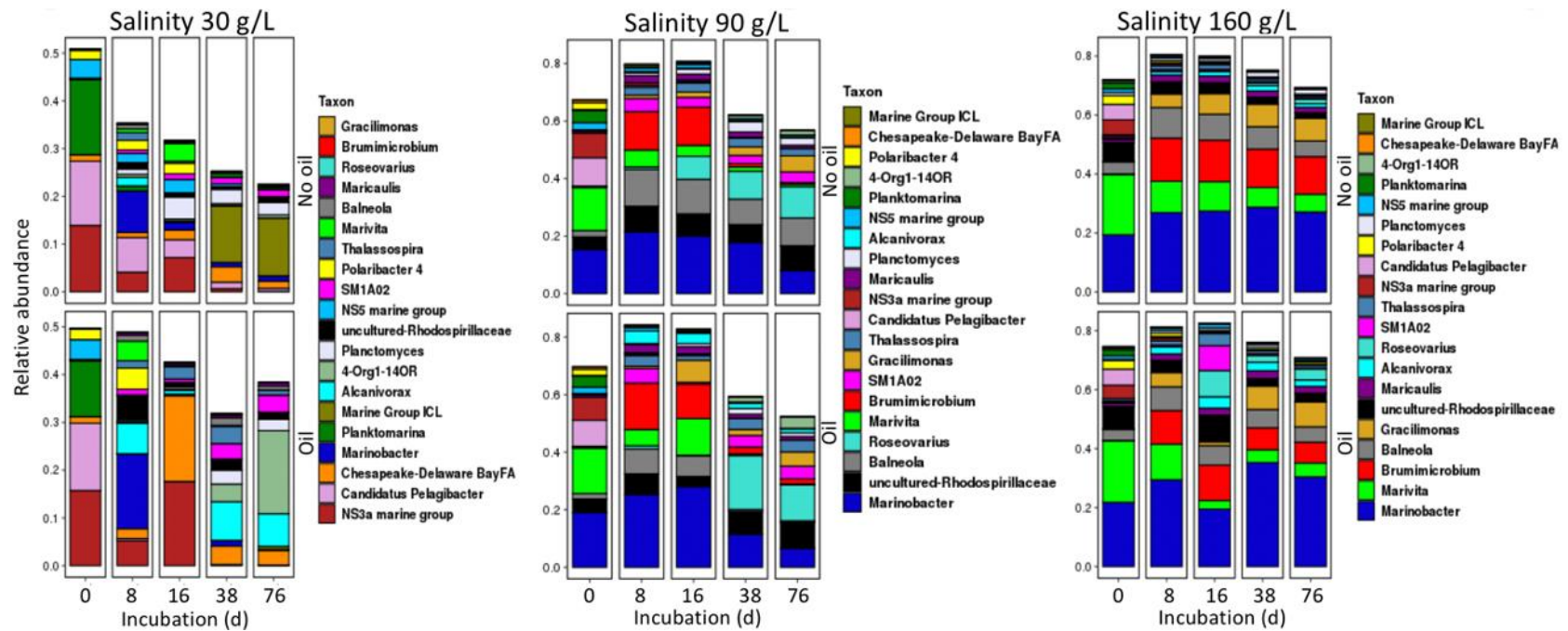


Figure 3.12 Taxonomic profiles of the 20 most abundant genera identified in the microcosms with 30, 90 or 160 g/L salt at the beginning of the experiment and after 8, 16, 38, and 76 days of incubation, in the presence (bottom panels) and absence of oil (top panels). Note that the total contribution of these most abundant genera was lower in the 30 g/l microcosms, indicating the greater diversity in those incubations.

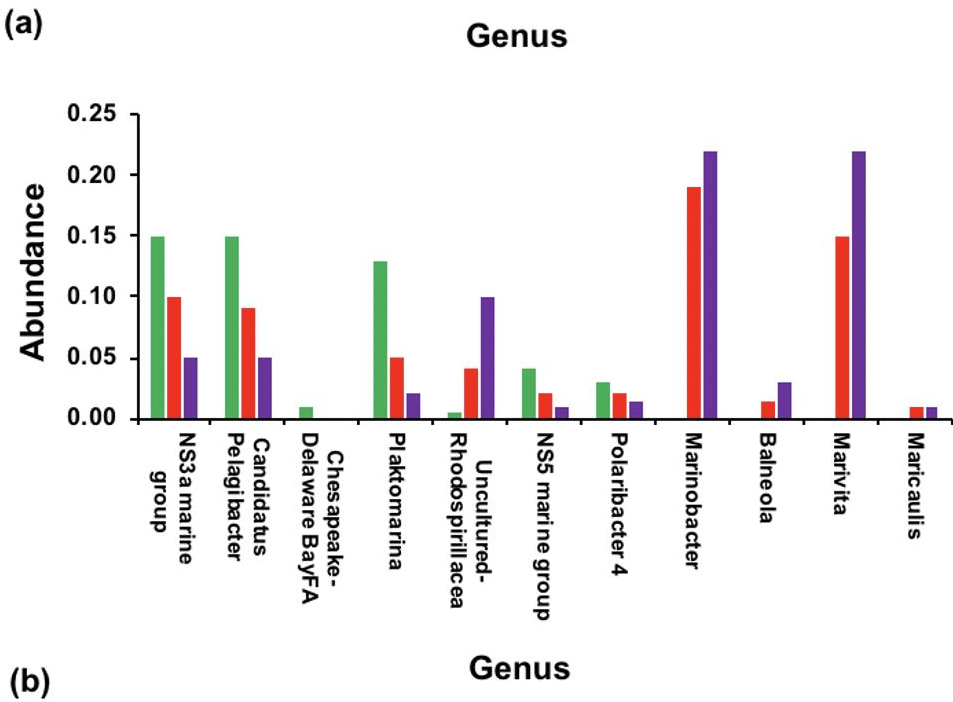
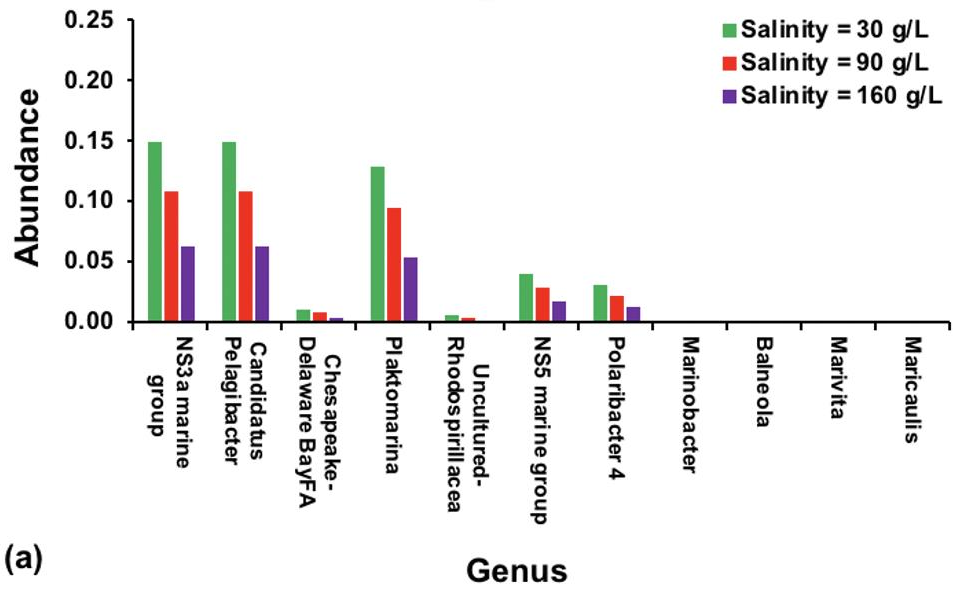


Figure 3.13 Most abundant genera at T = 0; (a) abundance calculated from the 30 g/L salt microcosms and the seawater to concentrated brine ratios, and (b) actual observed abundance

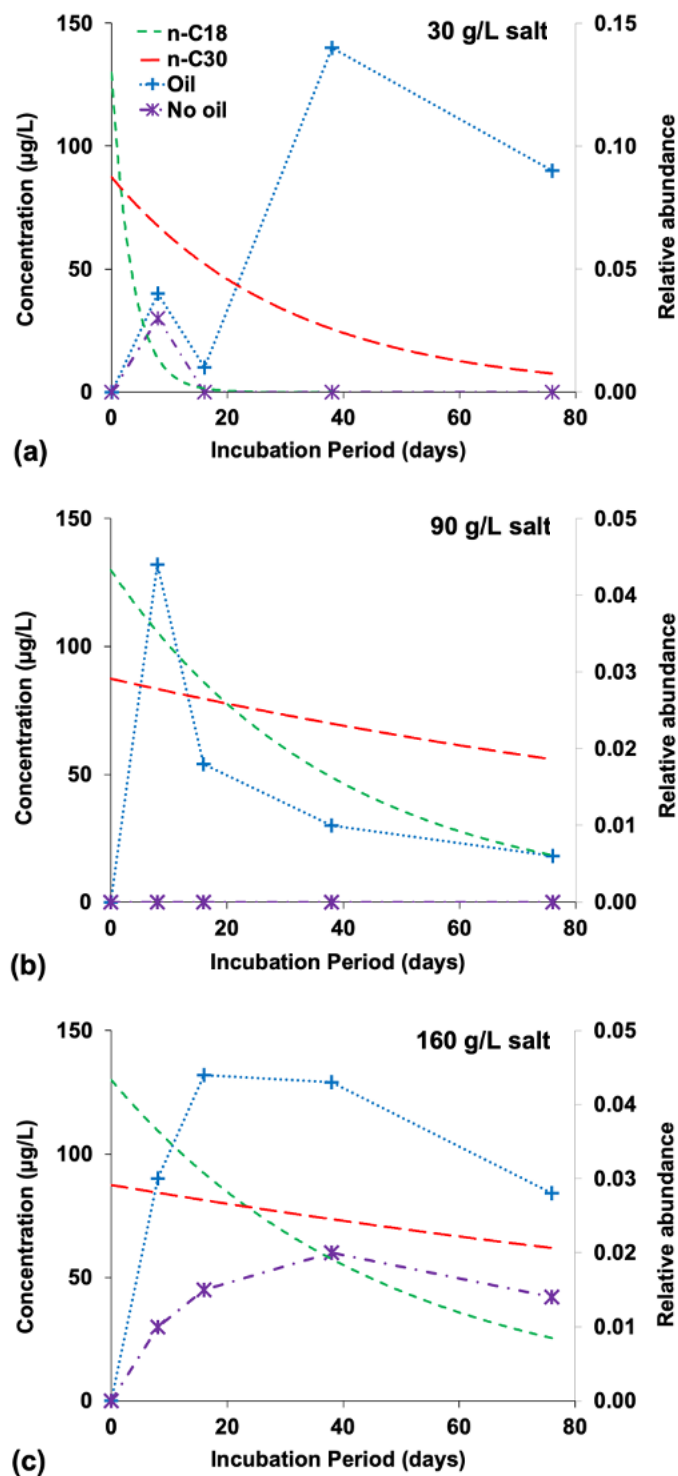


Figure 3.14 The average concentration of a short-chain (n-C18) and a long-chain (n-C30) alkane vs. the relative abundance of the *Alcanivorax* genus in the microcosms with respect to time at a salinity of (a) 30 g/L, (b) 90 g/L, and (c) 160 g/L. Note that, in the oiled and non-oiled microcosms at 30 g/L salt, the abundance of *Alcanivorax* increased at $t = 8$ days, and then increased again only in the oiled microcosms after $t = 16$ days.

Table 3.2 Dominant 100 Bacterial Amplicon Sequence Variants Identified in Microcosms at Different Salinities in the Absence of Oil (Continued)

Salinities	Total	Elements
30 g/L, 90 g/L, and 160 g/L	41	Methylophilaceae. OM43 clade Rhodobacteraceae. Sulfitobacter Flavobacteriaceae. Algibacter Comamonadaceae. BAL58 marine group Rhodobacteraceae. uncultured-Rhodobacteraceae Chesapeake-Delaware Bay. Chesapeake-Delaware BayFA Planctomycetaceae. Blastopirellula Rhodospirillaceae. Thalassospira Cryomorphaceae. Phaeocystidibacter Flavobacteriaceae. Formosa NS11-12 marine group. NS11-12 marine groupFA Rhodobacteraceae. Ruegeria SAR116 clade. Candidatus Puniceispirillum Flavobacteriaceae. Polaribacter 4 Rhodospirillaceae. Magnetospira Planctomycetaceae. Planctomyces Alteromonadaceae. Glaciecola Flavobacteriaceae. Tenacibaculum Rhodospirillaceae. Uncultured- Rhodospirillaceae Rhodobacteraceae. Marivita Flavobacteriaceae. Ulvibacter Rhodobacteraceae. Planktomarina Flavobacteriaceae. NS3a marine group BD7- 11CL. BD7-11CL SPOTSOCT00m83CL. SPOTSOCT00m83CL Flavobacteriaceae. NS5 marine group Rhodobacteraceae. Marinovum Flammeovirgaceae. Ekhidna. Other Flavobacteriaceae. Polaribacter 1 Unknown Family (bacteroidetes-bacteroidetes incertae sedis-order iii). Balneola Saprospiraceae. Lewinella T9d. T9dFA Surface 1. Candidatus Pelagibacter 4- Org1-14OR. 4-Org1-14OR Phycisphaeraceae. SM1A02 Alteromonadaceae. Marinobacter Alcanivoracaceae. Alcanivorax NS9 marine group. NS9 marine groupFA Surface 1. Surface 1FA Planctomycetaceae. Rhodopirellula.
30 g/L and 90 g/L	8	OPB35 soil groupCL. OPB35 soil groupCL Bacteroidetes VC2.1 Bac22CL. Bacteroidetes VC2.1 Bac22CL Oceanospirillaceae. Pseudohongiella JTB255 marine benthic group. JTB255 marine benthic groupFA Rhodobacteraceae. Loktanelia Nitrospinaceae. Nitrospina Surface 2. Surface 2FA BD2-11 terrestrial groupCL. BD2-11 terrestrial groupCL.
30 g/L and 160 g/L	7	OM182 clade. OM182 cladeFA OM190CL. OM190CL Halomonadaceae. Halomonas Halieaceae. Haliea OCS116 clade. OCS116 cladeFA Rhodothermaceae. uncultured-Rhodothermaceae Rhodobacteraceae.
90 g/L and 160 g/L	29	Unknown Family (bacteroidetes-bacteroidetes incertae sedis-order iii). Unknown FamilyFA Alcanivoracaceae. Kangiella OPB56. OPB56FA Flavobacteriaceae. Gillisia Piscirickettsiaceae. Methylophaga Alcaligenaceae. Kerstesia Hyphomicrobiaceae. Maritalea Sneathiellaceae. Sneathiella Rhodospirillaceae. Tistlia Porticoccaceae. C1-B045 Cryomorphaceae. Owenweeksia Hyphomonadaceae. Maricaulis Rhodobacteraceae. Roseovarius Hyphomonadaceae. Oceanicaulis Rhodobiaceae. uncultured-Rhodobiaceae Unknown Family (bacteroidetes-bacteroidetes incertae sedis-order iii). Gracilimonas Unknown Family (proteobacteria-alphaproteobacteria- alphaproteobacteria incertae sedis). Micavibrio Halobacteriaceae. Haloferax Planctomycetaceae. Pirellula Cryomorphaceae. Other Hyphomicrobiaceae. Filomicrobium Hyphomonadaceae. Uncultured-Hyphomonadaceae Cryomorphaceae. Brumimicrobium Saccharospirillaceae. Saccharospirillum Flammeovirgaceae. Fulvivirga Caldilineaceae, CaldilineaceaeFA Microbacteriaceae. ML602J-51 Saprospiraceae, Phaeodactylibacter Hyphomonadaceae. Hyphomonas.

Table 3.2 (Continued) Dominant 100 Bacterial Amplicon Sequence Variants Identified in Microcosms at Different Salinities in the Absence of Oil

30 g/L	38	<p>Saprospiraceae. Portibacter RhizobialesOR. RhizobialesOR Burkholderiaceae. Limnobacter Flavobacteriaceae. Aquibacter DEV007. DEV007FA Solimonadaceae. Polycyclovorans 070125-BRIC7-5OR. 070125-BRIC7-5OR Rhodobacteraceae. Pseudorhodobacter Cryomorphaceae. Luteibaculum PAUC34fPH. PAUC34fPH SAR202 cladeCL. SAR202 cladeCL SAR116 clade. SAR116 cladeFA Bdellovibrionaceae. OM27 clade Vibrionaceae. Aliivibrio Rhodobacteraceae. Pseudophaeobacter ARKDMS-49CL. ARKDMS-49CL Subgroup 22CL. Subgroup 22CL Salinisphaeraceae. Oceanococcus Saprospiraceae. Rubidimonas Oceanospirillaceae. Neptuniibacter Rhodospirillaceae. Lacibacterium Rhodospirillaceae. Other Nitrosomonadaceae. Nitrosomonas SAR11 cladeOR. SAR11 cladeOR Solibacteraceae (Subgroup 3). PAUC26f Bacteriovoraceae. Peredibacter JG30-KF-CM66CL. JG30-KF-CM66CL SBR1093PH. SBR1093PH Colwelliaceae. Thalassotalea Flavobacteriaceae. Other Rhodospirillaceae. OM75 clade Woesearchaeota (DHVEG-6)PH. Woesearchaeota (DHVEG-6) PH Marine Group ICL. Marine Group ICL Oceanospirillaceae. Motiliproteus Sva0996 marine group. Sva0996 marine groupFA Spongiibacteraceae. Zhongshania HydrogenedentesPH. HydrogenedentesPH Pseudoalteromonadaceae. Pseudoalteromonas.</p>
90 g/L	18	<p>S15-21. S15-21FA Cryomorphaceae. Crocinitomix Nitriliruptoraceae. NitriliruptoraceaeFA Flavobacteriaceae. Muricauda Phycisphaeraceae. Phycisphaera Saprospiraceae. uncultured-Saprospiraceae Rhodobacteraceae. Roseobacter E01-9C-26 marine groupOR. E01-9C-26 marine groupOR AT-s3-44. AT-s3-44FA Rhodospirillaceae. Thalassobaculum Flavobacteriaceae. Zeaxanthinibacter Rhodobacteraceae. Octadecabacter Rhodobacteraceae. Ketogulonicigenium Flavobacteriaceae. Sediminicola Flavobacteriaceae. Gramella Alcaligenaceae. Pusillimonas Flammeovirgaceae. Marinoscillum Cryomorphaceae. CryomorphaceaeFA.</p>
160 g/L	19	<p>BradymonadalesOR. BradymonadalesOR TM6 (Dependentiae) PH. TM6 (Dependentiae) PH Flammeovirgaceae. Marivirga Halobacteriaceae. Halohasta Rhodobacteraceae. Sedimentitalea Rhodobacteraceae. Mmeliella Halobacteriaceae. Natronomonas Rhizobiales Incertae Sedis. Pyruvatibacter Unknown Family (bacteroidetes-bacteroidetes incertae sedis-order iii). Aliifodinibius Rhodobacteraceae. Antarctobacter Pseudomonadaceae. Pseudomonas SM2D12. SM2D12FA Lentimicrobiaceae. LentimicrobiaceaeFA Halobacteriaceae. Halogranum Saprospiraceae. Other Rhodobacteraceae. Donghicola Porticoccaceae. Porticoccus Rhodospirillaceae. RhodospirillaceaeFA Halobacteriaceae. Halolamina.</p>

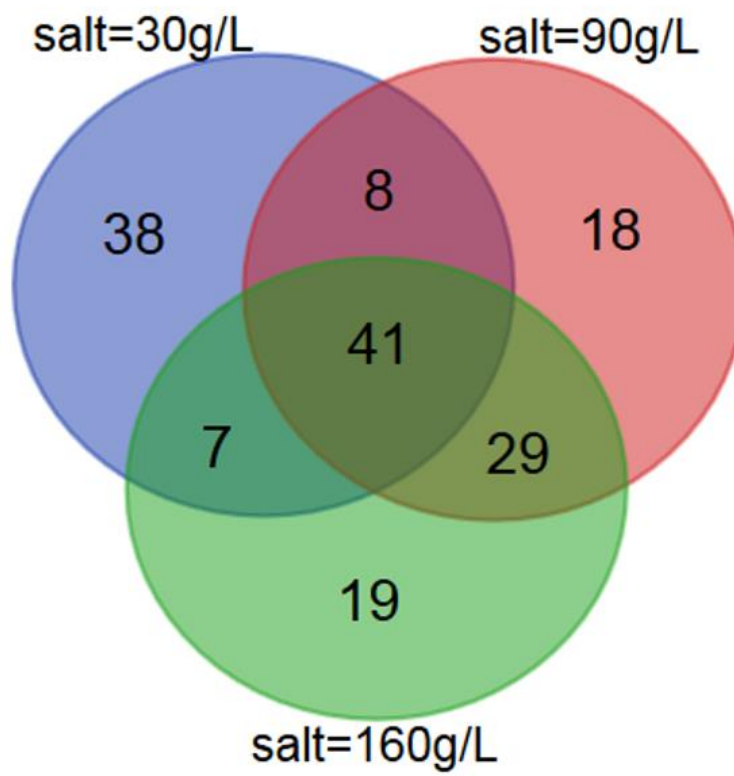


Figure 3.15 Venn diagram of the dominant 100 bacterial amplicon sequence variants of Table 3.2.

Table 3.3 Dominant 100 Bacterial Amplicon Sequence Variants Identified in Microcosms at Different Salinities in the Presence of Oil (Continued)

Salinities	Total	Elements
30 g/L, 90 g/L, and 160 g/L	50	Methylophilaceae. OM43 clade Flavobacteriaceae. Gillisia Rhodobacteraceae. Sulfitobacter Flavobacteriaceae. Algibacter Comamonadaceae. BAL58 marine group Rhodobacteraceae. Uncultured-Rhodobacteraceae Chesapeake-Delaware Bay. Chesapeake-Delaware BayFA Planctomycetaceae. Blastopirellula Rhodospirillaceae. Thalassospira Cryomorphaceae. Phaeocystidibacter Flavobacteriaceae. Formosa NS11-12 marine group. NS11-12 marine groupFA Oceanospirillaceae. Pseudohongiella SAR116 clade. Candidatus Puniceispirillum Porticoccaceae. C1-B045 Hyphomonadaceae. Maricaulis Flavobacteriaceae. Polaribacter 4 Rhodospirillaceae. Magnetospira Planctomycetaceae. P lanctomyces Alteromonadaceae. Glaciecola Flavobacteriaceae. Tenacibaculum Rhodobacteraceae. Marivita Rhodospirillaceae. uncultured-Rhodospirillaceae Flavobacteriaceae. Ulvibacter Rhodobacteraceae. Roseobacter Rhodobacteraceae. Planktomarina Rhodobiaceae. Uncultured-Rhodobiaceae Flavobacteriaceae. NS3a marine group BD7-11CL. BD7-11CL Unknown Family (proteobacteria-alphaproteobacteria-alphaproteobacteria incertae sedis). Micavibrio SPOTSOCT00m83CL. SPOTSOCT00m83CL Rhodobacteraceae. Loktanela Flavobacteriaceae. NS5 marine group Rhodospirillaceae. Thalassobaculum Other. Other Flavobacteriaceae. Polaribacter 1 Unknown Family (bacteroidetes-bacteroidetes incertae sedis-order iii). Balneola Saprospiraceae. Lewinella T9d. T9dFA Surface 1. Candidatus Pelagibacter Rhodobacteraceae. Donghicola 4-Org1-14OR. 4-Org1-14OR Phycisphaeraceae. SM1A02 Alteromonadaceae. Marinobacter Alcanivoracaceae. Alcanivorax Microbacteriaceae. ML602J-51 NS9 marine group. NS9 marine groupFA Surface 1. Surface 1FA Rhodobacteraceae. Other Hyphomonadaceae. Hyphomona.
30 g/L and 90 g/L	2	OPB35 soil groupCL. OPB35 soil groupCL PYR10d3OR. PYR10d3OR.
30 g/L and 160 g/L	3	Rhizobiales Incertae Sedis. Pyruvatibacter Lentimicrobiaceae. LentimicrobiaceaeFA Rhodothermaceae. Uncultured-Rhodothermaceae.
90 g/L and 160 g/L	33	Alcanivoracaceae. Kangiella OPB56. OPB56FA Piscirickettsiaceae. Methylophaga Alcaligenaceae. Kerstersia Hyphomicrobiaceae. Maritalea Halomonadaceae. Halomonas Flavobacteriaceae. Muricauda Sneathiellaceae. Sneathiella Rhodospirillaceae. Tistlia Rhodobacteraceae. Ruegeria Unknown Family (bacteroidetes-bacteroidetes incertae sedis-order iii). Aliifodinibius Cryomorphaceae. Owenweeksia Rhodobacteraceae. Roseovarius Hyphomonadaceae. Oceanicaulis JTB255 marine benthic group. JTB255 marine benthic groupFA Unknown Family (bacteroidetes-bacteroidetes incertae sedis-order iii). Gracilimonas Rhodobacteraceae. Marinovum Halieaceae. Haliea Flavobacteriaceae. Zeaxanthinibacter Halobacteriaceae. Haloferax Surface 2. Surface 2FA Halobacteriaceae. Halogranum Hyphomicrobiaceae. Filomicrobium Hyphomonadaceae. uncultured-Hyphomonadaceae Cryomorphaceae. Brumimicrobium Saccharospirillaceae. Saccharospirillum Flavobacteriaceae. Gramella Flammeovirgaceae. Fulvivirga Saprospiraceae. Phaeodactylibacter Rhodobacteraceae. Pelagibaca Hyphomonadaceae. Henriciella Planctomycetaceae. Rhodopirellula Halobacteriaceae. Halolamina.

Table 3.3 (Continued) Dominant 100 Bacterial Amplicon Sequence Variants Identified in Microcosms at Different Salinities in the Presence of Oil

30 g/L	44	<p>Legionellaceae. LegionellaceaeFA Halieaceae. Halioglobus OM190CL. OM190CL DEV007. DEV007FA Sandaracinaceae. SandaracinaceaeFA Rhodospirillaceae. Nisaea Hyphomonadaceae. Ponticaulis Puniceicoccaceae. Pelagicoccus Rhodobacteraceae. Roseobacter clade CHAB-I-5 lineage Oceanospirillaceae. Thalassolituus SS1-B-06-26. SS1-B-06-26FA PAUC34fPH. PAUC34fPH Rhodospirillaceae. Oceanibaculum Piscirickettsiaceae. Cycloclasticus Flavobacteriaceae. Polaribacter 2 Bdellovibrionaceae. OM27 clade Rhodobacteraceae. Aestuariivita Spongiibacteraceae. Spongiibacter Rhodobacteraceae. Celeribacter Phycisphaeraceae. PhycisphaeraceaeFA Verrucomicrobiaceae. Roseibacillus Rhizobiales Incertae Sedis. Candidatus Phaeomarinobacter Oceanospirillaceae. Neptuniibacter Oceanospirillaceae. Other Rhodobiaceae. Parvibaculum Rhodospirillaceae. Other SAR11 cladeOR. SAR11 cladeOR Legionellaceae. Legionella Rhodobacteraceae. Labrenzia Bacteriovoracaceae. Peredibacter P3OB-42. P3OB-42FA Opitutaceae. Diplosphaera Flavobacteriaceae. Other Marine Group ICL. Marine Group ICL Parvularculaceae. ParvularculaceaeFA Oceanospirillaceae. Motiliproteus Oceanospirillaceae. Oleibacter Rhodobacteraceae. Albimonas Hyphomonadaceae. Other Spongiibacteraceae. Zhongshania HydrogenedentesPH. HydrogenedentesPH.</p>
90 g/L	12	<p>Nitriliruptoraceae. NitriliruptoraceaeFA Caulobacteraceae. Amorphus Phycisphaeraceae. Phycisphaera Rhodobacteraceae. Oceanicella Saprospiraceae. uncultured-Saprospiraceae AT-s3-44. AT-s3-44FA Erythrobacteraceae. Erythrobacter Planctomycetaceae. Pirellula Flavobacteriaceae. Sediminicola Alcaligenaceae. Pusillimonas Caldilineaceae. CaldilineaceaeFA Flammeovirgaceae. Marinoscillum</p>
160 g/L	11	<p>Unknown Family (bacteroidetes-bacteroidetes incertae sedis-order iii). Unknown FamilyFA TM6 (Dependentiae)PH. TM6 (Dependentiae)PH Flammeovirgaceae. Marivirga Halobacteriaceae. Halohasta Granulosicoccaceae. Granulosicoccus Halobacteriaceae. Halostagnicola Pseudomonadaceae. Pseudomonas Halobacteriaceae. Halorubrum SM2D12. SM2D12FA Flammeovirgaceae. Ekhidna Rhodospirillaceae. RhodospirillaceaeFA</p>

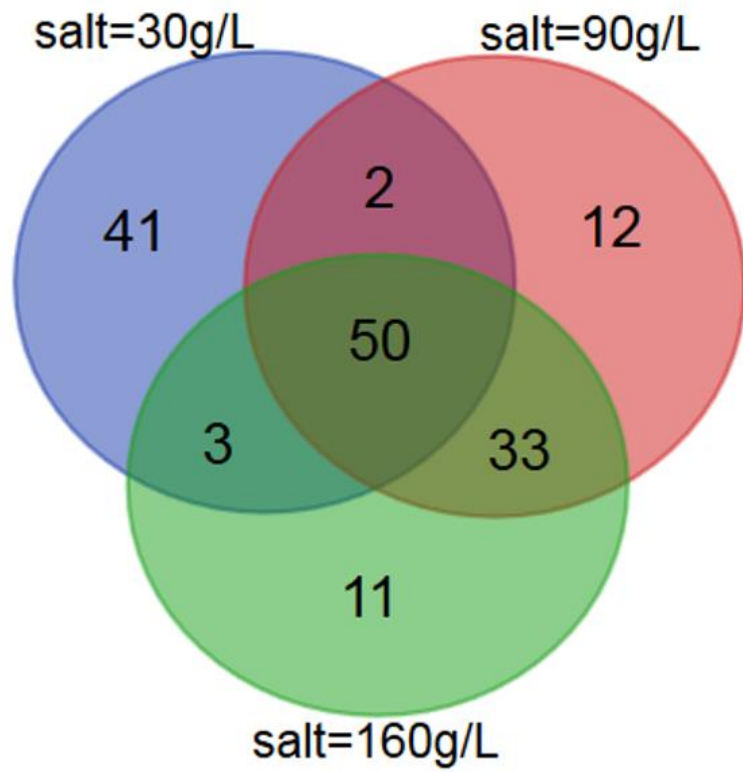


Figure 3.16 Venn diagram of the dominant 100 bacterial amplicon sequence variants of Table 3.3.

3.4 Discussion

The results clearly show that the biodegradation of petroleum hydrocarbons by indigenous seawater organisms decreases when salinity increases, by two-fold at 90 g/L and four-fold at 160 g/L salt (Figure 3.6). Figure 3.7 shows that, at seawater salinity, there is a drop in the apparent rate of biodegradation at alkane C24, implying that different chain length alkanes are biodegraded by distinctive enzymes (Wang et al., 2016; Brakstad et al., 2018), and might be the reason for the persistence of heavier alkanes in sunken oil residues after a catastrophic oil spill (Stout & Payne, 2016; Passow & Stout, 2020). This was not apparent at high salinities, where the biodegradation of alkanes gradually decreased with the size of the hydrocarbons. For instance, at 30 g/L salt, the rate constant k of C24 was ~65% lower than that of C23, while at 160 g/L salt, the difference was only ~12%, (Figure 3.7). In addition, the biodegradation of alkanes and low-molecular-weight PAHs was substantially slowed at high salinities (Table 3.1), although the effect was less apparent with the larger PAHs such as C3- and C4-phenanthrenes, benz[a]anthracene, and chrysenes. The apparent first-order rate constants of the biodegradation of most alkanes and some low-weight PAHs (e.g., naphthalenes and fluorenes) decreased by ~90% when the salinity of seawater increased by about five-fold (30–160 g/L), while that of chrysenes decreased only by ~50% (Figures 3.7 and 3.8). High pressure did not have this discriminatory effect, slowing the biodegradation of all measured compounds by about 30% (Prince et al., 2016b). Nonetheless, Figure 3.8 clearly shows that the rate constant k of heavy PAHs, such as chrysenes, is relatively low even at the ocean's salinity (Prince et al., 2013; Wang et al., 2016; Prince et al., 2017; Brakstad et al., 2018), and these molecules can persist for years in contaminated shorelines (Yin et al., 2015).

Previous studies showed a higher rate of oil biodegradation by halophiles isolated from hypersaline coastal sediments (Abed et al., 2006; Al-Mailem et al., 2010), but these studies relied on isolated extremely halophilic strains and may have enriched rare hypersaline microbes at the expense of more typical marine microorganisms, and hence, might not represent the natural in-situ oil biodegradation in contaminated coastal sediments. The microbial analysis clearly showed that the abundance of genera was different at high salt relative to that at seawater's salinity.

Microorganisms of the *Marinobacter* genus, which were rare at normal seawater salinity (except at $t = 8$ days), were among the most abundant at 90 and 160 g/L salt and remained abundant throughout most of the incubation period (Figure 3.12). Previous studies have examined the hydrocarbonolastic activity of the *Marinobacter* genus. Such extremely halotolerant microorganisms were capable of degrading petroleum hydrocarbons under hypersaline conditions, where the salinity was about five-fold (Wang et al., 2020), seven-fold (Wang et al., 2020), and ten-fold (Wang et al., 2020) higher than seawater. Consequently, the *Marinobacter* genus may be important in the bioremediation of oil-contaminated hypersaline ecosystems (Gauthier et al., 1992; Berlendis et al., 2010; Al-Mailem et al., 2013). Other genera, such as *Marivita* (*Rhodobacteriaceae*) and *Brumimicrobium* (Bacteroidetes), also became dominant at higher salt concentrations, with and without oil, even if only transiently. Several genera of well-known hydrocarbonoclastic activity (*Thalassolituus*, *Cycloclasticus*, and *Oleibacter*) were identified amongst the most dominant 100 bacteria only in 30 g/L salt with oil (Table 3.3, Figure 3.16), and were not detected amongst the most dominant bacteria under any other conditions (e.g., high salt, no oil). This may be part of the reason why the hydrocarbonoclastic activity was slowed at high salt.

Members of the domain Archaea were also observed, mainly at higher salt concentrations with or without oil, and this group has been observed in coastal sediments contaminated with oil, but only as minor components (Wang et al., 2020). The only detection of members of the phylum *Woesearchaeota* was in the 30 g/L microcosms without oil, whereas different *Halobacteriaceae* (Euryarchaeota) were evident at higher salt concentrations (90 and 160 g/L) in the presence or absence of oil. The relative abundance of Archaea was low under all conditions, and as has been suggested by previous studies (Röling et al., 2004), this domain does not appear to be important in oil biodegradation, with bacteria playing the dominant role in the degradation of petroleum hydrocarbons in the ocean (Hazen et al., 2016).

CHAPTER 4

MICROBIAL ACTIVITY IN VADOSE ZONES

4.1 Overview

Based on the experimental results of Chapter 3, it seems that high salinity can significantly inhibit the hydrocarbon degraders in seawater. Therefore, the biodegradation of stranded oil will most likely slow down in the upper parts of sandy beaches which are transiently hypersaline. Nonetheless, the microbial population and diversity on sandy shorelines might drastically differ from that in seawater. Understanding the microbial activity and characteristics of such sedimentary ecosystems is particularly important for properly analyzing the experimental results of Chapter 5 whereby the oil biodegradation in beach sand infiltrated with hypersaline seawater is investigated.

In unsaturated porous media, both the viscosity and pressure are altered near solid-water interfaces (i.e., at the walls of the sediments). It is expected that such changes will not alter the bacteria's efficiency in terms of metabolism and survival. Nevertheless, a low degree of saturation (i.e., low moisture content) is not without its challenges since it can restrict mobility, lead to desiccation, and make it harder to access nutrients. Consequently, the microbes might become less active, and in extreme cases, could perish. This chapter discusses the microbial activity in the vadose zone along with the effects of pressure, viscosity, and moisture content.

4.2 Characteristics and Challenges

4.2.1 Microbial Density and Diversity

Under most conditions, natural sediments are unsaturated where the fragmented aqueous habitats and thin liquid films detain bacterial cells within small volumes and close proximity for extended periods (Franklin & Mills, 2007; Or et al., 2007; Young et al., 2008; Tecon et al., 2018). The unsaturated layer, also called the vadose zone, supports the highest microbial density of all biosphere compartments, and the diversity estimates exceed those of the oceans by several orders of magnitude (Torsvik et al., 2002). Interestingly, microorganisms occupy no more than a few percent of the pore spaces of an average soil and only a small fraction (< 1%) of the available soil surfaces (Young & Crawford, 2004; Young et al., 2008). In addition, the richness of microbial species is enhanced by the sediments' coarseness (Chau et al., 2011). For instance, soils which possess larger pores (e.g., sandy soils) results in the formation of isolated water films, thus providing more opportunities for increased bacterial diversity (Chau et al., 2011).

4.2.2 Biofilms

Or et al. (2007), who reviewed the physical constraints affecting bacterial habitats and activity in unsaturated porous media, described how fewer flagellated cells are found in soil because they mostly attach to the solids (sediments) by biosynthesizing extracellular polymeric substances (EPS). Consequently, an important fraction of microorganisms in porous media doesn't rely on flagella to move and obtain their nourishment. The supracellular structures, called biofilms (comprised of surface-associated microbial cells embedded in hydrated EPS), enable intensive inter- and intra-species interactions, hence increasing the degradation efficiency of organic matter (Cai et al., 2019). Even though

sedimentary environments are complex and dynamic, biofilms stabilize the conditions surrounding the microorganisms by protecting them, to some extent, against predation, desiccation, and exposure to antibiotics, while improving the availability of nutrients and oxygen and providing a niche for horizontal gene transfer (Costerton, 1999; Sørensen et al., 2005). Figure 4.1 displays the life cycle of biofilms on sediments, taken from Cai et al. (2019).

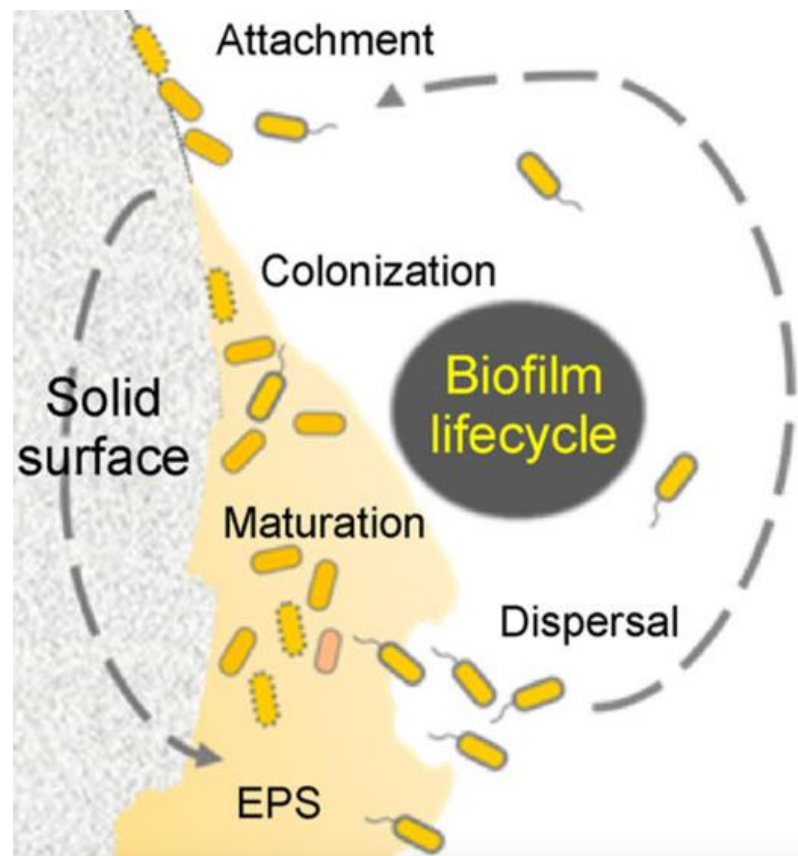


Figure 4.1 The life cycle of a soil biofilm consists of four phases: attachment, colonization, maturation, and dispersal. At maturation, the biofilm structure and composition are relatively stable. However, with the depletion of nutrients or external disturbances, the cells within can respond quickly by releasing enzymes capable of dispersing the biofilm and triggering the scattering of cells. During biofilm dispersal, cells can detach from the biofilm matrix, colonize another site and start a new biofilm cycle.

Source: (Oppenheimer-Shaanan et al., 2013; Cai et al., 2019)

4.2.3 Microbial Motility and Retainment

Bacteria are generally transported by the flowing water and may be retained as they interact with interfaces. Such attachments have been explained by the DLVO-theory – Derjaguin, Landau, Verwey, and Overbeek – of colloidal stability (Verwey et al., 1948; Derjaguin & Landau, 1993), which describes the interaction between the charged particles (e.g., bacteria) and solid surfaces as a sum of attractive Van der Waals forces and repulsive electrostatic forces. The attractive and repulsive forces have also been considered on the level of bacterial surface polymers, which can either promote or impede bacterial attachment (Rijnaarts et al., 1995). In addition, hydrophobic interactions (Tsao et al., 1993) between solids and cells can promote attachment. Such interactions explain the reason for microbial retention in water-filled porous media.

Generally, the amount of retained bacteria on solids increases with the decrease in the size and increase in the surface roughness of sediments (Gargiulo et al., 2007; Chau et al., 2011). Microbe deposition mechanisms in unsaturated porous media include attachment, interfacial attachment, straining, and film straining. Attachment refers to the deposition on the solid-water interface, while interfacial attachment is the deposition on the air-water interface. Microbial deposition by straining refers to those processes via which microbes are retained in pore throats that are too small to allow the transit of the bacteria across them (Díaz et al., 2010). Film straining is when the transport of suspended colloids can be impeded due to physical constraints imposed by thin water films in unsaturated porous media (Wan & Tokunaga, 1997). Therefore, straining is caused by the pore geometry's physical restrictions, while film straining depends on the water film

thickness. Generally, straining increases with smaller sediment sizes whereas film straining increases with the decrease in moisture content (Gargiulo et al., 2007).

In the case of sandy beaches, a large fraction of microorganisms in coastal sediments comes from seawater. In the ocean, some marine microorganisms possess flagella to move and obtain their nourishment. Figure 4.2 shows the arrangement of flagella in different organisms, taken from Aryal (2019). Microbial motility is guided by several processes, such as chemotaxis, where microorganisms either move toward food and nutrients or repel themselves from toxic compounds (Stock & Baker, 2009). Nonetheless, some marine microbes don't have flagella and rely on the ocean's natural physical processes to move from one place to another. For instance, Planktons – derived from the Greek word *planktos* meaning 'drifters', and *planao* meaning 'to wander' – rely on tides and water currents to move (Brierley, 2017).

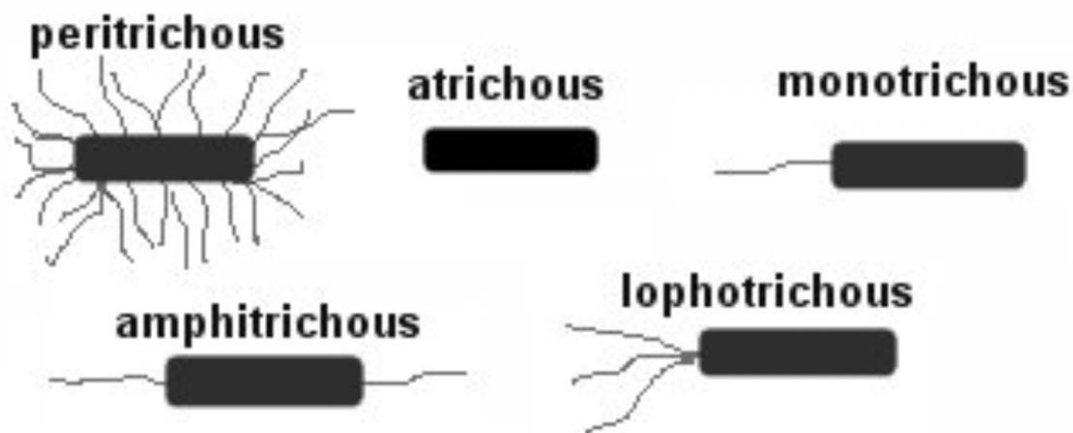


Figure 4.2 Different types of bacteria with respect to flagellar arrangement and abundance. Some don't have any and are classified as atrichous, while others are covered with flagella and are called peritrichous. Trichous comes from a Greek word which means "hairy" or "hair".

Source: (Aryal, 2019)

One of the challenges that microorganisms face in the upper parts of sandy shorelines, however, is the restriction of motility. This is due to the low degree of saturation

(prolonged evaporation) and the absence of natural physical processes (tides and currents). Therefore, other microbial movement mechanisms may become necessary on the liquid film-coated surfaces of coastal sediments. For instance, some microbes produce wetting agents to overcome the direct influence of attractive intermolecular forces due to proximity to the solid's surface and the strong surface tension of the water-gas interface (Matsuyama & Nakagawa, 1996). There are four types of microbial movement mechanisms in film-coated structures: swarming, gliding, twitching, and sliding (Harshey, 2003). Swarming motility is a quick (2–10 $\mu\text{m/s}$) and coordinated translocation of microorganisms (by using their flagella) across solid or semi-solid surfaces, and some species produce biosurfactants for swarming to occur (Bees et al., 2002). Gliding bacteria move by a process that does not usually involve the use of propulsive structures (e.g., flagella, pili, and fimbriae) to travel along low aqueous films. Nonetheless, some gliding mechanisms (e.g., social gliding) require the use of the IV Pilus, which can be used for movement by active extension and retraction (McBride, 2001). Gliding occurs when the bacterium moves smoothly in the general direction of its long axis using different mechanisms depending on the type of microorganism (McBride, 2001). For example, the secretion of polysaccharides assists the surface gliding of certain bacteria, in which the rate of extrusion of polysaccharides is similar to the rate of movement, and the direction of secretion is opposite to that of cell movement (McBride, 2001). Twitching motility is also a flagella-independent form of bacterial translocation, which involves the extension, tethering, and then retraction of the IV Pilus, operating like a grappling hook (Kaiser, 2000). Although some gliding mechanisms also use the IV pilus, as discussed earlier, twitching requires a very moist surface, and the movement isn't smooth like gliding since it occurs discontinuously by

short and intermittent jerks of up to several micrometers (McBride, 2001). Sliding motility, which is the least investigated, is defined as surface translocation produced by expansive forces in the growing colony combined with special surface properties to lower the friction between the cells and the substrate. Hence, sliding does not require the use of propulsive structures (Martínez et al., 1999). Figure 4.3 shows the propulsive structures of a bacterium.

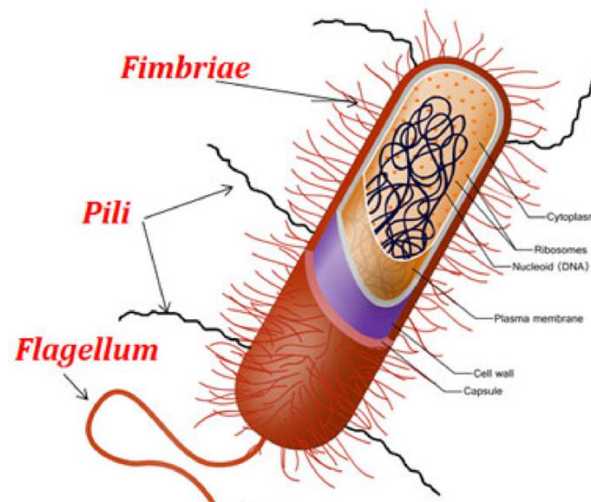


Figure 4.3 The different propulsive structures of a bacterium.
Source: (Orbibiotech, 2018)

4.2.4 Film Thickness and Microbial Immersion

When soil becomes unsaturated, the remaining liquid is either retained in corners and crevices behind liquid-gas interfaces (Figure 4.4-c) or adsorbed as thin liquid films on solid surfaces (Figure 4.4-b) (Long & Or, 2005; Or et al., 2007). Liquid film thickness is related to the degree of saturation and pore space geometry. Or et al. (2007) explain water film thickness on sediments due to Van der Waals surface forces using the following equation:

$$l = \left(\frac{H}{6\pi\rho\mu} \right)^{1/3}$$

where l is the film thickness in meters, H is the Hamaker constant (-6×10^{-20} J for water on silicate surfaces (Takagishi et al., 2019)), ρ is the water density ($\sim 1,000$ kg/m³), and μ is the matric water potential in J/kg (Iwamatsu & Horii, 1996; Tuller et al., 1999), which is proportional to the moisture content. Note that the matric potential is negative, so when it decreases (e.g., from -10 to -40 J/kg), the film thickness decreases. Under wet conditions (i.e., field capacity, where water in large pores has drained), the matric potential is between -10 and -30 J/kg, leading to a film thickness of 10 nm on a smooth mineral surface (Figure 4.5), which clearly cannot support complete immersion of typical microbial cells (0.5 to 2 μ m). When liquid films are too thin for a bacterium cell's complete immersion, the mobility between remaining aquatic habitats in unsaturated soils becomes severely restricted (Harris, 1981). In addition, the microorganisms will most likely be immersed in corners and cylindrical capillaries when the films are too thin (Figure 4.4-a). Figure 4.4-d displays the maximal radius of a fully-immersed microbe in a cylindrical capillary and corners with different angles for a range of matric potentials. It is clear that even under relatively wet conditions (matric potential -50 J/kg), the size of typical liquid element in corners and cylindrical capillaries is smaller than the average microbial diameter (~ 1 μ m). Figure 4.5 shows the correlation between the matric potential and the effective film thickness of flat and rough surfaces. In Figure 4.5, L is the depth of a roughness element, β is a dimensionless scaling factor for film-covered spacing between groove elements, and γ is the pit or groove angle.

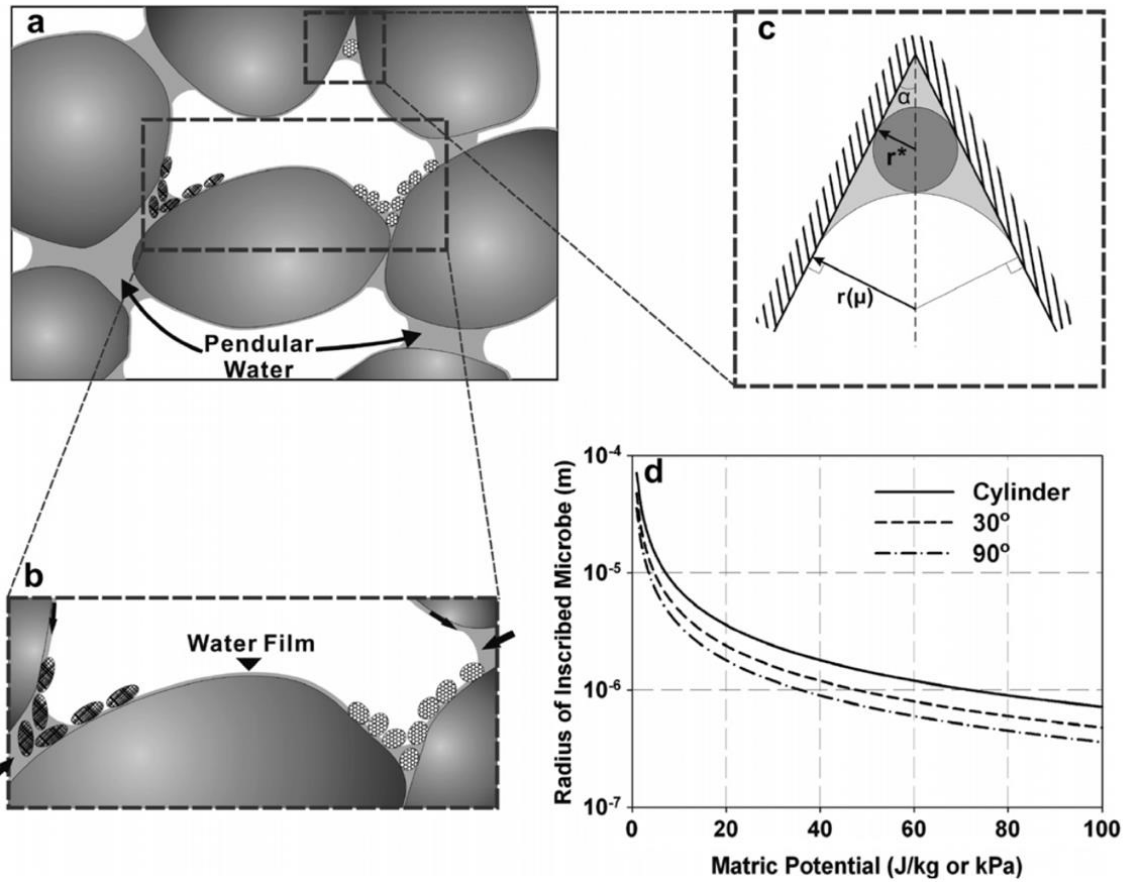


Figure 4.4 (a) An illustration of microbes inhabiting soil pore spaces concentrating in corners and crevices where water is comparatively abundant; (b) potential for nutrient flux interception due to diffusion limitation and microbial consumption (arrows indicate nutrient flux); (c) definition sketch for the size of aquatic habitat in a corner bounded by liquid-vapor interface and a spherical or cylindrical fully-immersed microbe behind the interface; and (d) calculated maximal radius of fully-immersed microbe in a cylindrical capillary, and in corners with different angles for a range of matric potential values. Note that (d) does not represent the immersion in thin films.

Source: (Long & Or, 2005)

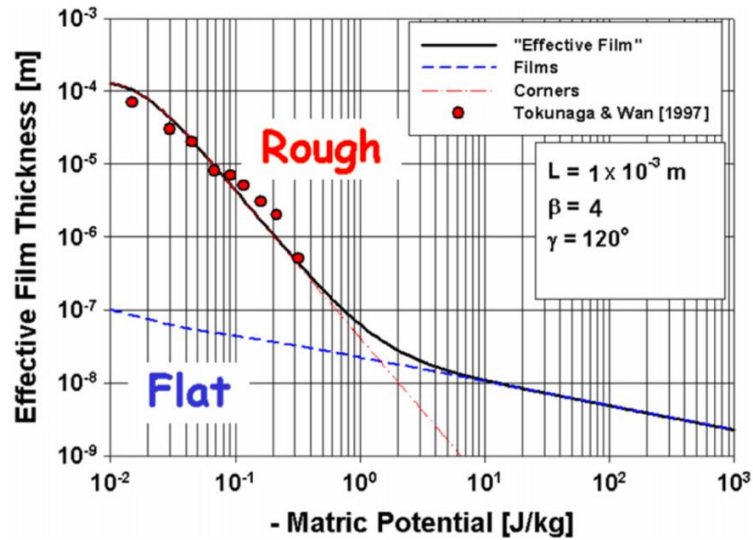


Figure 4.5 Comparison of theoretical effective film thickness on smooth and rough surfaces as a function of matric potential, based on measurements from Tuff rock surface obtained by Wan and Tokunaga (1997).

Source: (Or & Tuller, 1999; Or et al., 2007)

4.2.5 Viscosity

The effective viscosity of water near the walls of sediments (within 10 to 20 nm) increases by up to ten-fold, as predicted based on the Eyring equation amended with the solid surface energy barrier (Feng et al., 2018). A bacterium's motility is usually affected by viscosity, depending on the type of microorganism involved and its flagellar arrangement (Schneider & Doetsch, 1974). However, because water's viscosity only increases in a very thin layer near the walls, it would most probably not affect the microorganisms given their relatively much larger size.

4.2.6 Solid-water and Air-water Interfaces

The retention of microbes by porous media is partly a function of the degree of saturation. When the degree of saturation is very low, the bacteria will most likely be attached to the solid-water interface, with limited mobility, which is not necessarily the case when the pores are fully saturated. Ebrahimi and Or (2014) explain how the fragmented aqueous

phase occupying complex soil pore spaces suppresses motility and limits dispersal ranges – an important mechanism for maintaining microbial diversity and soil ecological functions – in unsaturated soils. On the other hand, if the water content is high (about 40 to 80% saturation), the microbes tend to attach to air-water interfaces (Blanchard & Syzdek, 1972; Marshall & Cruickshank, 1973; Dahlbäck et al., 1981; Wan et al., 1994; Powelson & Mills, 1996) since the interaction energy of cell-air bubbles is more attractive than that of the cell-solid interface. Attachment to air-water interfaces, which is irreversible because of capillary forces, strongly influences the movement and spatial distribution of microorganisms (Wan et al., 1994).

4.2.7 Nutrients and Desiccation

A low degree of saturation can negatively affect the nutrient availability for microorganisms (Or et al., 2007). Though, this might not be necessarily the case in coastal sediments. Based on Geng et al. (2021), a relatively high nutrient concentration was detected in the upper parts of shorelines. Nevertheless, the moisture content in the supratidal zones was low. Under such conditions, bacteria might need to rely on biofilms to protect them from desiccation. In extreme cases, however, some bacteria could react against dryness by producing endospores (Chen & Alexander, 1973), which are dormant, tough, and non-reproductive structures produced by some microorganisms to protect their genetic material (Nicholson et al., 2000). Moreover, the microorganisms in the transiently hypersaline supratidal zones might be more vulnerable to desiccation since high salinities cause the bacterium to lose water due to osmosis, especially if the microorganisms involved are not halophilic or halotolerant. Generally, microbial biomass and activity tend to be

reduced in saline soils (Rietz & Haynes, 2003), and modeling studies on the effects of porewater salinity in sediments on microorganisms are lacking (König et al., 2020).

4.2.8 Pressure

In unsaturated sediments, water would be held in place by suction (i.e., negative pressure) due to its cohesion, adhesion, and surface tension properties. However, such pressure might not necessarily affect the microorganism's activity. Prince et al. (2016b) analyzed the biodegradation of oil in the deep ocean. Seawater (natural inoculum) from a depth of eight meters was used in the experiment. The biodegradation rate decreased only by 30% when increasing the pressure from 0.1 MPa (atmospheric pressure) to 15 MPa, representing the deep sea at a depth of 1,500 m (Prince et al., 2016b). This indicates that the suction pressure near the moist wall of sediments might not necessarily inhibit the microbial activity. Nonetheless, the pressure imposed on bacteria in the deep ocean comes from all directions, and therefore, it might cancel out. But for the case of unsaturated sediments, the pressure (suction) is coming only from one direction (the solid's surface), which might affect the microorganisms differently.

4.3 Conclusion

It seems that there are several factors that might negatively affect the microbial activity in unsaturated soils. However, various microorganisms possess several physical, chemical, and biological mechanisms to overcome such challenges. The next chapter presents an experiment whereby oil biodegradation is investigated in unsaturated beach sand by conducting oil chemistry, metataxonomic, and metagenomic analyses.

CHAPTER 5

BIOREMEDIATION OF HYDROCARBONS IN SANDY BEACHES

5.1 Objectives of the Experiment

The results of the experiment in Chapter 3 indicate that the hydrocarbonoclastic activity in marine and coastal ecosystems will drastically slow down when subject to hypersaline conditions. Therefore, it is most likely that the biodegradation of petroleum hydrocarbons in the upper parts of oil-contaminated sandy beaches will be much slower relative to that of dispersed plumes (i.e., seawater with dispersed oil at few ppm). However, the experimental design in Chapter 3 did not account for the other effects that might allow the persistence of petroleum hydrocarbons in oil-contaminated sandy beaches, such as high oil concentrations (i.e., thousands of ppm), low moisture content (i.e., degree of saturation), and nutrient limitation (i.e., low availability of inorganic N and P).

In this chapter, oil biodegradation was investigated using sand columns prepared by mixing sampled beach sand infiltrated with natural inoculum (seawater) at different salinities while achieving a moisture content similar to that in supratidal zones. In addition, the oil concentrations used were similar to those observed on beaches contaminated by large oil spills. Furthermore, the loss of hydrocarbons due to evaporation was assessed using sterile experiments to dissociate between biotic and abiotic hydrocarbon removal, and positive controls consisted of dispersed oil in natural seawater. Oil chemistry, 16S rRNA gene amplicon, and metagenomic sequencing analyses were conducted every 30 days for 180 days.

5.2 Materials and Methods

5.2.1 Seawater Sampling, Evaporation, and Analysis

Seawater (100 L) was collected from the Manasquan Inlet, New Jersey, USA (40.1021° N – 74.0332° W), and then slowly evaporated as discussed in Subsection 3.2.1. After the formation of the concentrated brine, another batch of fresh seawater was collected from the same location to prepare the saline blends (Subsection 5.2.2). The collected seawater and the concentrated brine were analyzed for salinity, pH, dissolved oxygen, nutrients, and ions (Table 5.1). Salinity was determined by measuring the total dissolved solids content using standard method 2540D (APHA et al., 2017), the pH was measured using a pH meter (Aqua Shock, Sper Scientific, 850056), the DO was measured using CHEMets visual kit (K-7512), and nutrients (N-NH₄⁺, P-PO₄³⁻, N-NO₃⁻, and N-NO₂⁻) were measured through spectrophotometry (ultra-vis spectrophotometer, Cole-Parmer, 4802) using Low Range Hach reagents (HACH Company, Loveland, Colorado). Ions, comprising most of the dissolved components in seawater (Cl⁻, K⁺, Na⁺, SO₄²⁻, Mg²⁺, and Ca²⁺), were measured through colorimetry using Hach reagents (HACH Company, Loveland, Colorado).

Table 5.1 Properties of Seawater and Concentrated Brine

Parameter	Seawater For Evaporation	Concentrated Brine	Seawater For Setup
Volume (L)	100	10	40
pH	7.6	7.8	7.7
DO (ppm)	8.2	3.1	8.7
TDS (ppm)	32800	282060	31200
Cl ⁻ (ppm)	17700	159500	16900
Na ⁺ (ppm)	9900	83100	9600
Mg ²⁺ (ppm)	1200	8300	1100
Ca ²⁺ (ppm)	380	2900	410
SO ₄ ²⁻ (ppm)	2500	21500	2400
K ⁺ (ppm)	360	2400	350
N as NO ₃ ⁻ (ppm)	0.2	2.1	0.3
N as NO ₂ ⁻ (ppm)	< 0.1	0.2	< 0.1
N as NH ₄ ⁺ (ppm)	< 0.1	0.5	< 0.1
P as PO ₄ ³⁻ (ppm)	< 0.1	0.3	< 0.1

Note: DO = Dissolved Oxygen, TDS = Total Dissolved Solids.

5.2.2 Preparing the Saline Blends

Two sets of three live blends were prepared by mixing the brine with fresh seawater at different proportions to achieve salinities of 30, 90, and 160 g/L, as discussed in Subsection 3.2.2. In one of the sets, nutrients were added (10 mg N/L by adding NH₄NO₃, and 2 mg P/L by adding KH₂PO₄) to the recommended nutrient concentration range for bioremediation of oil-polluted sandy beaches (2 - 10 mg N/L (Du et al., 1999) with an N:P ratio of 5:1 (Smith et al., 1998)). Concomitantly, one set of three sterile blends to assess abiotic losses was prepared by mixing Milli-Q water with mercuric chloride (50 mg/L) to halt any microbial activity, and sea salt (Pentair Aquatic Eco-Systems INC IS160) to achieve the same salinities (30, 90, and 160 g/L). Ultimately, there were three sets of saline

blends: one live without additional nutrients (i.e., indigenous nutrients), one live with additional nutrients, and one sterile.

5.2.3 Sand Sampling and Analysis

Sand (20 kg) was collected from the supratidal zone of Manasquan beach, New Jersey, USA (40.1021° N – 74.0332° W). The sand’s porosity, moisture content, and density were measured using ASTM methods D2216 and D7263. The grain size distribution of sand was derived through sieve analysis (Figure 5.1), and the organic content was determined by measuring the volatile solid content using standard method 2540E (APHA et al., 2017). The characteristics and properties of the collected sand are shown in Table 5.2. The sand was used for the experimental setup on the same day of sampling.

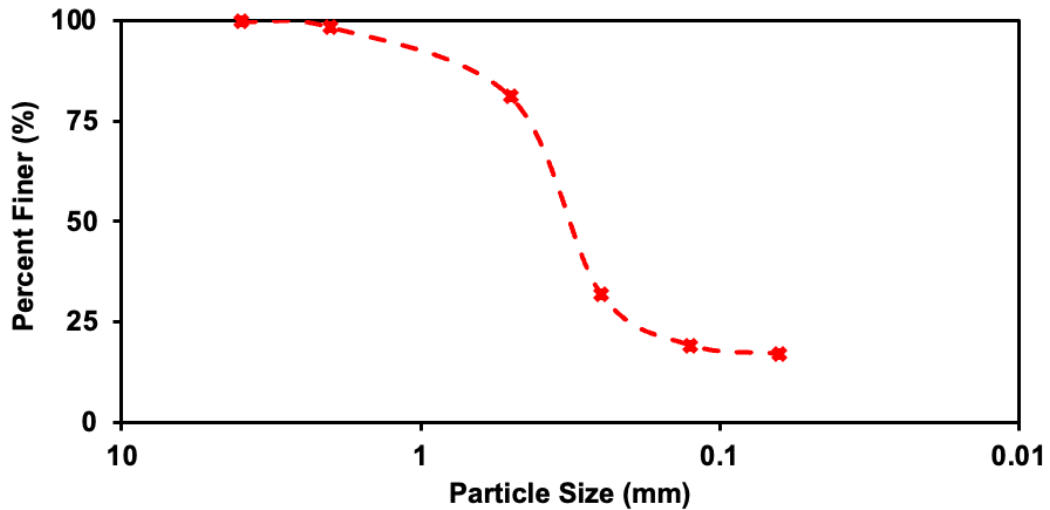


Figure 5.1 Particle size distribution curve of the sand.

Table 5.2 Properties of Sand

Sand Properties	Value
Dry Density (kg/m ³)	1575
Saturated Density* (kg/m ³)	1890
Porosity	0.32
Void Ratio	0.46
Moisture Content (%)	< 0.1
Volatile Solids (%)	< 0.1
D60 (mm)	0.65
D30 (mm)	0.45
D10 (mm)	0.3
Coefficient of Curvature	1.04
Coefficient of Uniformity	2.17

*The density at which the sand's voids are completely filled with seawater

Note: D₆₀ = 60% of sand particles that are finer than this size, D₃₀ = 30% of sand particles that are finer than this size, D₁₀ = 10% of sand particles that are finer than this size.

5.2.4 Experimental Setup

Hibernia crude oil (also used in the experiment of Chapter 3, Subsection 3.2.2) was used in this experiment. The oil was artificially weathered in a hood for five days (~20% loss by weight) to mimic the condition of weathered stranded oil on beaches. The initial concentration of representative GC-detectable hydrocarbons is presented in Figure 5.2. The crude oil was well mixed with the sand at a concentration of 1 mL/kg, which is an average of what was found in the supratidal zones of sandy beaches contaminated by the *Deepwater Horizon* blowout (Geng et al., 2021). The oiled sand was mixed with the live and sterile blends, resulting in nine sand mixtures: three live without additional nutrients, three live with additional nutrients, and three sterile. The degree of water saturation (i.e., % of water within the voids) used during preparation was 20% (i.e., volumetric moisture content of 6.3%), which is an average value of what is detected in the supratidal zones of beaches

(Geng et al., 2021). To ensure complete sterilization of the sterile mixtures, the sand was autoclaved (120°C and 0.16 MPa) before adding the oil and sterile saline blends. Another two sand mixtures were prepared at a much higher oil concentration (10 mL/kg) and infiltrated with fresh seawater (i.e., 30 g/L salt), one with additional nutrients and one without, to investigate the microbial activity at relatively high oil loadings. In addition, three sets of uncontaminated sand (i.e., without oil) were prepared by infiltrating with the live blends without additional nutrients to investigate the changes in the microbial population in the absence of oil.

Consequently, there was a total of 14 sand mixtures (Table 5.3), each placed in three glass columns (cylindrical glass tanks, 6.5 cm diameter, 10.5 cm height) to obtain triplicates. The sand mixtures were gently placed between two layers (2 cm each) of 4 mm glass beads (Fisher Scientific, Springfield, NJ) and without compression (i.e., as it would be on beaches). Ultimately, there were five batches of sand columns, ending up with a total of 51 microcosms, kept at room temperature (~20°C) for 180 days.

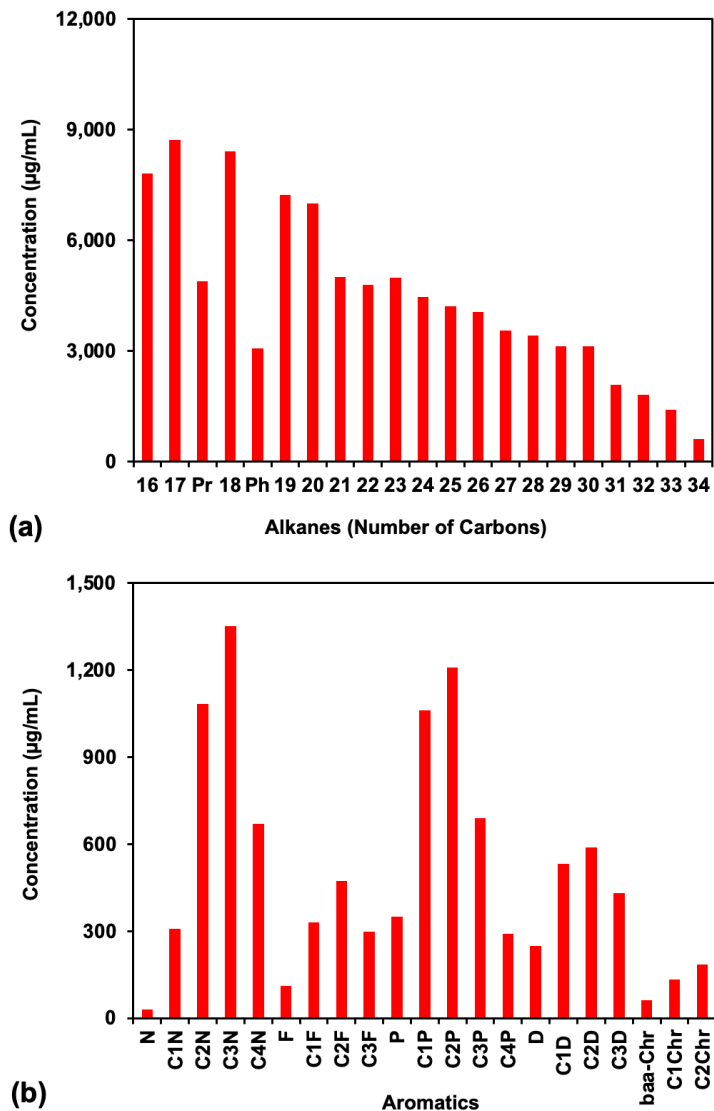


Figure 5.2 Initial concentration of the GC-detectable (a) alkanes and (b) aromatics in the Hibernia oil that was used in this experiment. Alkanes that were analyzed are from carbon number 16 (n-hexadecane) to carbon number 34 (n-tetraatriacontane). Pr and Ph represents pristane and phytane, respectively. Aromatics represent parent and alkylated naphthalenes (N), fluorenes (F), phenanthrenes (P), dibenzothiophenes (D), benz[a]anthracene (baa), and chrysenes (Chr), with C1-N indicating the sum of all methyl naphthalenes, C2-N indicating the sum of all dimethyl and ethyl naphthalenes, etc.

Table 5.3 Sand Mixtures

Sand mixture	Matrix	Pore water salinity (g/L)	Blend/ Batch #	Oil added (mL/kg)	Nutrients added
1	Sand infiltrated	30			
2	with	90	Live/1	1	No
3	seawater/brine	160			
4	Sand infiltrated	30			
5	with	90	Live/2	1	Yes
6	seawater/brine	160			
7*	Sand infiltrated	30			
8*	with poisoned	90	Sterile/3	1	No
9*	saline water	160			
10	Sand infiltrated	30			No
11	with seawater	30	Live/4	10	Yes
12	Sand infiltrated	30			
13	with	90	Live/5	None	No
14	seawater/brine	160			

*Sand was autoclaved and saline water was poisoned by adding HgCl₂ at a concentration of 50 mg/L

As a positive control, the same oil was added to 1 L of fresh seawater at a concentration of 10 µL/L in capped, but not sealed, flasks (GL 45 Media Bottle, Blue Polypropylene Cap), which were shaken vigorously to generate small oil droplets (i.e., dispersed plumes), and then left stationary. The seawater microcosms were prepared in duplicates, summing up to a total of 16 microcosms, of which four microcosms were sacrificed after each incubation period – two for oil chemistry analysis (Subsection 5.2.5) and two for microbial analysis (Subsections 5.2.6 and 5.2.7). The incubations lasted 30, 60, 90, 120, 150, and 180 days for all microcosms for oil chemistry analysis and 30, 90, and 180 days for microbial analysis. Figure 5.3 displays a flowchart of the experimental design and Figure 5.4 shows an image of the microcosms.

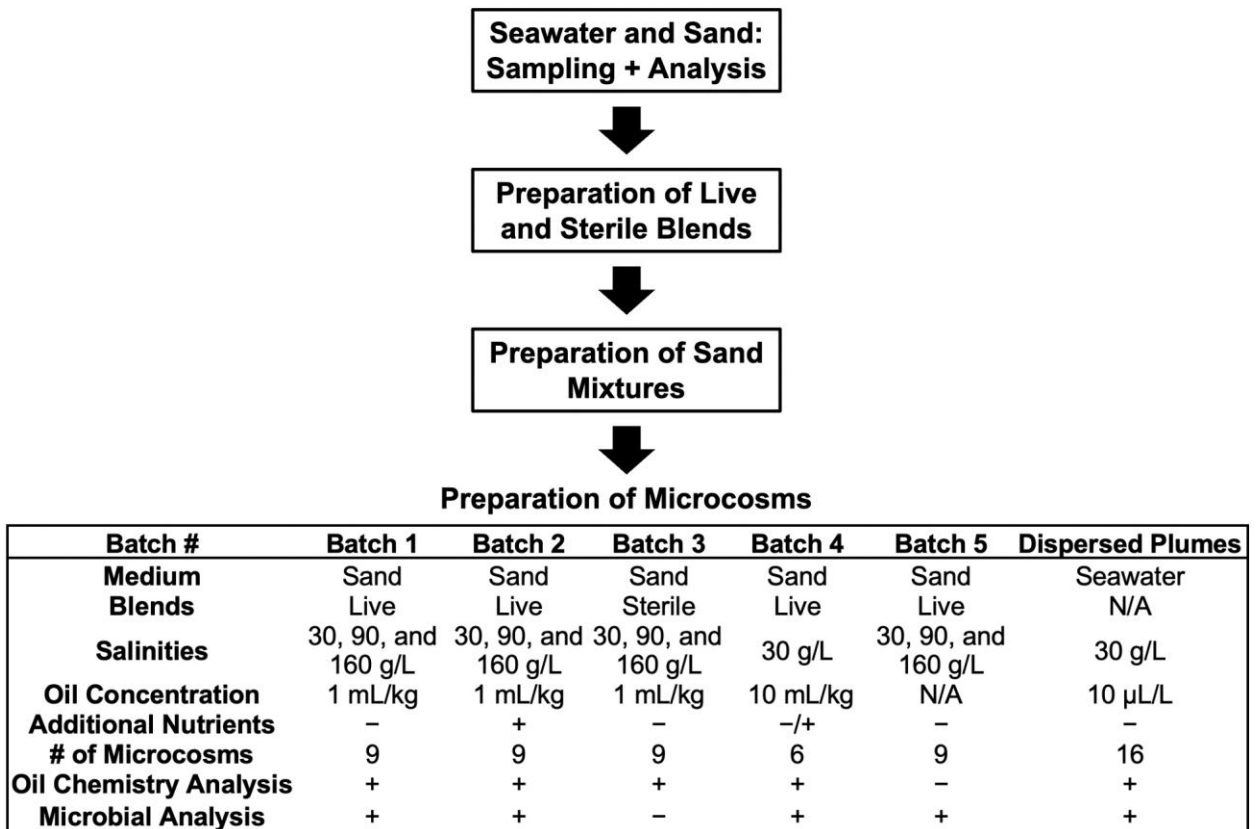


Figure 5.3 Flowchart of the experimental design. N/A = Not Applicable.



Figure 5.4 Sand column microcosms and seawater bottle (positive control). Note that there was a total of 42 columns and 16 bottles.

5.2.5 Oil Extraction and GC-MS Analysis

After each incubation period, 2 g samples were carefully removed from the sand columns and analyzed for moisture content to confirm that the degree of water saturation remained stable at 20%. An additional 20 g were carefully removed from the oil-containing sand columns (i.e., batches 1, 2, 3, and 4; Figure 5.3), dried using anhydrous sodium sulfate, and extracted with dichloromethane, as described in Abou-Khalil et al. (2022). The heavily oiled columns (10 mL/kg), were extracted only at the end of the experimental period (i.e., 180 days). For the positive control flasks (i.e., dispersed plumes), two of the seawater bottles were tested for dissolved oxygen and then sacrificed to extract the oil (Abou Khalil et al., 2021a). Extracted oils were analyzed using GC-MS (Gas Chromatography-Mass Spectrometry, Agilent 5973N, Benchtop GC having a 30 m X 0.25 mm ID film column DB-5ms, Millipore Sigma), along with appropriate standard samples (10 μ L of oil per mL of dichloromethane) before and after each run, and hydrocarbon removal was assessed using hopane as a conserved internal standard (Prince et al., 1994).

5.2.6 Preparation and Sampling for Microbial Analyses

Sampling. 10 g samples were carefully removed from the live sand columns (i.e., batches 1, 2, 4, and 5; Figure 5.3) and then placed in 50 mL sterile screw-cap tubes and stored in a freezer at -20°C . Sampling of the heavily oiled columns (10 mL/kg) was conducted only at the end of the experimental period (180 days). For the seawater flasks, two of them were filtered after each incubation period onto 0.2 μm polyethersulfone hydrophilic filters (Fisher Scientific, Springfield, NJ), using a Gast Vacuum pump (Fisher Model#: 0211-V45F-G8CX), and autoclaved filtration units. After filtration, the filters were immediately inserted into 15 mL sterile screw-cap tubes and stored in a freezer at -20°C . At the end of

the experimental period (180 days), the sand samples and filters, along with samples of the originally collected beach sand, fresh seawater, and concentrated brine were shipped overnight in a cooler with dry ice for microbial analyses.

Sample extraction and purification. Nucleic acids were recovered using the Quick-DNA Fecal/Soil Microbe MidiPrep kit from Zymo Research following the instructions of the manufacturer with the following modifications: DL-Dithiothreitol (Sigma-Aldrich, Oakville, ON, Canada) was added to the genomic lysis buffer instead of beta-mercaptoethanol. DNA samples were treated with RNase If (New England Biolabs, Whitby, ON, Canada), purified using a 1:1 volume ratio of magnetic beads from the Macherey-Nagel NucleoMag NGS Clean-up and Size Select kit (D-MARK Biosciences, Toronto, ON, Canada), then quantified using the Quant-iT PicoGreen assay from Fisher Scientific Ltd. (Edmonton, AB, Canada).

Preparation of 16S rRNA gene amplicon libraries and sequencing. The preparation of 16S rRNA gene amplicon libraries and sequencing were performed as described in Subsection 3.2.5

Preparation of metagenomic libraries and sequencing. Metagenomic sequencing libraries were prepared with 1 ng of DNA using the Nextera XT DNA Library Preparation Kit from Illumina (San Diego, CA, USA) following the instructions of the manufacturer. Normalization was performed by pooling equimolar amounts of libraries after quantification on the Agilent 4200 TapeStation System using the TapeStation High Sensitivity D5000 assay (Agilent Technologies, Mississauga, ON, Canada). The quality of the pooled library was assessed using the Agilent 4200 TapeStation System as described

above. The pool was sequenced on an Illumina NovaSeq 6000 S4 PE150 system on a rapid mode 2×150 bp configuration at the “Centre d'expertise et de services Génome Québec”.

5.2.7 Metataxonomics and Metagenomics

The sequencing of the 16S rRNA gene amplicon in 110 samples yielded a total of 6.8 Gb (i.e., Giga-base) of raw sequencing reads. They were analyzed using the NRC's amplicon bioinformatics pipeline AmpliconTagger (Tremblay & Yergeau, 2019), in which the reads are first subjected to a trimming and quality filtering step, then clustered according to their unique amplicon sequence variant sequence using the R package dada2 (v1.14.1; Callahan et al., 2016). A step of classification (RDP classifier v2.5; Wang et al., 2007) assigns the taxonomy to each ASV and a few more downstream analyses generate taxonomy tables and alpha/beta diversity matrices that are fed to a custom R package called Microbiomics to obtain principal coordinate analysis plots and abundance outputs. The custom online tool Shiny App was also used to create taxonomy graphs (Tremblay, <https://jtremblay2.shinyapps.io/taxonomy/>).

The 110 shotgun metagenomics sequence libraries represented 607 Gb of raw sequencing data. Once controlled for quality (removal and/or trimming of low-quality reads), 527 Gb packed in 3,516 M reads went into the novo co-assembly. Sequencing adapters were removed from each read and bases at the end of reads having a quality score <30 were cut off (Trimmomatic v0.39; Bolger et al., 2014) and scanned for sequencing adapter contaminant reads using BBDUK (<https://jgi.doe.gov/data-and-tools/bbtools/>) to generate quality controlled (QC) reads. The QC-passed reads from each sample were co-assembled using Megahit v1.2.9 (Li et al., 2016) on a three Tera-Bytes of RAM computer node with iterative kmer sizes of 31, 41, 51, 61, 71, 81, 91, 101, 111 and 121 bases.

Gene prediction was performed on each assembled contig using Prodigal v2.6.3 (Hyatt et al., 2010). Genes were annotated following the JGI's guidelines (Huntemann et al., 2015) including the assignment of KEGG orthologs (KO; Kanehisa and Goto, 2000). The QC-passed reads were mapped (BWA-MEM v0.7.17; Li and Durbin, 2009) against contigs to assess the quality of metagenome assembly and to obtain contig abundance profiles. Alignment files in bam format were sorted by read coordinates using samtools v1.9 (Li et al., 2009), and only properly aligned read pairs were kept for downstream steps. Each bam file (containing only properly aligned paired-reads only) was analyzed for coverage of called genes and contigs using bedtools (v2.23.0; Quinlan and Hall, 2010) using a custom bed file representing gene coordinates on each contig. Only paired reads both overlapping their contig or gene were considered for gene counts. Coverage profiles of each sample were merged to generate an abundance matrix (rows = contig, columns = samples) for which a corresponding CPM matrix (Counts Per Million – normalized using the TMM method, edgeR v3.36.0; Robinson et al., 2010) was generated. Taxonomic summaries were performed using a combination of in-house Perl and R scripts and DIAMOND blastp vs nr (v0.9.25) (Buchfink et al., 2014), part of the CAT package (v5.0.3) (von Meijenfeldt et al., 2019).

The gene abundance bubble plot was generated using the Calgary approach to ANnoTating HYDrocarbon degradation genes (CANT-HYD), a database of 37 Hidden Markov Models (HMMs) designed for the identification and annotation of marker genes that are critical for the aerobic and anaerobic degradation of alkane and aromatic hydrocarbons. The set of predicted genes was aligned against the CANT-HYD HMM database using HMM search (HMMER 3.3.2; Eddy, 1998) and an in-house R script was

used to convert the abundance values into RPKM (Reads Per Kilobase Million) and generate the bubble plot.

5.3 Oil Chemistry Analysis

5.3.1 Sterile Control Experiment

Figure 5.5 displays the GC-MS total ion traces of sterile experiments (Batch 3) along with the respective % loss of GC-detectable hydrocarbons. The evaporation rate of oil did not vary at different salinities, reaching about 18% loss after 180 days (Figure 5.5). In addition, the % loss from the sterile microcosms was considerably lower than what was observed in dispersed plumes (Chapter 3). This was expected since the sand column microcosms were capped and tightly sealed. Also, the Hibernia crude used in this experiment was artificially weathered for five days (20% loss by mass, Subsection 3.2.2), while in the previous experiment (Chapter 3, Subsection 3.2.2) the oil was artificially weathered for only one day (about 12% loss by mass), and therefore contained relatively a higher content of lighter components.

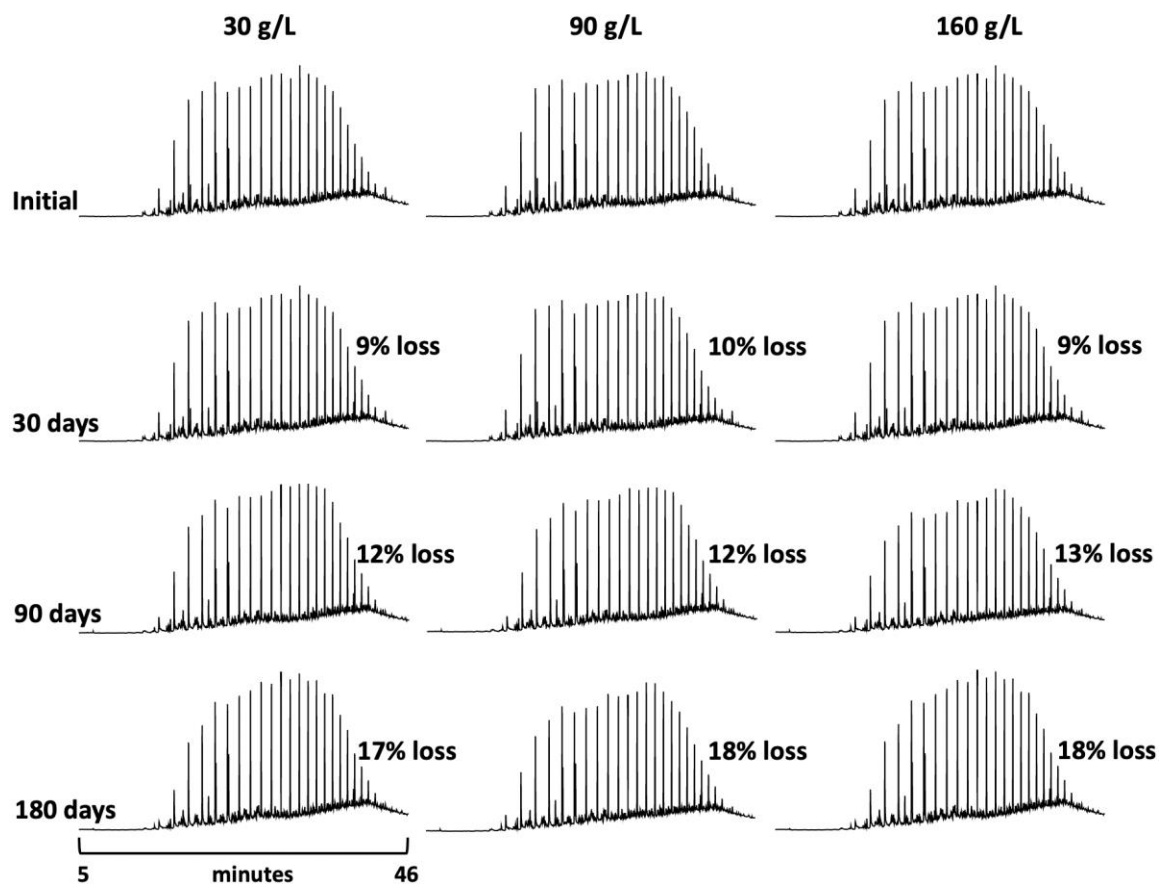


Figure 5.5 GC-MS profiles of crude oil remaining after 30, 90, and 180 days of incubation under sterile conditions: %loss represents abiotic removal, and chromatograms are normalized to hopane.

5.3.2 Biodegradation of Hydrocarbons

The moisture content in the sand column microcosms was $6.3 \pm 0.5\%$ (saturation of $20 \pm 1.2\%$) throughout the experiment. In the seawater flasks (positive control), dissolved oxygen levels were about 6.5 ± 1.6 mg/L during the entire experimental period, indicating favorable aerobic conditions where oil biodegradation can be sufficiently supported (Chiang et al., 1989; Michaelsen et al., 1992). Figure 5.6 shows the GC-MS traces of oil remaining in the sand column microcosms of batches 1 (indigenous nutrients) and 2 (additional nutrients) after 30, 90, and 180 days of incubation. Note that the “% loss” represents the loss due to both biodegradation and (minimal) evaporation. Figure 5.7 shows

the percentage of GC-detectable hydrocarbons remaining in microcosms of batches 1 and 2, due to biodegradation, without including the minor evaporation losses. For comparison, the percentage remaining from the sterile microcosms (batch 3) and the seawater flasks (positive control) is also provided (Figure 5.7).

As expected, the biodegradation of hydrocarbons was extensive in natural seawater (positive control), and most of the alkanes and aromatics were degraded within 30 days (Prince et al., 2013; Prince et al., 2016b; Wang et al., 2016; Zhuang et al., 2016; Olson et al., 2017; Prince et al., 2017; Brakstad et al., 2018; Ribicic et al., 2018; Abou Khalil et al., 2021a). In the sand column microcosms, however, the degradation of hydrocarbons was much slower at all salinities, most probably due to the much higher effective oil concentration (Figures 5.6 and 5.7). The biodegradation of pristane and phytane (both branched alkanes), which are among the highest peaks in the 30 g/L salt microcosms at $t = 30$ days, was slower relative to other alkanes (Pirnik et al., 1974; Prince et al., 2007; Prince et al., 2016b), but they were mostly consumed within 180 days (Figure 5.6).

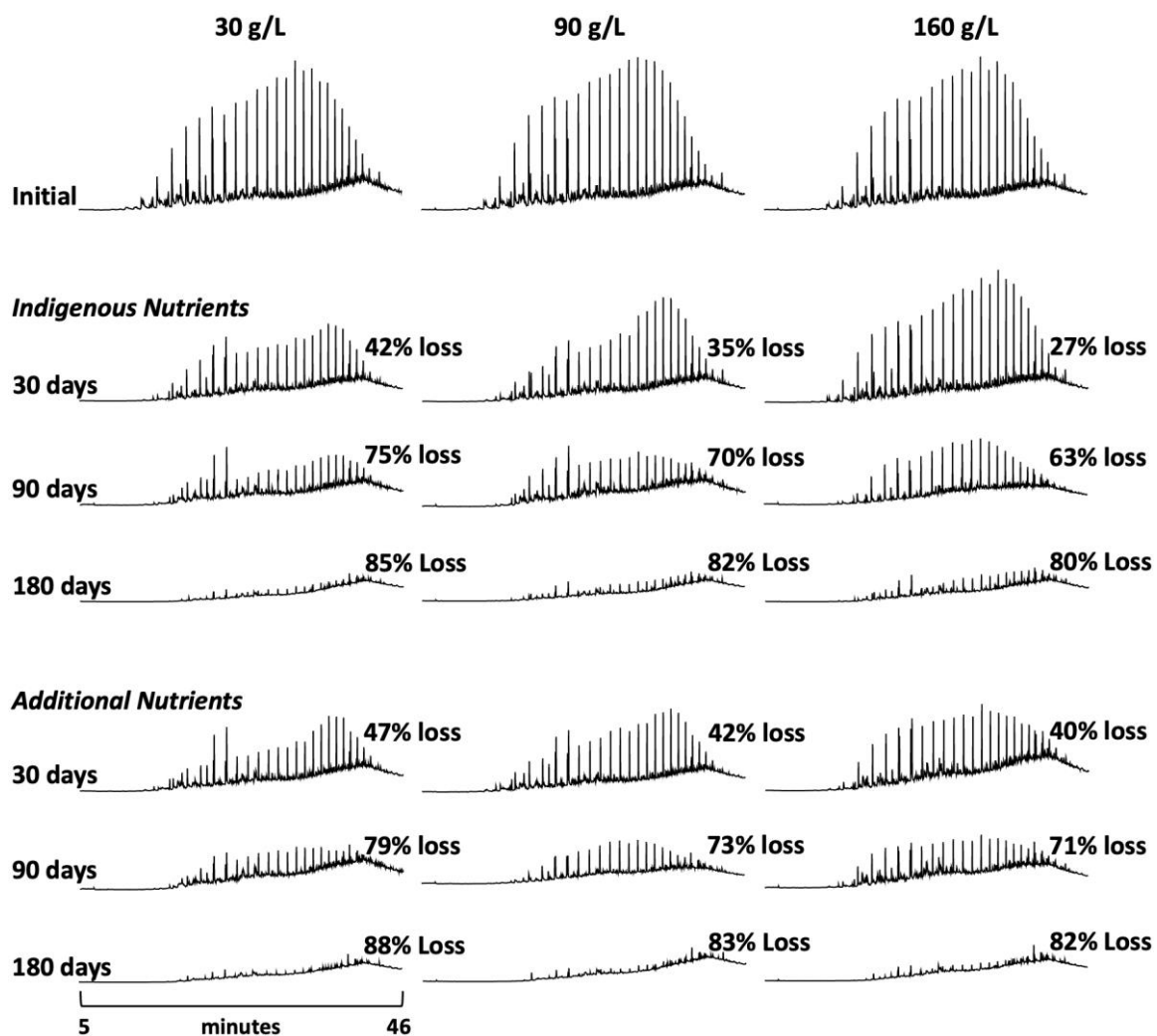


Figure 5.6 GC-MS profiles of crude oil remaining after 30, 90, and 180 days of incubation with and without the addition of nutrients: % loss represents total removal, and chromatograms are normalized to hopane.

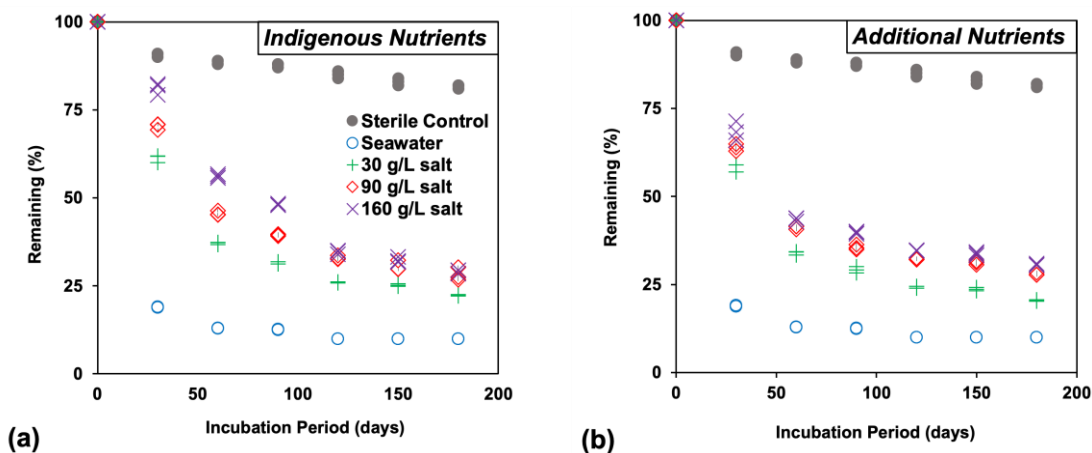


Figure 5.7 The %remaining of the GC-detectable hydrocarbons with (a) indigenous nutrients and (b) additional nutrients, due to the effect of biodegradation. Data from the sterile control and seawater flasks is also provided for comparison. Half-life of dispersed oil in seawater was 18.5 days. Half-lives in microcosms that underwent natural attenuation were 40.2, 58.1, and 76.5 days at 30, 90, and 160 g/L salt. Half-lives in microcosms that underwent biostimulation were 34.4, 43.2, and 49.1 days at 30, 90, and 160 g/L salt.

Biodegradation of oil was clearly slower at higher salinities but somewhat reached the same endpoint after 180 days (Figures 5.6 and 5.7). The apparent half-life of crude oil in the sand column microcosms slowed by about 50 and 30% in batches 1 (indigenous nutrients) and 2 (additional nutrients), respectively, when increasing the salinity from 30 to 160 g/L (Figure 5.7). In our previous work, however, the crude oil half-life slowed by 20-fold as salinity increased from 30 to 160 g/L (Section 3.3). This is illustrated in Figure 5.8 which displays how the decrease in the apparent rate constant (k) at higher salinities was much more significant in seawater than in sand. In fact, the half-life of the oil in the sand was relatively slow even at the salinity of seawater (Figure 5.7). This is most probably due to the higher effective oil concentration in contaminated sandy beaches (average of 25,000 ppm at 6.3% volumetric moisture content) relative to dispersed plumes (few ppm). Nonetheless, this doesn't imply that the biodegradation rate of oil (as mass per unit time) decreases at higher oil concentrations. Actually, it is expected that, when increasing

bioavailability (i.e., oil concentration), the biodegradation rate of oil (mass per unit time) increases while the half-life becomes longer (Prince et al., 2017).

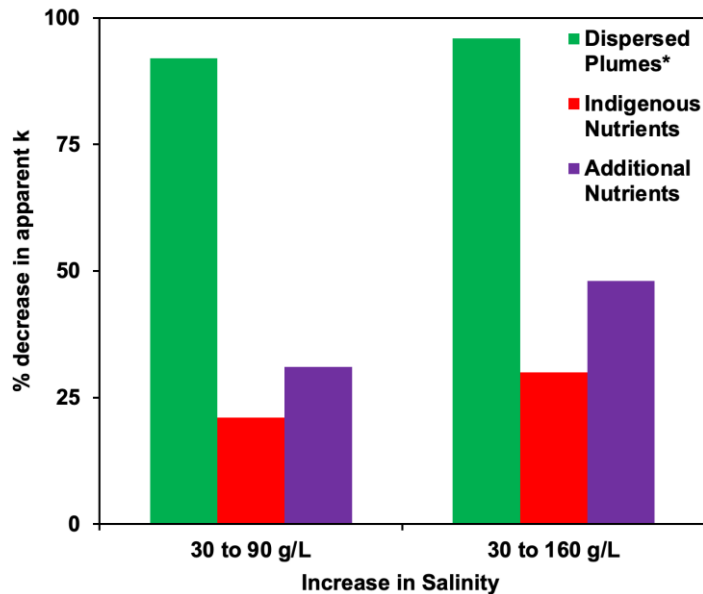


Figure 5.8 The % decrease in apparent first-order rate constants (k) at different salinities of GC-detectable hydrocarbons in seawater (dispersed plumes) and sand (with and without additional nutrients). *Data for dispersed plumes was taken from Chapter 3.

The addition of nutrients (Batch 2) enhanced the degradation of hydrocarbons in the sand (Figure 5.6, 5.7, and 5.8), decreasing the apparent half-life between 14 and 36%. This is similar to that seen in other laboratory and small-scale field experiments (Venosa et al., 1996; Pontes et al., 2013; Becker et al., 2016) but smaller than that seen in the relatively nutrient-poor waters of Prince William Sound (3 to 5-fold, (Bragg et al., 1994)) and Svalbard (2-fold, (Prince et al., 2003)), where nutrient limitation of biodegradation would be expected to be more evident. Due to evaporation and infrequent inundations, the upper parts of beaches are rich in nutrients relative to the intertidal zones (Geng et al., 2021), and our experiments mimicked that by using evaporated seawater, not inorganic

salt, to raise the salinity in our microcosms. Thus, it is not surprising that nutrient availability is not a limiting factor as it is in nutrient-poor environments.

Figure 5.9 illustrates the apparent first-order rate constant of individual hydrocarbons for the unfertilized and fertilized columns. Note that Figure 5.9 represents the effect of biodegradation derived from the sterile and live data, by subtracting the small losses due to evaporation. Small alkanes (< C16) were mostly lost through evaporation. Alkanes from C16 to C19 were also subject to evaporation (Figure 5.5), but biodegradation was the major contributor to their removal in the active incubations. Similarly, some PAHs such as the naphthalenes, fluorenes, phenanthrenes (P and C1-P), and dibenzothiophenes (D and C1-D) showed some evidence of evaporation, but biodegradation was more important. Interestingly, the biodegradation of the aromatics was much more affected at high salt than the alkanes (Figure 5.9). This was not the case in seawater (Section 3.3), where the degradation of both alkanes and aromatics was substantially inhibited at high salinities.

As expected, biodegradation of phenanthrene (P) and its alkylated congeners (up to those with the equivalent of two methyl substituents, C1-P – C2-P), was almost complete after 30 days in seawater (Prince et al., 2013; Prince et al., 2016b; Prince et al., 2017). In the sand column microcosms (batches 1 and 2), however, the phenanthrenes (parent and alkylated) partly remained in the oil, for up to 120 days at 30 g/L salt and 180 days at higher salinities, with and without additional nutrients. The apparent rate constant of benz[*a*]anthracene (Baa) and chrysene (Chr) – the most abundant 4-ring aromatics in crude oil – and chrysene's alkylated congeners (up to those with the equivalent of two methyl

substituents, C1-Chr and C2-Chr) was relatively very low, in both seawater and sand column microcosms, and again losses were lower at higher salinities (Figure 5.9).

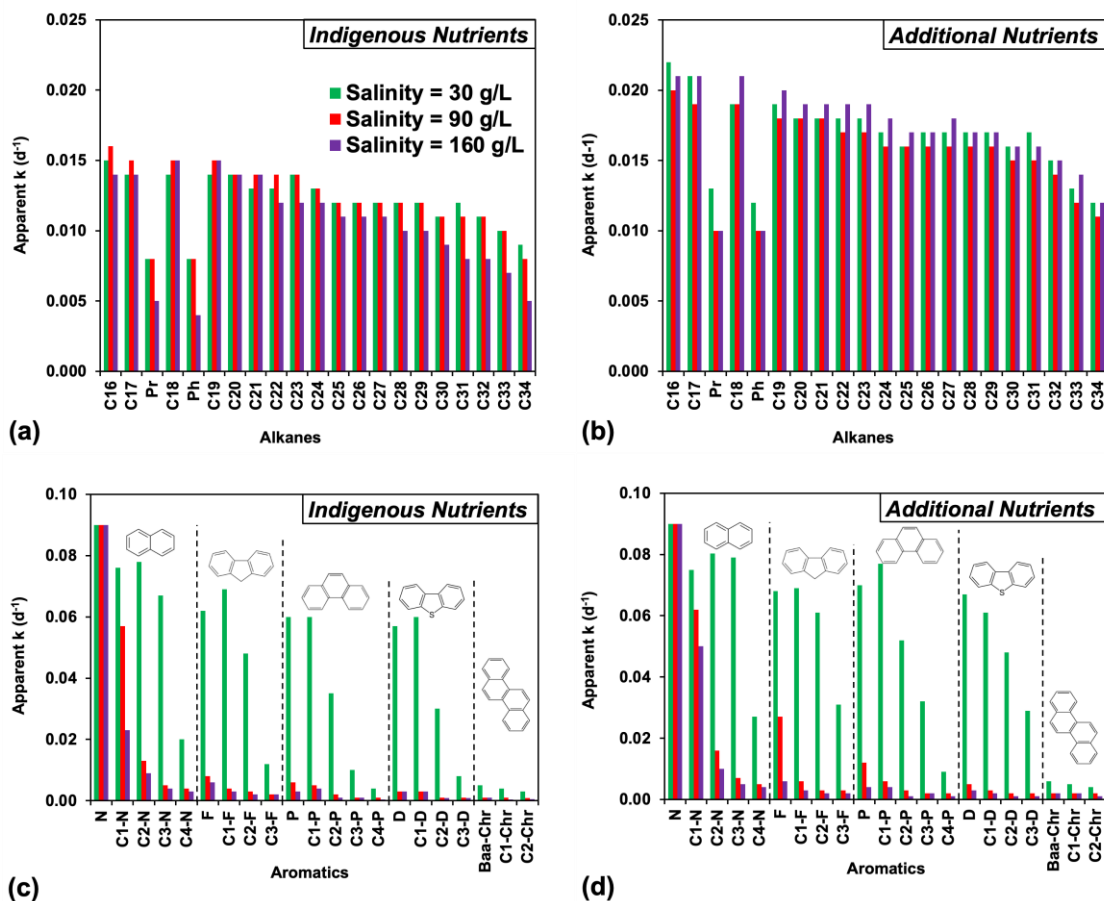


Figure 5.9 Apparent first-order rate constants (k) at different salinities of (a, b) measurable alkanes from carbon number 16 (n-hexadecane) to carbon number 34 (n-tetratriacontane), (c, d) and parent and alkylated naphthalenes (N), fluorenes (F), phenanthrenes (P), dibenzothiophenes (D), benz[a]anthracene (Baa), and chrysenes (Chr), with C1-N indicating the sum of all methyl naphthalenes, C2-N indicating the sum of all dimethyl and ethyl naphthalenes, etc. (a) and (c) are for microcosms that underwent natural attenuation, and (b) and (d) are for the microcosms that underwent biostimulation. Apparent k for naphthalene (N) could be higher since it was not detected at any incubation period.

Figure 5.10 displays the GC-MS traces of the oil in the seawater flasks and in the unfertilized and fertilized sand columns at different oil concentrations (1 and 10 mL/kg) after 180 days of incubations, at the salinity of seawater (30 g/L). As anticipated, the half-life of oil in seawater (positive control) was relatively rapid (only 18 days, see (Wang et

al., 2016; Prince et al., 2017; Brakstad et al., 2018)). The half-life of crude oil in the sand columns at a concentration of 1 mL/kg was about double that observed in seawater and slightly varied between batches 1 (indigenous nutrients) and 2 (additional nutrients). The apparent half-life of oil increased substantially when increasing the concentration of crude oil in the sand by 10-fold, and although adding nutrients somewhat improved the degradation of petroleum hydrocarbons, the concentration of oil seems to be the most impactful on the degradation rate.

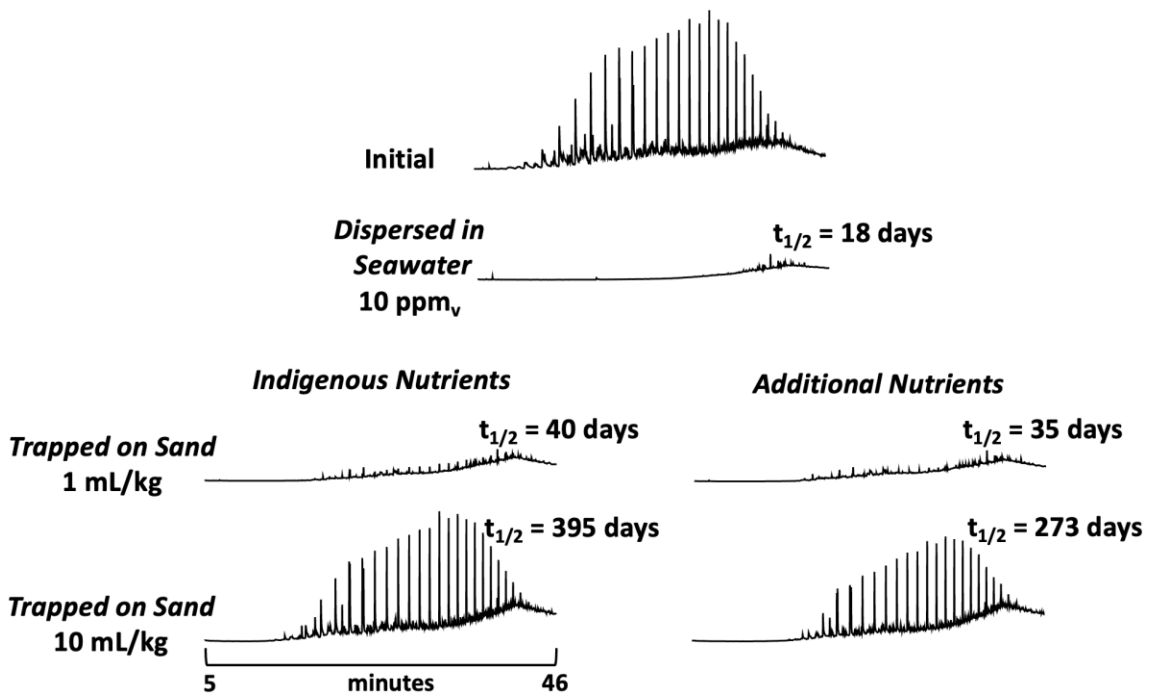


Figure 5.10 GC-MS profiles of crude oil remaining after 180 days for the seawater microcosms (positive control), and the oiled sand columns at a concentration of 1 and 10 mL/kg, with and without nutrients, at a salinity of 30 g/L. Chromatograms are normalized to hopane.

5.4 Microbial Analysis

5.4.1 Metataxonomic Analysis

The taxonomy profiles of the 20 most abundant genera identified in fresh seawater and concentrated brine using 16S rRNA gene amplicon analysis are presented in Figure 5.11. As anticipated, the relative abundance of the detectable genera in seawater (e.g., *Planktomarina*, *Clade 1a*, *Rickettsiales*, *NS5 marine group*, *NS3a marine group*, etc.) was significantly lower in the concentrated brine, while the abundance of halophilic bacteria, such as *Methylophaga* (Doronina et al., 2003), and *Rubinisphaera* (Ferreira et al., 2016), increased substantially, indicating that such genera were capable of surviving the extremely hypersaline conditions (280 g/L salt). The microbial population in the dry sand was mainly composed of bacteria pertaining to the *Gillisia*, *Gramella*, *Deinococcus*, and *Nocardioides* genera (Figure 5.12), which were not among the 20 most abundant genera in the seawater or concentrated brine (Figure 5.11). The taxonomy of the sand was not affected after infiltrating with the live blends (Figure 5.12) most probably because the unsaturated layer in sedimentary ecosystems (i.e., the vadose zone) supports the highest microbial density of all biosphere compartments, exceeding the oceans by several orders of magnitude (Torsvik et al., 2002), and sediments with relatively large pores, such as beach sand, could allow the formation of isolated water films which provide more opportunities for increased bacterial diversity and abundance (Chau et al., 2011).

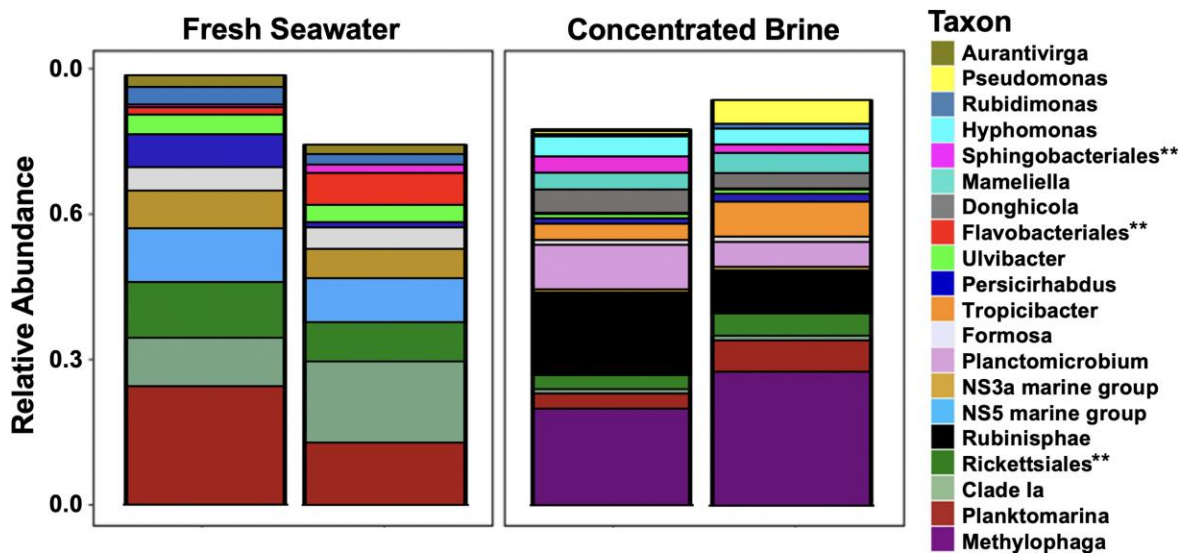


Figure 5.11 Taxonomy of the 20 most abundant genera identified in fresh seawater and concentrated brine at the beginning of the experiment. The color coding in the stacked graphs follows the same sequence as the colors in the legend from bottom to top. The sequences are essentially 'equivalent taxonomic units' identified to the genus, but based on the database used, some are identified to the order (**).

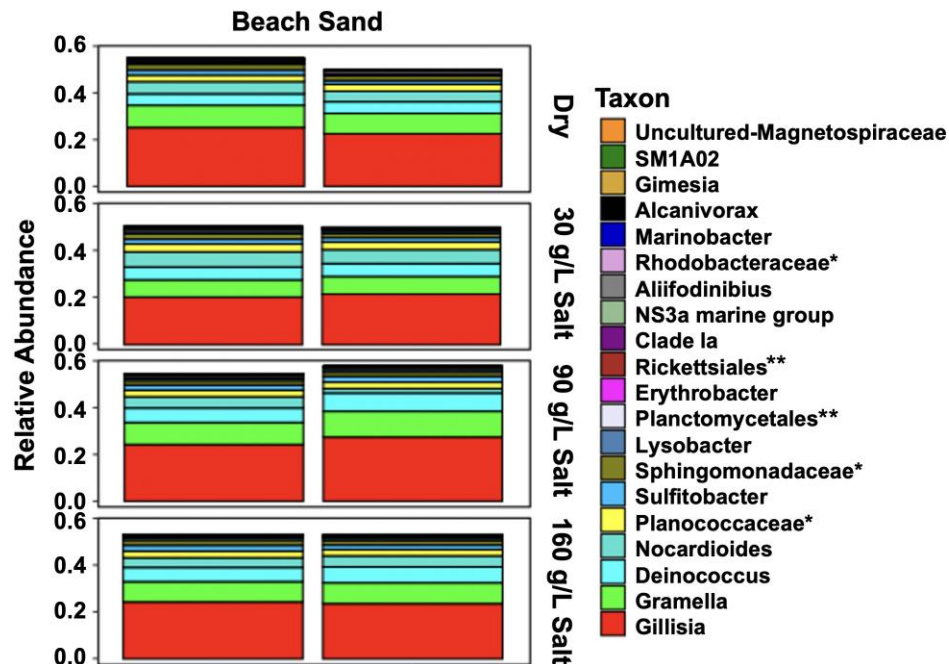


Figure 5.12 Taxonomy of the 20 most abundant genera identified in dry beach sand and in beach sand infiltrated with the live blends (20% saturation) at different salinities at the beginning of the experiment ($T = 0$). The color coding in the stacked graphs follows the same sequence as the colors in the legend from bottom to top. The sequences are essentially 'equivalent taxonomic units' identified to the genus, but based on the database used, some are identified to the family (*) or order (**). Note: It has been proposed to move *Planococcaceae* into *Caryophanaceae* (Gupta and Patel, 2020).

The bacterial alpha diversity for the seawater (i.e., dispersed plumes) and sand column microcosms at different salinities is presented in Figure 5.13. In the dispersed plumes, there was a slight initial increase in alpha diversity over time followed by a slow decrease, which is comparable to what was found in our previous study (Abou Khalil et al., 2021a). Similarly, alpha diversity showed an initial increase at 30 g/L salt but decreased somewhat over time. At 90 g/L salt, alpha diversity decreased initially and then increased to approximately initial levels by the end of the incubation period. At 160 g/L salinity, alpha diversity decreased substantially and became stable at a lower level till the end of the incubation period (Figure 5.13).

Principal coordinate analysis of the amplicon sequence variants showed that the microbial communities in the dispersed plumes were quite similar throughout the experiment but notably different from the populations associated with the sand column microcosms (Figure 5.14). At the beginning of the experiment, all sand samples clustered together, but they diverged as the incubations proceeded. The columns amended with 90 and 160 g/L salt clustered closely suggesting that they were more similar taxonomically than the ones at 30 g/L salt.

Figure 5.15 displays the taxonomic profiles of the 20 most abundant genera identified in the seawater bottles (i.e., dispersed plumes) at different incubation periods. At the beginning of the study ($T = 0$), hydrocarbon degraders, such as *Ulvibacter* (Prabakaran et al., 2007) as well as members of the *Sphingobacteriales* order (Pagé et al., 2015; Xue et al., 2016), were already observed in the dispersed plumes. After 30 days of incubation, additional hydrocarbon degraders, such as *NRL2* (pertaining to the *Alphaproteobacterial* class, (Kim & Kwon, 2010)) and *Alcanivorax* (Golyshin et al., 2003), became among the 20 most abundant taxons and remained relatively abundant throughout the study even after 180 days of incubation. *Thalassospira*, a genus

known for its ability to degrade aromatics (Zhao et al., 2010), was observed after 90 days of incubation and until the end of the experiment.

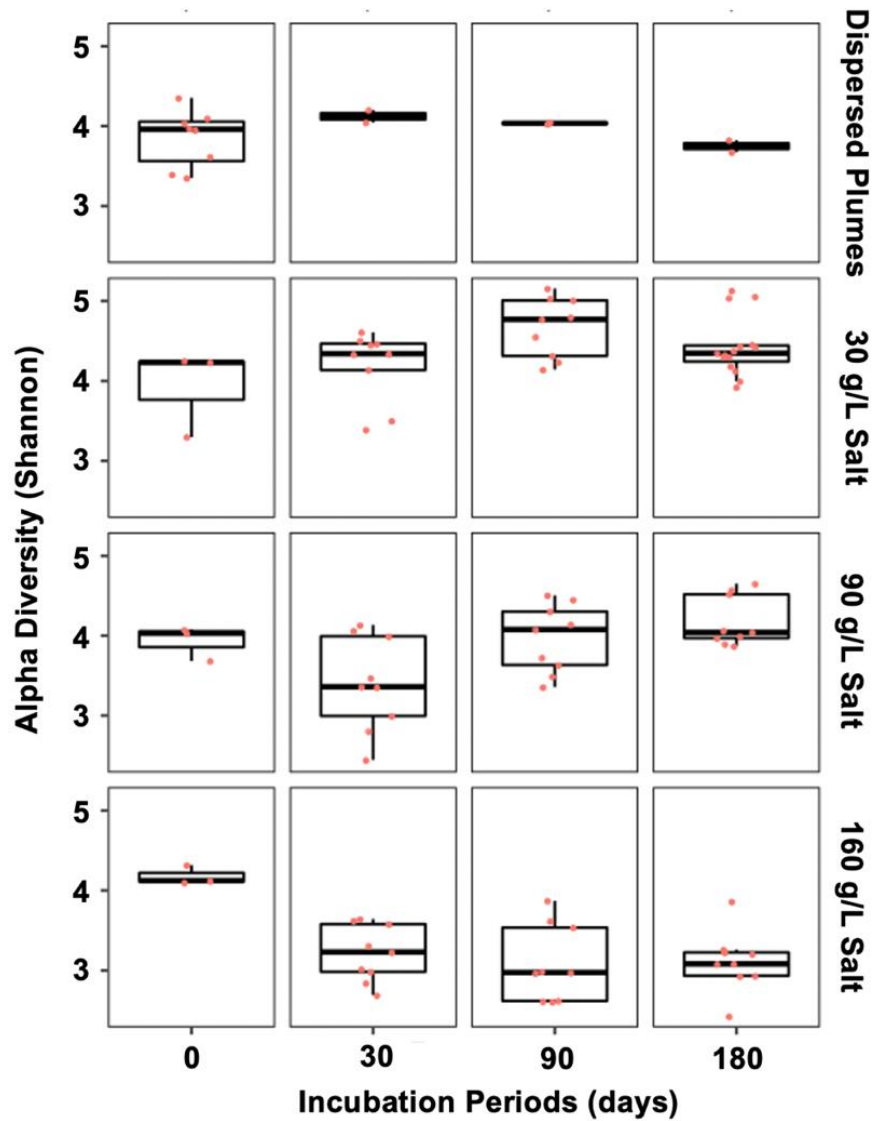


Figure 5.13 Bacterial alpha diversity in the seawater bottles and sand column microcosms at different salinities.

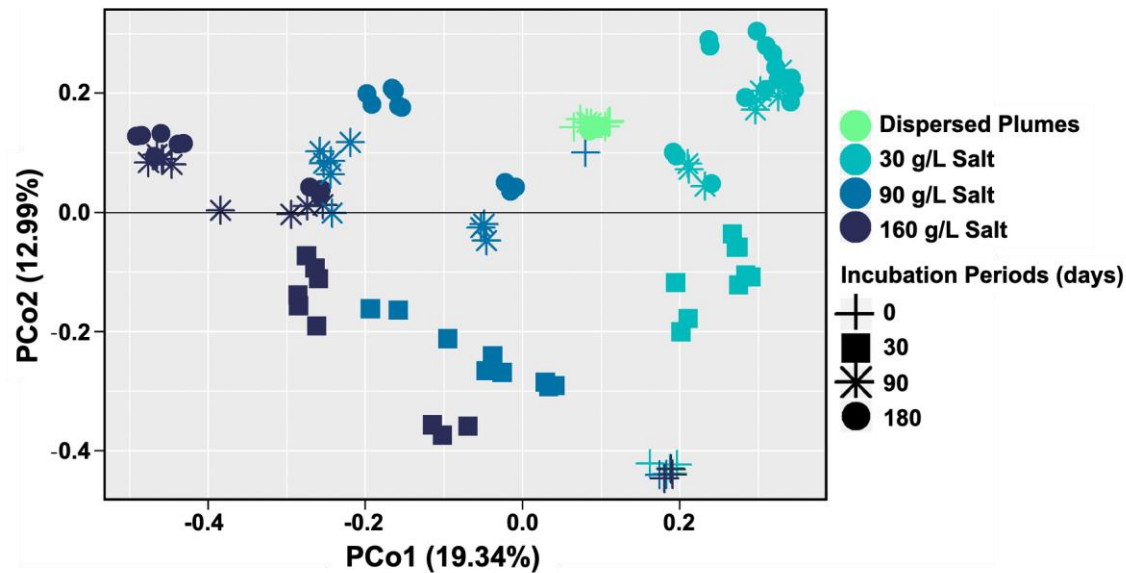


Figure 5.14 Beta diversity of the total microbial community in the seawater bottles and sand column microcosms with respect to salinity and incubation period.

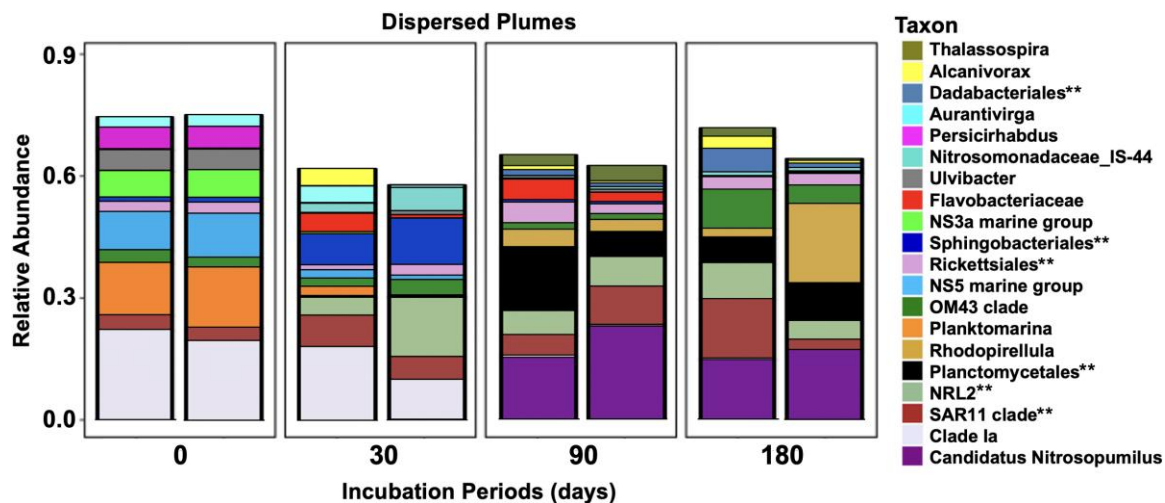


Figure 5.15 Taxonomy of the 20 most abundant genera identified in the seawater microcosms (i.e., dispersed plume). The color coding in the stacked graphs follows the same sequence as the colors in the legend from bottom to top. The sequences are essentially 'equivalent taxonomic units' identified to the genus, but based on the database used, some are identified to the order (**).

Figure 5.16 shows the taxonomy of the 20 most abundant genera identified in the sand column at different salinities and incubation periods. As expected, there was a notable difference in the abundance of microbial communities between the oiled and non-oiled microcosms, whereby hydrocarbon degraders such as *Marinobacter* (Mounier et al., 2014), *Gillisia* (Guibert et al., 2012;

Liang et al., 2021) and *Alcanivorax* (Golyshin et al., 2003) dominated the oiled microcosms. The abundance of several taxons varied with time, indicating that some microorganisms capable of growing on smaller hydrocarbons (e.g., alkanes shorter than C₂₀) flourished at the beginning, and then became less dominant as the small hydrocarbons became scarce. For instance, the relative abundance of *Alcanivorax*, known to biodegrade long-chain alkanes (Wang & Shao, 2014; SadrAzodi et al., 2019), was relatively low at t = 30 days in the oiled and non-oiled microcosms (except at 160 g/L salt), and then notably increased after 90 and 180 days only in the oiled microcosms, which is similar to what was observed in oiled hypersaline seawater (Abou Khalil et al., 2021a) and in the dispersed plumes (Figure 5.15). The addition of nutrients slightly enhanced the abundance of hydrocarbon degraders, such as *Gillisia* and *Alcanivorax*, thus enhancing the biodegradation of crude oil (Figures 5.6, 5.7, and 5.8). Nonetheless, the microbial population was mostly affected by salinity (Figure 5.16), whereby halophilic and halotolerant hydrocarbon-degrading genera, such as *Marinobacter* (Al-Awadhi et al., 2007) and *Alcanivorax* (SadrAzodi et al., 2019), dominated the hypersaline microcosms (Abou Khalil et al., 2021a). The relative abundance of the *Gillisia* genus, known to be halotolerant (Van Trappen et al., 2004; Bowman & Nichols, 2005) and capable of degrading hydrocarbons (Ping et al., 2009; Liang et al., 2021), was not significantly affected by different salinities. Furthermore, the *Aliifodinibius* genus, a moderately halophilic bacterium that may degrade hydrocarbons (Sun et al., 2022), became part of the 20 most abundant taxons only at 160 g/L salt after 90 days of incubation in both oiled and non-oiled microcosms.

The taxonomy profiles of the 20 most abundant genera identified in the sand microcosms at different oil concentrations and at 30 g/L salt after 180 days of incubation, with and without additional nutrients, are presented in Figure 5.17. The bacterial population did not seem to be

affected by the addition of nutrients at higher oil concentrations. The nutrient amendments were correlated with an increase in the relative abundance of *Alcanivorax* and *Marinobacter* and a decrease of *Gimesia* at lower oil concentrations. *Alcanivorax* practically disappeared in the microcosms amended with the highest concentrations of oil. A substantial decrease in the relative abundance of *Marinobacter* was also identified for that experiment.

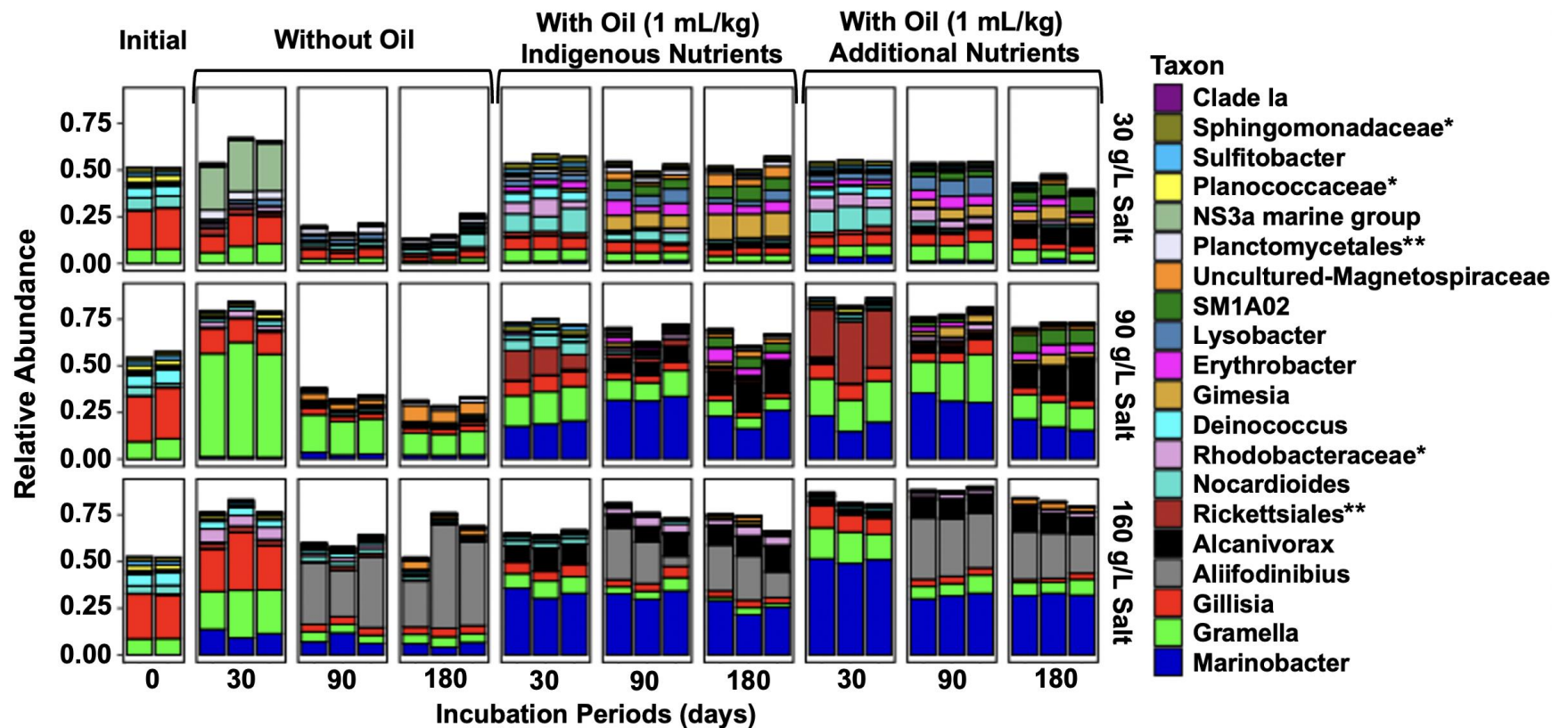


Figure 5.16 Taxonomy of the 20 most abundant genera identified in the sand microcosms with/without oil and with/without additional nutrients at different salinities and incubation periods. The color coding in the stacked graphs follows the same sequence as the colors in the legend from bottom to top. The sequences are essentially 'equivalent taxonomic units' identified to the genus, but based on the database used, some are identified to the family (*) or order (**). Note: It has been proposed to move *Planococcaceae* into *Caryophanaceae* (Gupta and Patel, 2020).

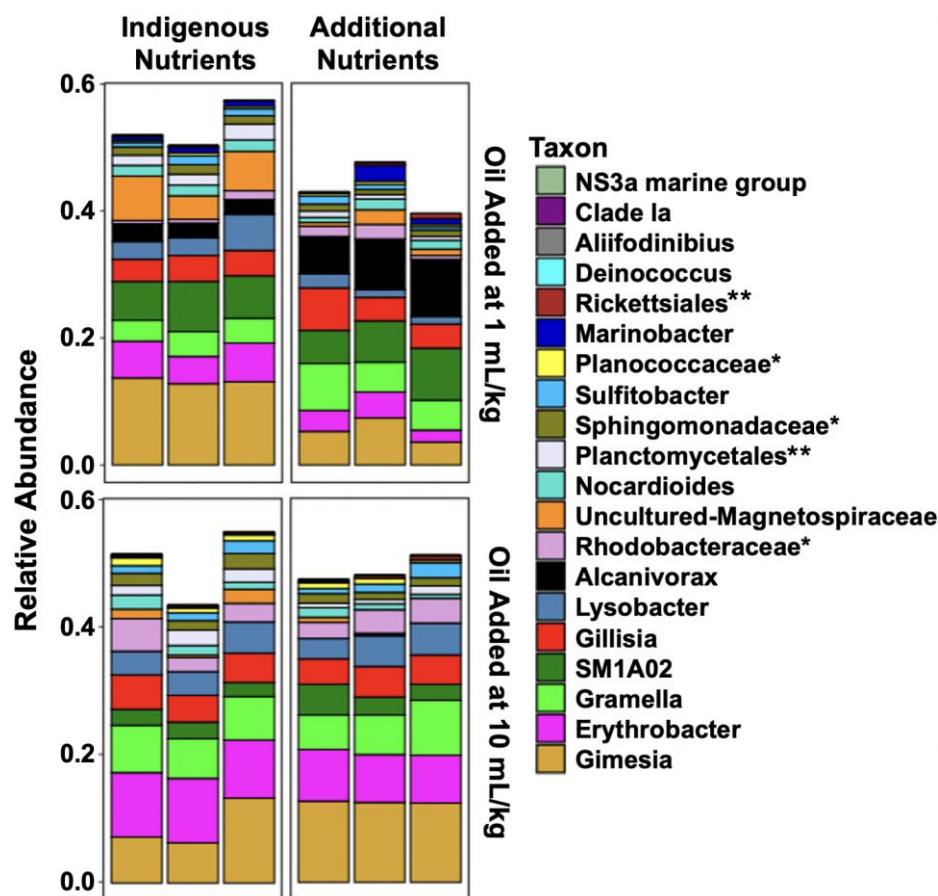
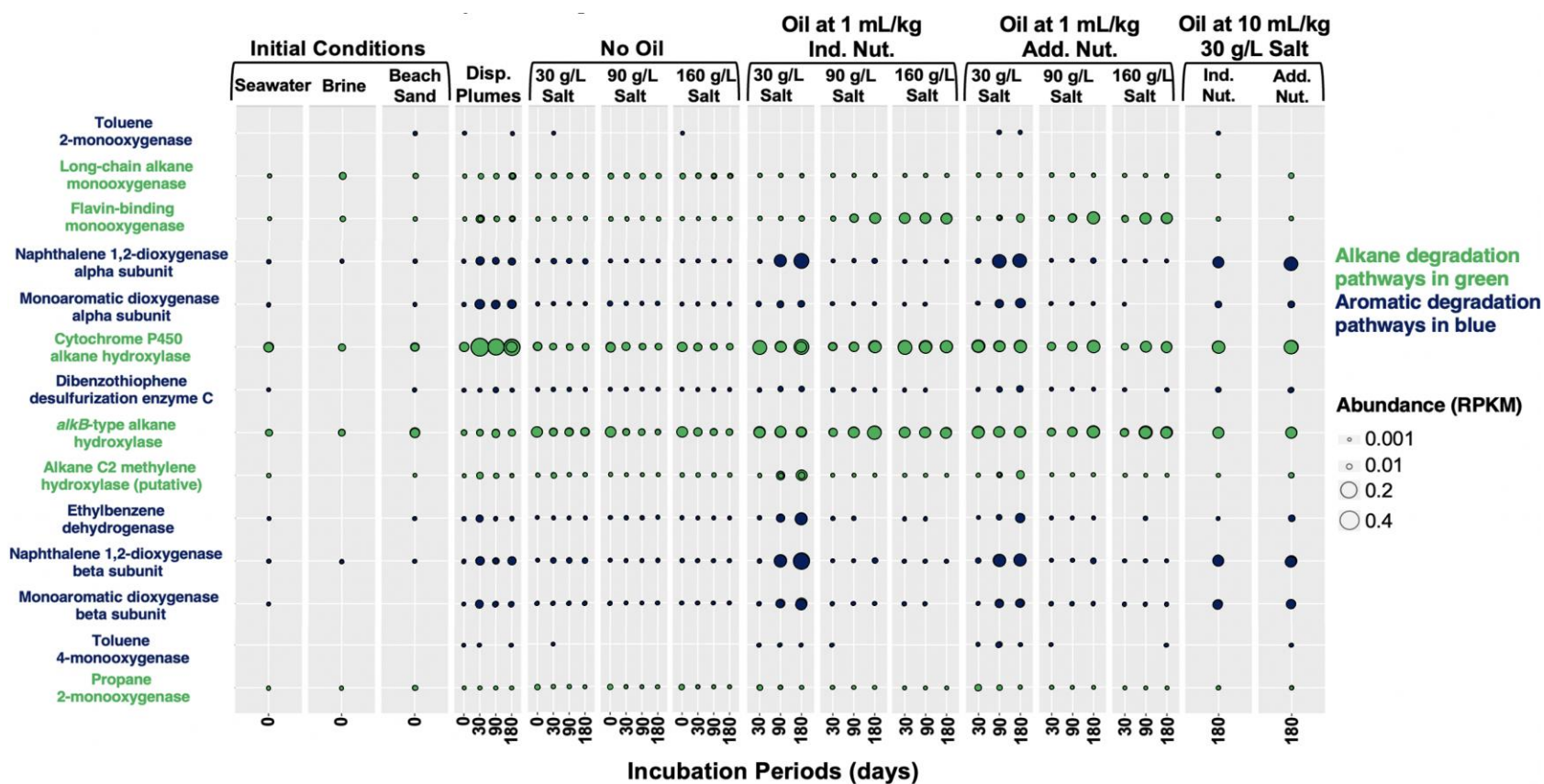


Figure 5.17 Taxonomy of the 20 most abundant genera identified in the sand microcosms at different oil concentrations with/without additional nutrients after 180 days of incubation. The color coding in the stacked graphs follows the same sequence as the colors in the legend from bottom to top. The sequences are essentially 'equivalent taxonomic units' identified to the genus, but based on the database used, some are identified to the family (*) or order (**). Note: It has been proposed to move *Planococcaceae* into *Caryophanaceae* (Gupta and Patel, 2020).

5.4.2 Metagenomic Analysis

Figure 5.18 displays the abundance of enzymes associated to alkane (in green) and aromatic (in blue) hydrocarbon degradation pathways. Both the sampled seawater and beach sand displayed similar enzymatic profiles, but enzymes associated to aromatic degradation pathways were not as prevalent in the concentrated brine. As expected, the oiled microcosms had a much higher abundance of enzymes related to hydrocarbon degradation than the non-oiled ones. The addition of nutrients and higher oil concentrations

doesn't seem to significantly affect the abundance, which corroborated the results generated with the metataxonomic analyses (Figures 5.16 and 5.17). The enzymes pertaining to the alkane degradation pathways were abundant in all the sand column microcosms, therefore agreeing with the oil chemistry results which indicated that the half-life of alkanes was essentially unaffected by the salinity (Figure 5.9). On the other hand, the relative abundance of reads for enzymes involved in the degradation of aromatics was substantially lower under hypersaline conditions, which is in accordance with oil chemistry data (Figure 5.9). This discriminatory effect was not observed in our previous experiment (Chapter 3) using oiled hypersaline seawater (Abou Khalil et al., 2021a). This suggests the presence of different microbial populations in beach sand and seawater (Figures 5.11 and 5.12).



5.5 Discussion

Both results from Chapter 3 and this study clearly show that the biodegradation of crude oil in coastal ecosystems by the indigenous hydrocarbon degraders slows down when salinity increases. The apparent half-life of oil increased by about 45 and 93% when increasing the porewater salinity from 30 g/L (seawater concentrations) to 90 g/L and 160 g/L, respectively (Section 5.3). Previous investigations showed higher biodegradation rates of petroleum hydrocarbons under hypersaline conditions when using halophiles isolated from hypersaline coastal sediments (Abed et al., 2006; Al-Mailem et al., 2010). Nonetheless, such studies, which relied on isolated extremely halophilic strains and may have enriched rare hypersaline microbes at the expense of more typical marine microorganisms, do not represent the natural in-situ oil biodegradation in contaminated coastal sediments. Metataxonomic analyses (Figures 5.16) clearly showed that the abundance and diversity of genera varied significantly with the increase in porewater salinity. Microorganisms of the *Marinobacter* genus, which were rare at seawater salinity, were among the 20 most abundant genera at 90 and 160 g/L salt throughout the experiment (Figure 5.16). This was expected since such microorganisms are generally classified as either halotolerant or halophilic (Gauthier et al., 1992; Martín et al., 2003; Qu et al., 2011; Liu et al., 2012; Boujida et al., 2019; Yoo et al., 2020; Nie et al., 2021). Several studies have investigated the hydrocarbonoclastic potential of *Marinobacter* strains, isolated from marine and hypersaline ecosystems, which were capable of degrading petroleum hydrocarbons under hypersaline conditions, where the salinity was about five-fold (Wang et al., 2020), seven-fold (Wang et al., 2020), and ten-fold (Wang et al., 2020) higher than seawater. Consequently, the *Marinobacter* genus may be important in the bioremediation

of oil-contaminated hypersaline ecosystems (Gauthier et al., 1992; Berlendis et al., 2010; Al-Mailem et al., 2013). Other moderately halophilic genera, such as *Alcanivorax*, which can degrade hydrocarbons (Golyshin et al., 2003; Qiao & Shao, 2010; Chernikova et al., 2020; Sun et al., 2022), were also relatively more abundant in the hypersaline microcosms (Figure 5.16)

The oil concentration in the sand column microcosms (1 mL/kg), which is an average of what is typically found in oil-contaminated sandy beaches (Geng et al., 2021) and is about 20-fold higher than in the hypersaline seawater microcosms (50 μ L/L) used in Chapter 3 and about 50-fold higher than in dispersed plumes (10 μ L/L), seems to significantly slow down the apparent half-life of oil, which implies that bioavailability also plays an important role in impeding the biodegradation of oil on seashores. Nonetheless, it is expected that the biodegradation rate measured as mass per unit time would increase at higher concentrations of petroleum hydrocarbons (Prince et al., 2017). Increasing the oil concentration from 1 to 10 mL/kg slowed down the half-life of oil by 10-fold and affected the relative abundance of microorganisms (Figure 5.17), whereby the abundance of some hydrocarbon degrading genera (e.g., *Alcanivorax*) significantly reduced.

The biodegradation rate of alkanes in the sand was essentially unaffected by the salinity (Figure 5.9-a and -b), while that of aromatics was substantially lower (Figure 5.9-c and -d), decreasing by 75 to 95% when the pore water salinity increased by about five-fold (i.e., from 30 to 160 g/L). High pressure did not have this discriminatory effect between alkanes and aromatics (Prince et al., 2016b), nor did sub-zero temperatures (McFarlin et al., 2014). Metagenomic data shows how the degradation pathways of aromatics were much more affected at higher salinities than those of alkanes, which

suggests that aromatic hydrocarbons would mostly persist on oil-contaminated beaches (Tronczyński et al., 2004; Kappell et al., 2014; Yin et al., 2015), especially in the upper intertidal and supratidal zones where the porewater in the sediments is transiently hypersaline. The biodegradation of petroleum hydrocarbons was slightly faster with additional nutrients (Figures 5.6 and 5.7), encouraging the fertilization of contaminated upper intertidal and supratidal zones of sandy beaches as a bioremediation option, in line with options for intertidal zones (Prince, 1993; Venosa et al., 1996; Atlas & Bragg, 2009; Prince et al., 2015). Metataxonomic and Metagenomic data (Figures 5.16, 5.17, and 5.18), however, did not show a notable change in microbial population and abundance of hydrocarbon metabolizing enzymes between the unfertilized and fertilized samples.

CHAPTER 6

CONCLUSIONS AND RECOMMENDATIONS

Both experiments of Chapters 3 and 5 suggest that the hypersaline conditions in the upper intertidal and supratidal zones would negatively affect the hydrocarbonoclastic activity of the indigenous marine and coastal microorganisms. Consequently, it is advisable that responders and decision-makers aiming to enhance the biodegradation rate of hydrocarbon contaminated shorelines should consider occasional inundation of the upper parts of sandy beaches. This replenishment would decrease the salinity of the pore water, and thereby enhance the oil's microbial degradation. The use of seawater would be particularly valuable since it would reseed the contaminated region with the marine's indigenous hydrocarbon degraders that might have perished due to the transiently hypersaline conditions. Fertilizing the oil-contaminated seashores is also recommended since it could enhance the biodegradation of petroleum hydrocarbons by avoiding the limitation of nutrients. High oil concentrations on contaminated beaches, however, are probably the most impactful on the persistence of oil on shorelines. Consequently, chemically dispersing the oil while at sea and preventing it from reaching the shorelines is most likely the most suitable action for speeding up the natural removal of spilled oil in marine environments.

REFERENCES

- Abdulrasheed, M., Zakaria, N. N., Roslee, A. F. A., Shukor, M. Y., Zulkharnain, A., Napis, S., Convey, P., Alias, S. A., Gonzalez-Rocha, G., & Ahmad, S. A. (2020). Biodegradation of diesel oil by cold-adapted bacterial strains of *Arthrobacter* spp. from Antarctica. *Antarctic Science*, 32(5), 341-353. doi: <https://doi.org/10.1017/S0954102020000206>
- Abed, R. M., Al-Thukair, A., & De Beer, D. (2006). Bacterial diversity of a cyanobacterial mat degrading petroleum compounds at elevated salinities and temperatures. *FEMS Microbiology Ecology*, 57(2), 290-301. doi: <https://doi.org/10.1111/j.1574-6941.2006.00113.x>
- Abou Khalil, C., Fortin, N., Prince, R. C., Greer, C. W., Lee, K., & Boufadel, M. C. (2021a). Crude oil biodegradation in upper and supratidal seashores. *Journal of Hazardous Materials*, 416, 125919. doi: <https://doi.org/10.1016/j.jhazmat.2021.125919>
- Abou Khalil, C., Prince, V. L., Prince, R. C., Greer, C. W., Lee, K., Zhang, B., & Boufadel, M. C. (2021b). Occurrence and biodegradation of hydrocarbons at high salinities. *Science of The Total Environment*, 762, 143165. doi: <https://doi.org/10.1016/j.scitotenv.2020.143165>
- Abou-Khalil, C., Prince, R. C., Greer, C. W., Lee, K., & Boufadel, M. C. (2022). Bioremediation of petroleum hydrocarbons in the upper parts of sandy beaches. *Environmental Science & Technology*. doi: <https://doi.org/10.1021/acs.est.2c01338>
- Aislabie, J., Saul, D. J., & Foght, J. M. (2006). Bioremediation of hydrocarbon-contaminated polar soils. *Extremophiles*, 10(3), 171-179. doi: <http://doi.org/10.1007/s00792-005-0498-4>
- Aislabie, J. M., Balks, M. R., Foght, J. M., & Waterhouse, E. J. (2004). Hydrocarbon spills on Antarctic soils: effects and management. *Environmental Science & Technology*, 38(5), 1265-1274. doi: <https://doi.org/10.1021/es0305149>
- Aitken, C. M., Jones, D. M., & Larter, S. R. (2004). Anaerobic hydrocarbon biodegradation in deep subsurface oil reservoirs. *Nature*, 431(7006), 291-294. doi: <https://doi.org/10.1038/nature02922>
- Al-Awadhi, H., Sulaiman, R. H., Mahmoud, H. M., & Radwan, S. (2007). Alkaliphilic and halophilic hydrocarbon-utilizing bacteria from Kuwaiti coasts of the Arabian Gulf. *Applied Microbiology and Biotechnology*, 77(1), 183-186. doi: <https://doi.org/10.1007/s00253-007-1127-1>

- Al-Mailem, D. M., Al-Deieg, M., Eliyas, M., & Radwan, S. S. (2017). Biostimulation of indigenous microorganisms for bioremediation of oily hypersaline microcosms from the Arabian Gulf Kuwaiti coasts. *Journal of Environmental Management*, *193*, 576-583. doi:<https://doi.org/10.1016/j.jenvman.2017.02.054>
- Al-Mailem, D. M., Eliyas, M., & Radwan, S. (2014). Enhanced bioremediation of oil-polluted, hypersaline, coastal areas in Kuwait via vitamin-fertilization. *Environmental Science and Pollution Research*, *21*(5), 3386-3394. doi:<https://doi.org/10.1007/s11356-013-2293-6>
- Al-Mailem, D. M., Eliyas, M., & Radwan, S. S. (2013). Oil-bioremediation potential of two hydrocarbonoclastic, diazotrophic Marinobacter strains from hypersaline areas along the Arabian Gulf coasts. *Extremophiles*, *17*(3), 463-470. doi:<http://doi.org/10.1007/s00792-013-0530-z>
- Al-Mailem, D. M., Sorkhoh, N. A., Al-Awadhi, H., Eliyas, M., & Radwan, S. S. (2010). Biodegradation of crude oil and pure hydrocarbons by extreme halophilic archaea from hypersaline coasts of the Arabian Gulf. *Extremophiles*, *14*(3), 321-328. doi:<http://doi.org/10.1007/s00792-010-0312-9>
- Al-Mueini, R., Al-Dalali, M., Al-Amri, I. S., & Patzelt, H. (2007). Hydrocarbon degradation at high salinity by a novel extremely halophilic actinomycete. *Environmental Chemistry*, *4*(1), 5-7. doi: <https://doi.org/10.1071/EN06019>
- Alipour, S. (2006). Hydrogeochemistry of seasonal variation of Urmia salt lake, Iran. *Saline Systems*, *2*(1), Article Number 9. doi: <https://doi.org/10.1186/1746-1448-2-9>
- Antunes, A., Ngugi, D. K., & Stingl, U. (2011). Microbiology of the Red Sea (and other) deep-sea anoxic brine lakes. *Environmental Microbiology Reports*, *3*(4), 416-433. doi: <https://doi.org/10.1111/j.1758-2229.2011.00264.x>
- APHA, AWWA, & WEF. (2017). Solids 2540. *Standard methods for the examination of water and wastewater 23th ed.* Retrieved from https://edgeanalytical.com/wp-content/uploads/Inorganic_SM2540.pdf (Accessed on 19 September, 2020).
- Arocena, J. M., & Rutherford, P. M. (2005). Properties of hydrocarbon-and salt-contaminated flare pit soils in northeastern British Columbia (Canada). *Chemosphere*, *60*(4), 567-575. doi: <https://doi.org/10.1016/j.chemosphere.2004.12.077>
- Arrigo, K. R., Mock, T., & Lizotte, M. P. (2010). Primary producers and sea ice. In D. N. Tomas & G. S. Dieckmann (Eds.), *Sea Ice* (Vol. 2, pp. 283-325): Willey-Blackwell, Hoboken, New Jersey, USA.

- Arulazhagan, P., & Vasudevan, N. (2011). Biodegradation of polycyclic aromatic hydrocarbons by a halotolerant bacterial strain *Ochrobactrum sp. VAI*. *Marine Pollution Bulletin*, 62(2), 388-394. doi: <https://doi.org/10.1016/j.marpolbul.2010.09.020>
- Aryal, S. (2019). Flagella – Introduction, Types, Examples, Parts, Functions and Flagella Staining- Principle, Procedure and Interpretation. Retrieved from <https://microbiologyinfo.com/flagella-introduction-types-examples-parts-functions-and-flagella-staining-principal-procedure-and-interpretation/> (Accessed on 20 October, 2020).
- Asker, D., & Ohta, Y. (2002). *Haloferax alexandrinus sp. nov.*, an extremely halophilic canthaxanthin-producing archaeon from a solar saltern in Alexandria (Egypt). *International Journal of Systematic and Evolutionary Microbiology*, 52(3), 729-738. doi: <https://doi.org/10.1099/00207713-52-3-729>
- Atlas, R., & Bragg, J. (2009). Bioremediation of marine oil spills: when and when not—the Exxon Valdez experience. *Microbial Biotechnology*, 2(2), 213-221. doi: <https://doi.org/10.1111/j.1751-7915.2008.00079.x>
- Avrahamov, N., Antler, G., Yechieli, Y., Gavrieli, I., Joye, S., Saxton, M., Turchyn, A., & Sivan, O. (2014). Anaerobic oxidation of methane by sulfate in hypersaline groundwater of the Dead Sea aquifer. *Geobiology*, 12(6), 511-528. doi: <https://doi.org/10.1111/gbi.12095>
- Aydemir, A. (2008). Hydrocarbon potential of the Tuzgolü (Salt Lake) Basin, Central Anatolia, Turkey: a comparison of geophysical investigation results with the geochemical data. *Journal of Petroleum Science and Engineering*, 61(1), 33-47. doi: <https://doi.org/10.1016/j.petrol.2007.10.004>
- Baliga, N. S., Bonneau, R., Facciotti, M. T., Pan, M., Glusman, G., Deutsch, E. W., Shannon, P., Chiu, Y., Weng, R. S., & Gan, R. R. (2004). Genome sequence of *Haloarcula marismortui*: a halophilic archaeon from the Dead Sea. *Genome Research*, 14(11), 2221-2234. doi: <http://doi.org/10.1101/gr.2700304>
- Ballestero, H., & Magdol, Z. (2011). Biodegradation of polycyclic aromatic hydrocarbons in simulated Arctic Sea ice brine channels and protistan predation. *Paper presented at the International Oil Spill Conference Proceedings (IOSC)*. American Petroleum Institute.
- Bastin, E. S., Greer, F. E., Merritt, C., & Moulton, G. (1926). The presence of sulphate reducing bacteria in oil field waters. *Science*, 63(1618), 21-24. doi: <https://doi.org/10.1126/science.63.1618.21>

- Becker, B. R., de Souza, E. S., Martins, R. L., & da Luz Bueno, J. (2016). Bioremediation of oil-contaminated beach and restinga sediments using a slowrelease fertilizer. *CLEAN–Soil, Air, Water*, 44(9), 1154-1162. doi: <https://doi.org/10.1002/clen.201500023>
- Bees, M. A., Andresen, P., Mosekilde, E., & Givskov, M. (2002). Quantitative effects of medium hardness and nutrient availability on the swarming motility of *Serratia liquefaciens*. *Bulletin of Mathematical Biology*, 64(3), 565-587. doi: <https://doi.org/10.1006/bulm.2002.0287>
- Bell, T. H., Yergeau, E., Maynard, C., Juck, D., Whyte, L. G., & Greer, C. W. (2013). Predictable bacterial composition and hydrocarbon degradation in Arctic soils following diesel and nutrient disturbance. *The ISME Journal*, 7(6), 1200-1210. doi:<https://doi.org/10.1038/ismej.2013.1>
- Berlendis, S., Cayol, J.-L., Verhé, F., Laveau, S., Tholozan, J.-L., Ollivier, B., & Auria, R. (2010). First evidence of aerobic biodegradation of BTEX compounds by pure cultures of *Marinobacter*. *Applied Biochemistry and Biotechnology*, 160(7), 1992-1999. doi: <https://doi.org/10.1007/s12010-009-8746-1>
- Bertrand, J., Almallah, M., Acquaviva, M., & Mille, G. (1990). Biodegradation of hydrocarbons by an extremely halophilic archaeobacterium. *Letters in Applied Microbiology*, 11(5), 260-263. doi: <https://doi.org/10.1111/j.1472-765X.1990.tb00176.x>
- Bhupathiraju, V. K., McInerney, M. J., & Knapp, R. M. (1993). Pretest studies for a microbially enhanced oil recovery field pilot in a hypersaline oil reservoir. *Geomicrobiology Journal*, 11(1), 19-34. doi:<https://doi.org/10.1080/01490459309377929>
- Birkle, P., García, B. M., & Padrón, C. M. M. (2009). Origin and evolution of formation water at the Jujo–Tecominoacán oil reservoir, Gulf of Mexico. Part 1: Chemical evolution and water–rock interaction. *Applied Geochemistry*, 24(4), 543-554. doi: <https://doi.org/10.1016/j.apgeochem.2008.12.009>
- Biswas, J., Mandal, S., & Paul, A. (2015). Production, partial purification and some biophysicochemical properties of EPS produced by *Halomonas xianhensis* SUR308 isolated from a saltern environment. *Journal of Biologically Active Products from Nature*, 5(2), 108-119. doi: <https://doi.org/10.1080/22311866.2015.1038852>
- Blanchard, D. C., & Syzdek, L. D. (1972). Concentration of bacteria in jet drops from bursting bubbles. *Journal of Geophysical Research*, 77(27), 5087-5099. doi: <https://doi.org/10.1029/JC077i027p05087>

- Bociu, I., Shin, B., Wells, W. B., Kostka, J. E., Konstantinidis, K. T., & Huettel, M. (2019). Decomposition of sediment-oil-agglomerates in a Gulf of Mexico sandy beach. *Scientific Reports*, 9(1), 1-13. doi: <https://doi.org/10.1038/s41598-019-46301-w>
- Bock, M., Bosecker, K., Kämpfer, P., & Dott, W. (1994). Isolation and characterization of heterotrophic, aerobic bacteria from oil storage caverns in northern Germany. *Applied Microbiology and Biotechnology*, 42(2), 463-468. doi:<https://doi.org/10.1007/BF00902758>
- Bolger, A. M., Lohse, M., & Usadel, B. (2014). Trimmomatic: a flexible trimmer for Illumina sequence data. *Bioinformatics*, 30(15), 2114-2120. doi: <https://doi.org/10.1093/bioinformatics/btu170>
- Bonfá, M. R., Grossman, M. J., Mellado, E., & Durrant, L. R. (2011). Biodegradation of aromatic hydrocarbons by *Haloarchaea* and their use for the reduction of the chemical oxygen demand of hypersaline petroleum produced water. *Chemosphere*, 84(11), 1671-1676. doi: <https://doi.org/10.1016/j.chemosphere.2011.05.005>
- Bordenave, S., Chatterjee, I., & Voordouw, G. (2013). Microbial community structure and microbial activities related to CO₂ storage capacities of a salt cavern. *International Biodeterioration & Biodegradation*, 81, 82-87. doi: <https://doi.org/10.1016/j.ibiod.2012.08.001>
- Borzenkov, I., Milekhina, E., Gotoeva, M., Rozanova, E., & Belyaev, S. (2006). The properties of hydrocarbon-oxidizing bacteria isolated from the oilfields of Tatarstan, Western Siberia, and Vietnam. *Microbiology*, 75(1), 66-72. doi: <https://doi.org/10.1134/S0026261706010127>
- Boufadel, M. C., Wrenn, B. A., Moore, B. E., Boda, K. J., & Michel, J. (2011). A biodegradation assessment tool for decision on beach response. In proceedings of the *International Oil Spill Conference*, abs348. American Petroleum Institute.
- Boujida, N., Palau, M., Charfi, S., Manresa, À., Senhaji, N. S., Abrini, J., & Miñana-Galbis, D. (2019). *Marinobacter maroccanus* sp. nov., a moderately halophilic bacterium isolated from a saline soil. *International Journal of Systematic and Evolutionary Microbiology*, 69(1), 227-234. doi: <https://doi.org/10.1099/ijsem.0.003134>
- Bowman, J. P., & Nichols, D. S. (2005). Novel members of the family Flavobacteriaceae from Antarctic maritime habitats including *Subsaximicrobium wynnwilliamsii* gen. nov., sp. nov., *Subsaximicrobium saxinquilinus* sp. nov., *Subsaxibacter broadyi* gen. nov., sp. nov., *Lacinutrix copepodicola* gen. nov., sp. nov., and novel species of the genera *Bizionia*, *Gelidibacter* and *Gillisia*. *International Journal of Systematic and Evolutionary Microbiology*, 55(4), 1471-1486. doi: <https://doi.org/10.1099/ijms.0.63527-0>

- Bragg, J. R., Prince, R. C., Harner, E. J., & Atlas, R. M. (1994). Effectiveness of bioremediation for the Exxon Valdez oil spill. *Nature*, 368(6470), 413-418. doi: <https://doi.org/10.1038/368413a0>
- Brakstad, O. G., Lofthus, S., Ribicic, D., & Netzer, R. (2017). Biodegradation of petroleum oil in cold marine environments. In *Psychrophiles: From Biodiversity to Biotechnology* (pp. 613-644): Springer, Cham, Switzerland. doi: https://doi.org/10.1007/978-3-319-57057-0_27
- Brakstad, O. G., Nordtug, T., & Throne-Holst, M. (2015). Biodegradation of dispersed Macondo oil in seawater at low temperature and different oil droplet sizes. *Marine Pollution Bulletin*, 93(1-2), 144-152. doi:<https://doi.org/10.1016/j.marpolbul.2015.02.006>
- Brakstad, O. G., Ribicic, D., Winkler, A., & Netzer, R. (2018). Biodegradation of dispersed oil in seawater is not inhibited by a commercial oil spill dispersant. *Marine Pollution Bulletin*, 129(2), 555-561. doi: <https://doi.org/10.1016/j.marpolbul.2017.10.030>
- Brierley, A. S. (2017). Plankton. *Current Biology*, 27(11), R478-R483. doi: <https://doi.org/10.1016/j.cub.2017.02.045>
- Buchfink, B., Xie, C., & Huson, D. H. (2014). Fast and sensitive protein alignment usingDIAMOND. *NatMethods*12: 59–60. doi: <https://doi.org/10.1038/nmeth.3176>
- Budiyanto, F., Thukair, A., Al-Momani, M., Musa, M. M., & Nzila, A. (2018). Characterization of halophilic bacteria capable of efficiently biodegrading the high-molecular-weight polycyclic aromatic hydrocarbon pyrene. *Environmental Engineering Science*, 35(6), 616-626. doi: <https://doi.org/10.1089/ees.2017.0244>
- Cai, P., Sun, X., Wu, Y., Gao, C., Mortimer, M., Holden, P. A., Redmile-Gordon, M., & Huang, Q. (2019). Soil biofilms: microbial interactions, challenges, and advanced techniques for ex-situ characterization. *Soil Ecology Letters*, 1(3), 85-93. doi: <https://doi.org/10.1007/s42832-019-0017-7>
- Cameron, R., Morelli, F., & Randall, L. (1972). Aerial, aquatic, and soil microbiology of Don Juan Pond, Antarctica. *Antarctic Journal of the United States*, 7, 254-258.
- Camur, M. Z., & Mutlu, H. (1996). Major-ion geochemistry and mineralogy of the Salt Lake (Tuz Gölü) basin, Turkey. *Chemical Geology*, 127(4), 313-329. doi: [https://doi.org/10.1016/0009-2541\(95\)00129-8](https://doi.org/10.1016/0009-2541(95)00129-8)
- Cao, Y., Zhang, B., Zhu, Z., Song, X., Cai, Q., Chen, B., Dong, G., & Ye, X. (2020). Microbial eco-physiological strategies for salinity-mediated crude oil biodegradation. *Science of the Total Environment*, 138723. doi: <https://doi.org/10.1016/j.scitotenv.2020.138723>

- Castillo-Carvajal, L. C., Sanz-Martín, J. L., & Barragán-Huerta, B. E. (2014). Biodegradation of organic pollutants in saline wastewater by halophilic microorganisms: a review. *Environmental Science and Pollution Research*, 21(16), 9578-9588. doi:<https://doi.org/10.1007/s11356-014-3036-z>
- Chamkha, M., Mnif, S., & Sayadi, S. (2008). Isolation of a thermophilic and halophilic tyrosol-degrading *Geobacillus* from a Tunisian high-temperature oil field. *FEMS Microbiology Letters*, 283(1), 23-29. doi: <https://doi.org/10.1111/j.1574-6968.2008.01136.x>
- Chandler, R., & McMeekin, T. (1989). Combined effect of temperature and salt concentration/water activity on the growth rate of *Halobacterium* spp. *Journal of Applied Bacteriology*, 67(1), 71-76. doi:<https://doi.org/10.1111/j.1365-2672.1989.tb04956.x>
- Chang, W., Akbari, A., David, C. A., & Ghoshal, S. (2018). Selective biostimulation of cold-and salt-tolerant hydrocarbon-degrading *Dietzia maris* in petroleum-contaminated sub-Arctic soils with high salinity. *Journal of Chemical Technology & Biotechnology*, 93(1), 294-304. doi: <https://doi.org/10.1002/jctb.5385>
- Chau, J. F., Bagtzoglou, A. C., & Willig, M. R. (2011). The effect of soil texture on richness and diversity of bacterial communities. *Environmental Forensics*, 12(4), 333-341. doi:<https://doi.org/10.1080/15275922.2011.622348>
- Chen, M., & Alexander, M. (1973). Survival of soil bacteria during prolonged desiccation. *Soil Biology and Biochemistry*, 5(2), 213-221. doi:[https://doi.org/10.1016/0038-0717\(73\)90004-7](https://doi.org/10.1016/0038-0717(73)90004-7)
- Chen, W., Kong, Y., Li, J., Sun, Y., Min, J., & Hu, X. (2020). Enhanced biodegradation of crude oil by constructed bacterial consortium comprising salt-tolerant petroleum degraders and biosurfactant producers. *International Biodeterioration & Biodegradation*, 154, 105047. doi: <https://doi.org/10.1016/j.ibiod.2020.105047>
- Chernikova, T. N., Bargiela, R., Toshchakov, S. V., Shivaraman, V., Lunev, E. A., Yakimov, M. M., Thomas, D. N., & Golyshin, P. N. (2020). Hydrocarbon-degrading bacteria *Alcanivorax* and *Marinobacter* associated with microalgae *Pavlova lutheri* and *Nannochloropsis oculata*. *Frontiers in Microbiology*, 11, 572931. doi:<https://doi.org/10.3389/fmicb.2020.572931>
- Chiang, C., Salanitro, J., Chai, E., Colthart, J., & Klein, C. (1989). Aerobic biodegradation of benzene, toluene, and xylene in a sandy aquifer—data analysis and computer modeling. *Groundwater*, 27(6), 823-834. doi: <https://doi.org/10.1111/j.1745-6584.1989.tb01046.x>
- Connan, J. (1984). Biodegradation of crude oils in reservoirs. *Advances in Petroleum Geochemistry*, 1, 299-335.

- Corsellis, Y. Y., Krasovec, M. M., Sylvi, L. L., Cuny, P. P., & Milton, C. C. (2016). Oil removal and effects of spilled oil on active microbial communities in close to salt-saturation brines. *Extremophiles*, 20(3), 235-250. doi: <https://doi.org/10.1007/s00792-016-0818-x>
- Costerton, J. W. (1999). Introduction to biofilm. *International Journal of Antimicrobial Agents*, 11(3-4), 217-221.
- Cummings, S. P., & Gilmour, D. J. (1995). The effect of NaCl on the growth of a *Halomonas* species: accumulation and utilization of compatible solutes. *Microbiology*, 141(6), 1413-1418. doi: <https://doi.org/10.1099/13500872-141-6-1413>
- Dahal, R. H., Chaudhary, D. K., & Kim, J. (2017). *Acinetobacter halotolerans* sp. nov., a novel halotolerant, alkalitolerant, and hydrocarbon degrading bacterium, isolated from soil. *Archives of Microbiology*, 199(5), 701-710. doi: <https://doi.org/10.1007/s00203-017-1349-2>
- Dahlbäck, B., Hermansson, M., Kjelleberg, S., & Norkrans, B. (1981). The hydrophobicity of bacteria—An important factor in their initial adhesion at the air-water interface. *Archives of Microbiology*, 128(3), 267-270. doi: <https://doi.org/10.1007/BF00422527>
- Dastgheib, S. M. M., Amoozegar, M. A., Khajeh, K., Shavandi, M., & Ventosa, A. (2012). Biodegradation of polycyclic aromatic hydrocarbons by a halophilic microbial consortium. *Applied Microbiology and Biotechnology*, 95(3), 789-798. doi: <https://doi.org/10.1007/s00253-011-3706-4>
- de Carvalho, C. C. (2012). Adaptation of *Rhodococcus erythropolis* cells for growth and bioremediation under extreme conditions. *Research in Microbiology*, 163(2), 125-136. doi: <https://doi.org/10.1016/j.resmic.2011.11.003>
- Derjaguin, B., & Landau, L. (1993). Theory of the stability of strongly charged lyophobic sols and of the adhesion of strongly charged particles in solutions of electrolytes. *Progress in Surface Science*, 43(1-4), 30-59. doi: [https://doi.org/10.1016/0079-6816\(93\)90013-L](https://doi.org/10.1016/0079-6816(93)90013-L)
- Díaz, J., Rendueles, M., & Díaz, M. (2010). Straining phenomena in bacteria transport through natural porous media. *Environmental Science and Pollution Research*, 17(2), 400-409. doi: <https://doi.org/10.1007/s11356-009-0160-2>
- Díaz, M. P., Boyd, K. G., Grigson, S. J., & Burgess, J. G. (2002). Biodegradation of crude oil across a wide range of salinities by an extremely halotolerant bacterial consortium *MPD-M*, immobilized onto polypropylene fibers. *Biotechnology and Bioengineering*, 79(2), 145-153. doi: <https://doi.org/10.1002/bit.10318>

- Dolfing, J., & Hubert, C. R. (2017). Using thermodynamics to predict the outcomes of nitrate-based oil reservoir souring control interventions. *Frontiers in Microbiology*, 8, 2575. doi: <https://doi.org/10.3389/fmicb.2017.02575>
- Dornbusch, M. J., Limb, R. F., Tomlinson, H. A., Daigh, A. L., & Sedivec, K. K. (2020). Evaluation of soil treatment techniques on remediated brine spill sites in semi-arid rangelands. *Journal of Environmental Management*, 260, 110100. doi: <https://doi.org/10.1016/j.jenvman.2020.110100>
- Doronina, N. V., Darmaeva, T. D., & Trotsenko, Y. A. (2003). *Methylophaga alcalica sp. nov.*, a novel alkaliphilic and moderately halophilic, obligately methylophilic bacterium from an East Mongolian saline soda lake. *International Journal of Systematic and Evolutionary Microbiology*, 53(1), 223-229. doi: <https://doi.org/10.1099/ijs.0.02267-0>
- Du, X., Reeser, P., Suidan, M. T., Huang, T., Moteleb, M., Boufadel, M. C., & Venosa, A. D. (1999). Optimum nitrogen concentration supporting maximum crude oil biodegradation in microcosms. *Paper presented at the International Oil Spill Conference*. American Petroleum Institute. doi: <https://doi.org/10.7901/2169-3358-1999-1-485>
- Duarte, C. M., Røstad, A., Michoud, G., Barozzi, A., Merlino, G., Delgado-Huertas, A., Hession, B. C., Mallon, F. L., Afifi, A. M., & Daffonchio, D. (2020). Discovery of Afifi, the shallowest and southernmost brine pool reported in the Red Sea. *Scientific Reports*, 10(1), 1-17. doi: <https://doi.org/10.1038/s41598-020-57416-w>
- Ebrahimi, A. N., & Or, D. (2014). Microbial dispersal in unsaturated porous media: Characteristics of motile bacterial cell motions in unsaturated angular pore networks. *Water Resources Research*, 50(9), 7406-7429. doi: <https://doi.org/10.1002/2014WR015897>
- Eckle, P., Burgherr, P., & Michaux, E. (2012). Risk of large oil spills: a statistical analysis in the aftermath of *Deepwater Horizon*. *Environmental Science & Technology*, 46(23), 13002-13008. doi: <https://doi.org/10.1021/es3029523>
- Edbeib, M. F., Wahab, R. A., & Huyop, F. (2016). Halophiles: biology, adaptation, and their role in decontamination of hypersaline environments. *World Journal of Microbiology and Biotechnology*, 32(8), 1-23. doi: <https://doi.org/10.1007/s11274-016-2081-9>
- Eddy, S. R. (1998). Profile hidden Markov models. *Bioinformatics* (Oxford, England), 14(9), 755-763. doi: <https://doi.org/10.1093/bioinformatics/14.9.755>
- Effimoff, I. (2000). The oil and gas resource base of the Caspian region. *Journal of Petroleum Science and Engineering*, 28(4), 157-159. doi: [https://doi.org/10.1016/S0920-4105\(00\)00075-9](https://doi.org/10.1016/S0920-4105(00)00075-9)

- Erdoğmuş, S. F., Mutlu, B., Korcan, S. E., Güven, K., & Konuk, M. (2013). Aromatic hydrocarbon degradation by halophilic archaea isolated from Çamaltı Saltern, Turkey. *Water, Air, & Soil Pollution*, 224(3), 1449. doi: <https://doi.org/10.1007/s11270-013-1449-9>
- Eriksson, M., Ka, J.-O., & Mohn, W. W. (2001). Effects of low temperature and freeze-thaw cycles on hydrocarbon biodegradation in Arctic tundra soil. *Applied and Environmental Microbiology*, 67(11), 5107-5112. doi: <http://doi.org/10.1128/AEM.67.11.5107-5112.2001>
- Faber, E., Botz, R., Poggenburg, J., Schmidt, M., Stoffers, P., & Hartmann, M. (1998). Methane in red sea brines. *Organic Geochemistry*, 29(1-3), 363-379. doi: [https://doi.org/10.1016/S0146-6380\(98\)00155-7](https://doi.org/10.1016/S0146-6380(98)00155-7)
- Fakhru'l-Razi, A., Pendashteh, A., Abdullah, L. C., Biak, D. R. A., Madaeni, S. S., & Abidin, Z. Z. (2009). Review of technologies for oil and gas produced water treatment. *Journal of Hazardous Materials*, 170(2-3), 530-551. doi: <https://doi.org/10.1016/j.jhazmat.2009.05.044>
- Fang, T., Pan, R., Jiang, J., He, F., & Wang, H. (2016). Effect of salinity on community structure and naphthalene dioxygenase gene diversity of a halophilic bacterial consortium. *Frontiers of Environmental Science & Engineering*, 10(6), 16. doi: <http://doi.org/10.1007/s11783-016-0888-0>
- Fathepure, B. Z. (2014). Recent studies in microbial degradation of petroleum hydrocarbons in hypersaline environments. *Frontiers in Microbiology*, 5, 173. doi:<https://doi.org/10.3389/fmicb.2014.00173>
- Feng, D., Li, X., Wang, X., Li, J., & Zhang, X. (2018). Capillary filling under nanoconfinement: The relationship between effective viscosity and water-wall interactions. *International Journal of Heat and Mass Transfer*, 118, 900-910. doi: <https://doi.org/10.1016/j.ijheatmasstransfer.2017.11.049>
- Fernandes, C., Khandeparker, R. D., & Shenoy, B. D. (2020). High abundance of *Vibrio* in tarball-contaminated seawater from Vagator beach, Goa, India. *Marine Pollution Bulletin*, 150, 110773. doi:<https://doi.org/10.1016/j.marpolbul.2019.110773>
- Ferreira, C., Soares, A. R., Lamosa, P., Santos, M. A., & Da Costa, M. S. (2016). Comparison of the compatible solute pool of two slightly halophilic planctomycetes species, *Gimesia maris* and *Rubinisphaera brasiliensis*. *Extremophiles*, 20(6), 811-820. <https://doi.org/10.1007/s00792-016-0868-0>

- Fowler, S., Readman, J., Oregioni, B., Villeneuve, J.-P., & McKay, K. (1993). Petroleum hydrocarbons and trace metals in nearshore Gulf sediments and biota before and after the 1991 war: an assessment of temporal and spatial trends. *Marine Pollution Bulletin*, 27, 171-182. doi: [https://doi.org/10.1016/0025-326X\(93\)90022-C](https://doi.org/10.1016/0025-326X(93)90022-C)
- Franklin, R. B., & Mills, A. L. (2007). *The Spatial Distribution of Microbes in the Environment*: Springer, Cham, Switzerland. doi: <https://doi.org/10.1007/978-1-4020-6216-2>
- Gales, G., Tsesmetzis, N., Neria, I., Alazard, D., Coulon, S., Lomans, B. P., Morin, D., Ollivier, B., Borgomano, J., & Joulian, C. (2016). Preservation of ancestral Cretaceous microflora recovered from a hypersaline oil reservoir. *Scientific Reports*, 6, 22960. doi: <https://doi.org/10.1038/srep22960>
- Gao, C., Zhang, Y., Wang, X., Lin, J., & Li, Y. (2019). Geochemical Characteristics and Geological significance of the anaerobic biodegradation products of crude oil. *Energy & Fuels*, 33(9), 8588-8595. doi: <https://doi.org/10.1021/acs.energyfuels.9b00632>
- Gargiulo, G., Bradford, S., Šimůnek, J., Ustohal, P., Vereecken, H., & Klumpp, E. (2007). Bacteria transport and deposition under unsaturated conditions: The role of the matrix grain size and the bacteria surface protein. *Journal of Contaminant Hydrology*, 92(3-4), 255-273. doi: <https://doi.org/10.1016/j.jconhyd.2007.01.009>
- Gargouri, B., Mnif, S., Aloui, F., Karray, F., Mhiri, N., Chamkha, M., & Sayadi, S. (2012). Bioremediation of petroleum contaminated water and soils in tunisia. In F. Quercia & D. Vidojevic (Eds.), *Clean Soil and Safe Water* (pp. 153-165): Springer, Dordrecht, Netherlands. doi: https://doi.org/10.1007/978-94-007-2240-8_12
- Garneau, M.-È., Michel, C., Meisterhans, G., Fortin, N., King, T. L., Greer, C. W., & Lee, K. (2016). Hydrocarbon biodegradation by Arctic sea-ice and sub-ice microbial communities during microcosm experiments, Northwest Passage (Nunavut, Canada). *FEMS Microbiology Ecology*, 92(10), fiw130. doi: <https://doi.org/10.1093/femsec/fiw130>
- Gauthier, M. J., Lafay, B., Christen, R., Fernandez, L., Acquaviva, M., Bonin, P., & Bertrand, J.-C. (1992). *Marinobacter hydrocarbonoclasticus* gen. nov., sp. nov., a new, extremely halotolerant, hydrocarbon-degrading marine bacterium. *International Journal of Systematic and Evolutionary Microbiology*, 42(4), 568-576. doi: <https://doi.org/10.1099/00207713-42-4-568>
- Geng, X., & Boufadel, M. C. (2014). Modeling biodegradation of subsurface oil in sand beaches polluted with oil. In proceedings of the *International Oil Spill Conference*. American Petroleum Institute. doi: <https://doi.org/10.7901/2169-3358-2014.1.1113>

- Geng, X., & Boufadel, M. C. (2015). Impacts of evaporation on subsurface flow and salt accumulation in a tidally influenced beach. *Water Resources Research*, 51(7), 5547-5565. doi: <https://doi.org/10.1002/2015WR016886>
- Geng, X., & Boufadel, M. C. (2017). The influence of evaporation and rainfall on supratidal groundwater dynamics and salinity structure in a sandy beach. *Water Resources Research*, 53(7), 6218-6238. doi: <https://doi.org/10.1002/2016WR020344>
- Geng, X., Boufadel, M. C., & Jackson, N. L. (2016a). Evidence of salt accumulation in beach intertidal zone due to evaporation. *Scientific Reports*, 6(1), 1-5. doi: <https://doi.org/10.1038/srep31486>
- Geng, X., Khalil, C. A., Prince, R. C., Lee, K., An, C., & Boufadel, M. C. (2021). Hypersaline pore water in gulf of mexico beaches prevented efficient biodegradation of *Deepwater Horizon* beached oil. *Environmental Science & Technology*, 55(20), 13792-13801. doi: <https://doi.org/10.1021/acs.est.1c02760>
- Geng, X., Pan, Z., Boufadel, M. C., Ozigokmen, T., Lee, K., & Zhao, L. (2016b). Simulation of oil bioremediation in a tidally influenced beach: Spatiotemporal evolution of nutrient and dissolved oxygen. *Journal of Geophysical Research: Oceans*, 121(4), 2385-2404. doi: <https://doi.org/10.1002/2015JC011221>
- Ghai, R., Hernandez, C. M., Picazo, A., Mizuno, C. M., Ininbergs, K., Díez, B., Valas, R., DuPont, C. L., McMahon, K. D., & Camacho, A. (2012). Metagenomes of Mediterranean coastal lagoons. *Scientific Reports*, 2(1), 1-13. doi: <https://doi.org/10.1038/srep00490>
- Gleitz, M., vd Loeff, M. R., Thomas, D. N., Dieckmann, G. S., & Millero, F. J. (1995). Comparison of summer and winter inorganic carbon, oxygen and nutrient concentrations in Antarctic sea ice brine. *Marine Chemistry*, 51(2), 81-91. doi: [https://doi.org/10.1016/0304-4203\(95\)00053-T](https://doi.org/10.1016/0304-4203(95)00053-T)
- Golyshin, P. N., Dos Santos, V. A. M., Kaiser, O., Ferrer, M., Sabirova, Y. S., Lünsdorf, H., Chernikova, T. N., Golyshina, O. V., Yakimov, M. M., & Pühler, A. (2003). Genome sequence completed of *Alcanivorax borkumensis*, a hydrocarbon-degrading bacterium that plays a global role in oil removal from marine systems. *Journal of Biotechnology*, 106(2-3), 215-220. doi: <https://doi.org/10.1016/j.jbiotec.2003.07.013>
- Gordon, G., Hansen, B., Scott, J., Hirst, C., Graham, R., Grow, T., Spedding, A., Fairhead, S., Fullarton, L., & Griffin, D. (2010). The hydrocarbon prospectivity of the Egyptian North Red Sea basin. *Paper presented at the Geological Society, London, Petroleum Geology Conference series*. doi: <https://doi.org/10.1144/0070783>

- Grant, W. D., Pagaling, E., Márquez, M. C., Gutiérrez, M. C., Cowan, D. A., Ma, Y., Jones, B. E., Ventosa, A., & Heaphy, S. (2011). The hypersaline LAKES of Inner Mongolia: the MGAtch project. In A. Ventosa, A. Oren, & Y. Ma (Eds.), *Halophiles and Hypersaline Environments* (pp. 65-107): Springer-Verlag Berlin Heidelberg, Germany. doi: https://doi.org/10.1007/978-3-642-20198-1_4
- Gupta, R. S., & Patel, S. (2020). Robust demarcation of the family *Caryophanaceae* (*Planococcaceae*) and its different genera including three novel genera based on phylogenomics and highly specific molecular signatures. *Frontiers in Microbiology*, 10, 2821. doi: <https://doi.org/10.3389/fmicb.2019.02821>
- Gudiña, E. J., Pereira, J. F., Rodrigues, L. R., Coutinho, J. A., & Teixeira, J. A. (2012). Isolation and study of microorganisms from oil samples for application in microbial enhanced oil recovery. *International Biodeterioration & Biodegradation*, 68, 56-64. doi: <https://doi.org/10.1016/j.ibiod.2012.01.001>
- Gvirtzman, H., & Stanislavsky, E. (2000). Palaeohydrology of hydrocarbon maturation, migration and accumulation in the Dead Sea Rift. *Basin Research*, 12(1), 79-93. doi: <https://doi.org/10.1046/j.1365-2117.2000.00111.x>
- Halvorson, G. A., & Lang, K. J. (1989). Revegetation of a salt water blowout site. *Rangeland Ecology & Management/Journal of Range Management Archives*, 42(1), 61-65. doi: <https://doi.org/10.2307/3899660>
- Harris, R. (1981). Effect of water potential on microbial growth and activity. *Water Potential Relations in Soil Microbiology*, 9, 23-95. doi: <https://doi.org/10.2136/sssaspepub9.c2>
- Harshey, R. M. (2003). Bacterial motility on a surface: many ways to a common goal. *Annual Reviews in Microbiology*, 57(1), 249-273. doi: <https://doi.org/annurev.micro.57.030502.091014>
- Hase, T., Wakabayashi, S., Matsubara, H., Mevarech, M., & Werber, M. (1980). Amino acid sequence of 2Fe-2S ferredoxin from an extreme halophile, *Halobacterium* of the Dead Sea. *Biochimica et Biophysica Acta (BBA)-Protein Structure*, 623(1), 139-145. doi: [https://doi.org/10.1016/0005-2795\(80\)90016-1](https://doi.org/10.1016/0005-2795(80)90016-1)
- Hassan, H. A., & Aly, A. A. (2018). Isolation and characterization of three novel catechol 2, 3-dioxygenase from three novel haloalkaliphilic BTEX-degrading *Pseudomonas* strains. *International Journal of Biological Macromolecules*, 106, 1107-1114. doi: <https://doi.org/10.1016/j.ijbiomac.2017.08.113>
- Hassan, H. A., Rizk, N. M., Hefnawy, M., & Awad, A. M. (2012). Isolation and characterization of halophilic aromatic and chloroaromatic degrader from Wadi El-Natron Soda lakes. *Life Science Journal*, 9(3), 1565-1570.

- Hazen, T. C. (2018). Cometabolic Bioremediation In R. Steffan (Ed.), *Consequences of Microbial Interactions with Hydrocarbons, Oils, and Lipids: Biodegradation and Bioremediation, Handbook of Hydrocarbon and Lipid Microbiology* (pp. 233-248): Springer International Publishing.
- Hazen, T. C., Prince, R. C., & Mahmoudi, N. (2016). Marine oil biodegradation. *Environmental Science & Technology*, 50(5), 2121-2129. doi: <https://doi.org/10.1021/acs.est.5b03333>
- Heyer, J., Berger, U., Hardt, M., & Dunfield, P. F. (2005). *Methylohalobius crimeensis* gen. nov., sp. nov., a moderately halophilic, methanotrophic bacterium isolated from hypersaline lakes of Crimea. *International Journal of Systematic and Evolutionary Microbiology*, 55(5), 1817-1826. doi: <https://doi.org/10.1099/ijs.0.63213-0>
- Hosseini, M., Fakhari, J., Al-Rubaye, M. T. S., & Dezfouli, E. A. (2017). Screening of halophilic bacteria able to degrade crude oil contamination from Alborz Oil Field, Qom, Iran. *Journal of Pure and Applied Microbiology*, 11(2), 773-778. doi: <http://dx.doi.org/10.22207/JPAM.11.2.16>
- Huntemann, M., Ivanova, N. N., Mavromatis, K., Tripp, H. J., Paez-Espino, D., Palaniappan, K., Szeto, E., Pillay, M., Chen, I-A., Pati, A., Nielsen, T., Markowitz, M. V., & Kyrpides, N. C. (2015). The standard operating procedure of the DOE-JGI Microbial Genome Annotation Pipeline (MGAP v. 4). *Standards in Genomic Sciences*, 10(1), 1-6. doi: <https://doi.org/10.1186/s40793-015-0077-y>
- Hyatt, D., Chen, G. L., LoCascio, P. F., Land, M. L., Larimer, F. W., & Hauser, L. J. (2010). Prodigal: prokaryotic gene recognition and translation initiation site identification. *BMC Bioinformatics*, 11(1), 1-11. doi: <https://doi.org/10.1186/1471-2105-11-119>
- Ibrahim, A., Hawboldt, K., Bottaro, C., & Khan, F. (2018). Review and analysis of microbiologically influenced corrosion: the chemical environment in oil and gas facilities. *Corrosion Engineering, Science and Technology*, 53(8), 549-563. doi: <https://doi.org/10.1080/1478422X.2018.1511326>
- Igunnu, E. T., & Chen, G. Z. (2014). Produced water treatment technologies. *International Journal of Low-carbon Technologies*, 9(3), 157-177. doi: <https://doi.org/10.1093/ijlct/cts049>
- Ivanov, A. Y., Gerivani, H., & Evtushenko, N. V. (2020). Characterization of natural hydrocarbon seepage in the South Caspian Sea off Iran using satellite SAR and geological data. *Marine Georesources & Geotechnology*, 38(5), 527-538. doi: <https://doi.org/10.1080/1064119X.2019.1600175>
- Iwamatsu, M., & Horii, K. (1996). Capillary condensation and adhesion of two wetter surfaces. *Journal of Colloid and Interface Science*, 182(2), 400-406. doi: <https://doi.org/10.1006/jcis.1996.0480>

- Jaafari, A. (1963). History and development of the Alborz and Sarajeh fields of Central Iran. In proceedings of the *6th World Petroleum Congress, 19-26 June, Frankfurt am Main, Germany*. World Petroleum Congress.
- Jamal, M. T., & Pugazhendi, A. (2018). Degradation of petroleum hydrocarbons and treatment of refinery wastewater under saline condition by a halophilic bacterial consortium enriched from marine environment (Red Sea), Jeddah, Saudi Arabia. *3 Biotech*, 8(6), 276. doi: <https://doi.org/10.1007/s13205-018-1296-x>
- Jézéquel, R., & Poncet, F. (2011). The Erika Oil Spill, 10 Years After: Assessment of the natural weathering of the oil and natural recovery of vegetatio. In proceedings of the *International Oil Spill Conference, abs165*. American Petroleum Institute.
- Jia, R., Unsal, T., Xu, D., Lekbach, Y., & Gu, T. (2019). Microbiologically influenced corrosion and current mitigation strategies: a state of the art review. *International Biodeterioration & Biodegradation*, 137, 42-58. doi: <https://doi.org/10.1016/j.ibiod.2018.11.007>
- Johannesson, K. H., Lyons, W. B., & Bird, D. A. (1994). Rare earth element concentrations and speciation in alkaline lakes from the western USA. *Geophysical Research Letters*, 21(9), 773-776. doi: <https://doi.org/10.1029/94GL00005>
- Johnson, R. J., Folwell, B. D., Wirekoh, A., Frenzel, M., & Skovhus, T. L. (2017). Reservoir Souring—Latest developments for application and mitigation. *Journal of Biotechnology*, 256, 57-67. doi:<https://doi.org/10.1016/j.jbiotec.2017.04.003>
- Jones, D., Head, I., Gray, N., Adams, J., Rowan, A., Aitken, C., Bennett, B., Huang, H., Brown, A., & Bowler, B. (2008). Crude-oil biodegradation via methanogenesis in subsurface etroleum reservoirs. *Nature*, 451(7175), 176-180. doi:<https://doi.org/10.1038/nature06484>
- Kaiser, D. (2000). Bacterial motility: how do pili pull? *Current Biology*, 10(21), R777-R780. doi: [https://doi.org/10.1016/S0960-9822\(00\)00764-8](https://doi.org/10.1016/S0960-9822(00)00764-8)
- Kappell, A. D., Wei, Y., Newton, R. J., Van Nostrand, J. D., Zhou, J., McLellan, S. L., & Hristova, K. R. (2014). The polycyclic aromatic hydrocarbon degradation potential of Gulf of Mexico native coastal microbial communities after the *Deepwater Horizon* oil spill. *Frontiers in Microbiology*, 5, 205. doi: <https://doi.org/10.3389/fmicb.2014.00205>
- Khemili-Talbi, S., Kebbouche-Gana, S., Akmuoussi-Toumi, S., Angar, Y., & Gana, M. L. (2015). Isolation of an extremely halophilic archaeon *Natrialba* sp. C21 able to degrade aromatic compounds and to produce stable biosurfactant at high salinity. *Extremophiles*, 19(6), 1109-1120. doi: <https://doi.org/10.1007/s00792-015-0783-9>

- Kilic, O., & Kilic, A. (2010). Salt crust mineralogy and geochemical evolution of the Salt Lake (Tuz Gölü), Turkey. *Scientific Research and Essays*, 5(11), 1317-1324. doi: <https://doi.org/10.5897/SRE.9000817>
- Kim, S.-J., & Kwon, K. (2010). Marine, hydrocarbon-degrading *Alphaproteobacteria*. In *Handbook of Hydrocarbon and Lipid Microbiology*. doi: https://dx.doi.org/10.1007%2F978-3-540-77587-4_120
- Knol, M., & Arbo, P. (2014). Oil spill response in the Arctic: Norwegian experiences and future perspectives. *Marine Policy*, 50, 171-177. doi: <https://doi.org/10.1016/j.marpol.2014.06.003>
- König, S., Vogel, H.-J., Harms, H., & Worrlich, A. (2020). Physical, chemical and biological effects on soil bacterial dynamics in microscale models. *Frontiers in Ecology and Evolution*, 8, 53. doi: <https://doi.org/10.3389/fevo.2020.00053>
- Kosarev, A. N., Kostianoy, A. G., Zonn, I. S., & Zhiltsov, S. S. (2013). The caspian sea and Kara-bogaz-gol bay. In I. S. Zonn & A. G. Kostianoy (Eds.), *The Turkmen Lake Altyn Asyr and Water Resources in Turkmenistan (Vol. 28, pp. 69-94)*: Springer-Verlag Berlin Heidelberg, Germany. doi: https://doi.org/10.1007/698_2013_228
- Krembs, C., Gradinger, R., & Spindler, M. (2000). Implications of brine channel geometry and surface area for the interaction of sympagic organisms in Arctic sea ice. *Journal of Experimental Marine Biology and Ecology*, 243(1), 55-80. doi: [https://doi.org/10.1016/S0022-0981\(99\)00111-2](https://doi.org/10.1016/S0022-0981(99)00111-2)
- Kristanti, R. A., Hadibarata, T., Al Farraj, D. A., Elshikh, M. S., & Alkufeidy, R. M. (2018). Biodegradation mechanism of phenanthrene by halophilic *Hortaea sp.* B15. *Water, Air, & Soil Pollution*, 229(10), 324. doi: <https://doi.org/10.1007/s11270-018-3969-9>
- Kulichevskaya, I., Milekhina, E., Borzenkov, I., Zvyagintseva, I., & Belyaev, S. (1991). Oxidation of petroleum-hydrocarbons by extremely halophilic archaeobacteria. *Microbiology*, 60(5), 596-601.
- Kumar, M., León, V., Materano, A. D. S., & Ilzins, O. A. (2007). A halotolerant and thermotolerant *Bacillus sp.* degrades hydrocarbons and produces tensio-active emulsifying agent. *World Journal of Microbiology and Biotechnology*, 23(2), 211-220. doi: <https://doi.org/10.1007/s11274-006-9215-4>
- Kuznetsov, V., Zajtseva, T., Vakulenko, L., & Filippova, S. (1992). *Streptomyces albiacialis sp. nov.*—a new oil hydrocarbons degrading species of thermo- and halotolerant streptomyces. *Mikrobiologiâ (Moskva, 1932)*, 61(1), 84-91.

- Ladino-Orjuela, G., Gomes, E., Silva, R. d., Salt, C., & Parsons, J. R. (2016). Metabolic pathways for degradation of aromatic hydrocarbons by bacteria. *Reviews of Environmental Contamination and Toxicology* 237, 105-121. doi: https://doi.org/10.1007/978-3-319-23573-8_5
- Lamarche-Gagnon, G., Comery, R., Greer, C. W., & Whyte, L. G. (2015). Evidence of in situ microbial activity and sulphidogenesis in perennially sub-0 C and hypersaline sediments of a high Arctic permafrost spring. *Extremophiles*, 19(1), 1-15. doi: <http://doi.org/10.1007/s00792-014-0703-4>
- Larter, S., Huang, H., Adams, J., Bennett, B., Jokanola, O., Oldenburg, T., Jones, M., Head, I., Riediger, C., & Fowler, M. (2006). The controls on the composition of biodegraded oils in the deep subsurface: Part II—Geological controls on subsurface biodegradation fluxes and constraints on reservoir-fluid property prediction: Part I of this study was published in Organic Chemistry in 2003 (Larter et al., 2003). *AAPG Bulletin*, 90(6), 921-938. doi: <https://doi.org/10.1306/01270605130>
- Larter, S., Wilhelms, A., Head, I., Koopmans, M., Aplin, A., Di Primio, R., Zwach, C., Erdmann, M., & Telnaes, N. (2003). The controls on the composition of biodegraded oils in the deep subsurface—part 1: biodegradation rates in petroleum reservoirs. *Organic Geochemistry*, 34(4), 601-613. doi: [https://doi.org/10.1016/S0146-6380\(02\)00240-1](https://doi.org/10.1016/S0146-6380(02)00240-1)
- Lasserre, F. (2014). Case studies of shipping along Arctic routes. Analysis and profitability perspectives for the container sector. *Transportation Research Part A: Policy and Practice*, 66, 144-161. doi: <https://doi.org/10.1016/j.tra.2014.05.005>
- Ławniczak, Ł., Woźniak-Karczewska, M., Loibner, A. P., Heipieper, H. J., & Chrzanowski, Ł. (2020). Microbial degradation of hydrocarbons—basic principles for bioremediation: a review. *Molecules*, 25(4), 856. doi: <https://doi.org/10.3390/molecules25040856>
- Le Borgne, S., Paniagua, D., & Vazquez-Duhalt, R. (2008). Biodegradation of organic pollutants by halophilic bacteria and archaea. *Microbial Physiology*, 15(2-3), 74-92. doi: <https://doi.org/10.1159/000121323>
- Lenchi, N., Kebbouche-Gana, S., Servais, P., Gana, M. L., & Llirós, M. (2020). Diesel biodegradation capacities and biosurfactant production in saline-alkaline conditions by *Delftia* sp. n11, isolated from an algerian oilfield. *Geomicrobiology Journal*, 37(5), 454-466. doi: <https://doi.org/10.1080/01490451.2020.1722769>
- León, V. M., Moreno-González, R., González, E., Martínez, F., García, V., & Campillo, J. A. (2013). Interspecific comparison of polycyclic aromatic hydrocarbons and persistent organochlorines bioaccumulation in bivalves from a Mediterranean coastal lagoon. *Science of the Total Environment*, 463, 975-987. doi: <https://doi.org/10.1016/j.scitotenv.2013.06.075>

- Leskiw, L. A., Sedor, R. B., Welsh, C. M., & Zeleke, T. B. (2012). Soil and vegetation recovery after a well blowout and salt water release in northeastern British Columbia. *Canadian Journal of Soil Science*, 92(1), 179-190. doi:<https://doi.org/10.4141/cjss2011-018>
- Levy, J. S., Fountain, A. G., Welch, K. A., & Lyons, W. B. (2012). Hypersaline “wet patches” in Taylor Valley, Antarctica. *Geophysical Research Letters*, 39(5), 1-5. doi: <https://doi.org/10.1029/2012GL050898>
- Lewis, A., & Prince, R. C. (2018). Integrating dispersants in oil spill response in Arctic and other icy environments. *Environmental Science & Technology*, 52(11), 6098-6112. doi: <https://doi.org/10.1021/acs.est.7b06463>
- Li, D., Luo, R., Liu, C. M., Leung, C. M., Ting, H. F., Sadakane, K., Yamashita, H., & Lam, T. W. (2016). MEGAHIT v1. 0: a fast and scalable metagenome assembler driven by advanced methodologies and community practices. *Methods*, 102, 3-11. doi: <https://doi.org/10.1016/j.ymeth.2016.02.020>
- Li, H., & Durbin, R. (2009). Fast and accurate short read alignment with Burrows–Wheeler transform. *Bioinformatics*, 25(14), 1754-1760. doi: <https://doi.org/10.1093/bioinformatics/btp324>
- Li, H., Handsaker, B., Wysoker, A., Fennell, T., Ruan, J., Homer, N., Marth, G., Abecasis, G., & Durbin, R. (2009). The sequence alignment/map format and SAMtools. *Bioinformatics*, 25(16), 2078-2079. doi: <https://doi.org/10.1093/bioinformatics/btp352>
- Liang, J., Gao, S., Wu, Z., Rijnaarts, H. H., & Grotenhuis, T. (2021). DNA-SIP identification of phenanthrene-degrading bacteria undergoing bioaugmentation and natural attenuation in petroleum-contaminated soil. *Chemosphere*, 266, 128984. doi: <https://doi.org/10.1016/j.chemosphere.2020.128984>
- Lin, J.-L., Joye, S. B., Scholten, J. C., Schäfer, H., McDonald, I. R., & Murrell, J. C. (2005). Analysis of methane monooxygenase genes in Mono Lake suggests that increased methane oxidation activity may correlate with a change in methanotroph community structure. *Applied and Environmental Microbiology*, 71(10), 6458-6462. doi: <http://doi.org/10.1128/AEM.71.10.6458-6462.2005>
- Liu, C., Chen, C.-X., Zhang, X.-Y., Yu, Y., Liu, A., Li, G.-W., Chen, X.-L., Chen, B., Zhou, B.-C., & Zhang, Y.-Z. (2012). *Marinobacter antarcticus* sp. nov., a halotolerant bacterium isolated from Antarctic intertidal sandy sediment. *International Journal of Systematic and Evolutionary Microbiology*, 62(Pt_8), 1838-1844. doi: <https://doi.org/10.1099/ijs.0.035774-0>

- Liu, Y., Chen, J., Liu, Z., Shou, L., Lin, D., Zhou, L., Yang, S.-Z., Liu, J.-F., Li, W., & Gu, J.-D. (2020). Anaerobic degradation of paraffins by thermophilic Actinobacteria under methanogenic conditions. *Environmental Science & Technology*. doi: <https://doi.org/10.1021/acs.est.0c02071>
- Lizama, C., Monteoliva-Sánchez, M., Suárez-García, A., Roselló-Mora, R., Aguilera, M., Campos, V., & Ramos-Cormenzana, A. (2002). *Halorubrum tebenquichense* sp. nov., a novel halophilic archaeon isolated from the Atacama Saltern, Chile. *International Journal of Systematic and Evolutionary Microbiology*, 52(1), 149-155. doi:<https://doi.org/10.1099/00207713-52-1-149>
- Lloyd, K. G., Lapham, L., & Teske, A. (2006). An anaerobic methane-oxidizing community of ANME-1b archaea in hypersaline Gulf of Mexico sediments. *Applied and Environmental Microbiology*, 72(11), 7218-7230. doi: <http://doi.org/10.1128/AEM.00886-06>
- Long, T., & Or, D. (2005). Aquatic habitats and diffusion constraints affecting microbial coexistence in unsaturated porous media. *Water Resources Research*, 41(8). doi: <https://doi.org/10.1029/2004WR003796>
- Lux, K.-H. (2009). Design of salt caverns for the storage of natural gas, crude oil and compressed air: Geomechanical aspects of construction, operation and abandonment. *Geological Society, London, Special Publications*, 313(1), 93-128. doi: <https://doi.org/10.1144/SP313.7>
- MacDonald, I., Smith, M., & Huffer, F. (2010). Community structure comparisons of lower slope hydrocarbon seeps, northern Gulf of Mexico. *Deep Sea Research Part II: Topical Studies in Oceanography*, 57(21-23), 1904-1915. doi: <https://doi.org/10.1016/j.dsr2.2010.09.002>
- Maignien, L., Parkes, R. J., Cragg, B., Niemann, H., Knittel, K., Coulon, S., Akhmetzhanov, A., & Boon, N. (2013). Anaerobic oxidation of methane in hypersaline cold seep sediments. *FEMS Microbiology Ecology*, 83(1), 214-231. doi: <https://doi.org/10.1111/j.1574-6941.2012.01466.x>
- Manikandan, M., Kannan, V., & Pašić, L. (2009). Diversity of microorganisms in solar salterns of Tamil Nadu, India. *World Journal of Microbiology and Biotechnology*, 25(6), 1007-1017. doi: <https://doi.org/10.1007/s11274-009-9980-y>
- Marine Science, (2008). Seawater composition. Retrieved from <https://www.marinebio.net/marinescience/02ocean/swcomposition.htm> (Accessed on 17 September, 2020).
- Marshall, K., & Cruickshank, R. (1973). Cell surface hydrophobicity and the orientation of certain bacteria at interfaces. *Archiv für Mikrobiologie*, 91(1), 29-40. doi: <https://doi.org/10.1007/BF00409536>

- Martín, S., Márquez, M., Sánchez-Porro, C., Mellado, E., Arahál, D., & Ventosa, A. (2003). *Marinobacter lipolyticus* sp. nov., a novel moderate halophile with lipolytic activity. *International Journal of Systematic and Evolutionary Microbiology*, 53(5), 1383-1387. doi: <https://doi.org/10.1099/ijs.0.02528-0>
- Martinelli, M., Luise, A., Tromellini, E., Sauer, T. C., Neff, J. M., & Douglas, G. S. (1995). The M/C Haven oil spill: Environmental assessment of exposure pathways and resource injury. In proceedings of the *International Oil Spill Conference*, pp. 679-685. American Petroleum Institute. doi: <https://doi.org/10.7901/2169-3358-1995-1-679>
- Martínez, A., Torello, S., & Kolter, R. (1999). Sliding motility in mycobacteria. *Journal of Bacteriology*, 181(23), 7331-7338. doi: <https://doi.org/10.1128/JB.181.23.7331-7338.1999>
- Matsuyama, T., & Nakagawa, Y. (1996). Bacterial wetting agents working in colonization of bacteria on surface environments. *Colloids and Surfaces B: Biointerfaces*, 7(5-6), 207-214. doi: [https://doi.org/10.1016/0927-7765\(96\)01300-8](https://doi.org/10.1016/0927-7765(96)01300-8)
- McBride, M. J. (2001). Bacterial gliding motility: multiple mechanisms for cell movement over surfaces. *Annual Reviews in Microbiology*, 55(1), 49-75.
- McFarlin, K. M., Prince, R. C., Perkins, R., & Leigh, M. B. (2014). Biodegradation of dispersed oil in arctic seawater at -1°C. *PloS One*, 9(1), e84297. doi: <https://doi.org/10.1371/journal.pone.0084297>
- Meier, W. N., Hovelsrud, G. K., Van Oort, B. E., Key, J. R., Kovacs, K. M., Michel, C., Haas, C., Granskog, M. A., Gerland, S., & Perovich, D. K. (2014). Arctic sea ice in transformation: A review of recent observed changes and impacts on biology and human activity. *Reviews of Geophysics*, 52(3), 185-217. doi: <https://doi.org/10.1002/2013RG000431>
- Michaelsen, M., Hulsch, R., Höpner, T., & Berthe-Corti, L. (1992). Hexadecane mineralization in oxygen-controlled sediment-seawater cultivations with autochthonous microorganisms. *Applied and Environmental Microbiology*, 58(9), 3072-3077. doi: <https://doi.org/10.1128/aem.58.9.3072-3077.1992>
- Michel, J., Owens, E. H., Zengel, S., Graham, A., Nixon, Z., Allard, T., Holton, W., Reimer, P. D., Lamarche, A., & White, M. (2013). Extent and degree of shoreline oiling: *Deepwater Horizon* oil spill, Gulf of Mexico, USA. *PloS One*, 8(6), e65087. doi: <https://doi.org/10.1371/journal.pone.0065087>
- Miller, J. I., Techtmann, S., Fortney, J., Mahmoudi, N., Joyner, D., Liu, J., Olesen, S., Alm, E., Fernandez, A., & Gardinali, P. (2019). Oil hydrocarbon degradation by Caspian Sea microbial communities. *Frontiers in Microbiology*, 10, 995. doi: <https://doi.org/10.3389/fmicb.2019.00995>

- Mnif, S., Chamkha, M., & Sayadi, S. (2009). Isolation and characterization of *Halomonas* sp. strain C2SS100, a hydrocarbon-degrading bacterium under hypersaline conditions. *Journal of Applied Microbiology*, 107(3), 785-794. doi: <https://doi.org/10.1111/j.1365-2672.2009.04251.x>
- Mohn, W. W., & Stewart, G. R. (2000). Limiting factors for hydrocarbon biodegradation at low temperature in Arctic soils. *Soil Biology and Biochemistry*, 32(8-9), 1161-1172. doi: [https://doi.org/10.1016/S0038-0717\(00\)00032-8](https://doi.org/10.1016/S0038-0717(00)00032-8)
- Morrow, N. R., Tang, G.-q., Valat, M., & Xie, X. (1998). Prospects of improved oil recovery related to wettability and brine composition. *Journal of Petroleum Science and Engineering*, 20(3-4), 267-276. doi: [https://doi.org/10.1016/S0920-4105\(98\)00030-8](https://doi.org/10.1016/S0920-4105(98)00030-8)
- Mounier, J., Camus, A., Mitteau, I., Vaysse, P.-J., Goulas, P., Grimaud, R., & Sivadon, P. (2014). The marine bacterium *Marinobacter hydrocarbonoclasticus* SP17 degrades a wide range of lipids and hydrocarbons through the formation of oleolytic biofilms with distinct gene expression profiles. *FEMS Microbiology Ecology*, 90(3), 816-831. doi: <https://doi.org/10.1111/1574-6941.12439>
- Murray, A. E., Kenig, F., Fritsen, C. H., McKay, C. P., Cawley, K. M., Edwards, R., Kuhn, E., McKnight, D. M., Ostrom, N. E., & Peng, V. (2012). Microbial life at -13 C in the brine of an ice-sealed Antarctic lake. In proceedings of the *National Academy of Sciences*, 109(50), 20626-20631. doi: <https://doi.org/10.1073/pnas.1208607109>
- National Research Council, N. (1993). *In-situ* bioremediation: When does it work? : *National Academies Press*.
- Neifar, M., Chouchane, H., Najjari, A., El Hidri, D., Mahjoubi, M., Ghedira, K., Naili, F., Soufi, L., Raddadi, N., & Sghaier, H. (2019). Genome analysis provides insights into crude oil degradation and biosurfactant production by extremely halotolerant *Halomonas desertis* G11 isolated from Chott El-Djerid salt-lake in Tunisian desert. *Genomics*, 111(6), 1802-1814. doi: <https://doi.org/10.1016/j.ygeno.2018.12.003>
- Nicholson, W. L., Munakata, N., Horneck, G., Melosh, H. J., & Setlow, P. (2000). Resistance of *Bacillus* endospores to extreme terrestrial and extraterrestrial environments. *Microbiology and Molecular Biology Reviews*, 64(3), 548-572. doi: <https://doi.org/10.1128/MMBR.64.3.548-572.2000>
- Nie, Y., Su, X., Wu, D., Zhang, R., Wang, R., Zhao, Z., Xamxidun, M., Sun, C., & Wu, M. (2021). *Marinobacter caseinilyticus* sp. nov., isolated from saline soil. *Current Microbiology*, 78(3), 1045-1052. doi: <https://doi.org/10.1007/s00284-021-02351-w>

- Niederberger, T. D., Perreault, N. N., Tille, S., Lollar, B. S., Lacrampe-Couloume, G., Andersen, D., Greer, C. W., Pollard, W., & Whyte, L. G. (2010). Microbial characterization of a subzero, hypersaline methane seep in the Canadian High Arctic. *The ISME Journal*, 4(10), 1326-1339. doi: <https://doi.org/10.1038/ismej.2010.57>
- Nissenbaum, A. (1975). The microbiology and biogeochemistry of the Dead Sea. *Microbial Ecology*, 2(2), 139-161. doi: <https://doi.org/10.1007/BF02010435>
- Null, S. E., & Wurtsbaugh, W. A. (2020). Water development, consumptive water uses, and Great Salt Lake. In B. K. Baxter & J. K. Butler (Eds.), *Great Salt Lake Biology (pp. 1-21)*: Springer, Cham, Switzerland. doi: https://doi.org/10.1007/978-3-030-40352-2_1
- Obuekwe, C. O., Badrudeen, A. M., Al-Saleh, E., & Mulder, J. L. (2005). Growth and hydrocarbon degradation by three desert fungi under conditions of simultaneous temperature and salt stress. *International Biodeterioration & Biodegradation*, 56(4), 197-205. doi: <https://doi.org/10.1016/j.ibiod.2005.05.005>
- Office of Fossil Fuels (2020). About The SPR. Retrieved from <https://www.energy.gov/fe/services/petroleum-reserves/strategic-petroleum-reserve> (Accessed on 19 December, 2020).
- Oggier, M., Eicken, H., Wilkinson, J., Petrich, C., & O'Sadnick, M. (2020). Crude oil migration in sea-ice: laboratory studies of constraints on oil mobilization and seasonal evolution. *Cold Regions Science and Technology*, 174, 102924. doi: [https://doi.org/10.1016/S0146-6380\(00\)00015-2](https://doi.org/10.1016/S0146-6380(00)00015-2)
- Oh, S., Wang, Q., Shin, W. S., & Song, D.-I. (2013). Effect of salting out on the desorption-resistance of polycyclic aromatic hydrocarbons (PAHs) in coastal sediment. *Chemical Engineering Journal*, 225, 84-92. doi: <https://doi.org/10.1016/j.cej.2013.03.069>
- Oldenburg, T. B., Rullkötter, J., Böttcher, M. E., & Nissenbaum, A. (2000). Molecular and isotopic characterization of organic matter in recent and sub-recent sediments from the Dead Sea. *Organic Geochemistry*, 31(4), 251-265. doi: [https://doi.org/10.1016/S0146-6380\(00\)00015-2](https://doi.org/10.1016/S0146-6380(00)00015-2)
- Ollivier, B., Borgomano, J., & Oger, P. (2014). Petroleum: from formation to microbiology. *Microbial Life of the Deep Biosphere*, 8, 161-185.
- Olson, G. M., Gao, H., Meyer, B. M., Miles, M. S., & Overton, E. B. (2017). Effect of Corexit 9500A on Mississippi Canyon crude oil weathering patterns using artificial and natural seawater. *Heliyon*, 3(3), e00269. doi: <https://doi.org/10.1016/j.heliyon.2017.e00269>

- Oppenheimer-Shaanan, Y., Steinberg, N., & Kolodkin-Gal, I. (2013). Small molecules are natural triggers for the disassembly of biofilms. *Trends in Microbiology*, 21(11), 594-601. doi: <https://doi.org/10.1016/j.tim.2013.08.005>
- Or, D., Smets, B., Wraith, J., Dechesne, A., & Friedman, S. (2007). Physical constraints affecting bacterial habitats and activity in unsaturated porous media—a review. *Advances in Water Resources*, 30(6-7), 1505-1527. doi: <https://doi.org/10.1016/j.advwatres.2006.05.025>
- Or, D., & Tuller, M. (1999). Liquid retention and interfacial area in variably saturated porous media: Upscaling from single-pore to sample-scale model. *Water Resources Research*, 35(12), 3591-3605. doi: <https://doi.org/10.1029/1999WR900262>
- Orbitbiotech (2018). Cell-Surface-Appendages-of-Bacteria. Retrieved from <https://orbitbiotech.com/flagella-fimbrae-pili-monotrichous-amphitrichous-filament-hook/cell-surface-appendages-of-bacteria/> (Accessed on 20 January, 2020).
- Oren, A. (1983). *Halobacterium sodomense* sp. nov., a Dead Sea halobacterium with an extremely high magnesium requirement. *International Journal of Systematic and Evolutionary Microbiology*, 33(2), 381-386. doi:<https://doi.org/10.1007/BF01579551>
- Oren, A. (2019). Aerobic hydrocarbon-degrading Archaea. *Taxonomy, Genomics and Ecophysiology of Hydrocarbon Degrading Microbes*, 41-51. doi: https://doi.org/10.1007/978-3-030-14796-9_5
- Oren, A., Ginzburg, M., Ginzburg, B., Hochstein, L., & Volcani, B. (1990). *Haloarcula marismortui* (Volcani) sp. nov., nom. rev., an extremely halophilic bacterium from the Dead Sea. *International Journal of Systematic and Evolutionary Microbiology*, 40(2), 209-210. doi: <https://doi.org/10.1099/00207713-40-2-209>
- Pagé, A. P., Yergeau, É., & Greer, C. W. (2015). *Salix purpurea* stimulates the expression of specific bacterial xenobiotic degradation genes in a soil contaminated with hydrocarbons. *PloS One*, 10(7), e0132062. doi: <https://doi.org/10.1371/journal.pone.0132062>
- Pannekens, M., Kroll, L., Müller, H., Mbow, F. T., & Meckenstock, R. U. (2019). Oil reservoirs, an exceptional habitat for microorganisms. *New Biotechnology*, 49, 1-9. doi: <https://doi.org/10.1016/j.nbt.2018.11.006>
- Pašić, L., Ulrih, N. a. P., Črnigoj, M., Grabnar, M., & Velikonja, B. H. (2007). Haloarchaeal communities in the crystallizers of two adriatic solar salterns. *Canadian Journal of Microbiology*, 53(1), 8-18. doi:<https://doi.org/10.1139/w06-091>

- Passow, U., & Stout, S. A. (2020). Character and sedimentation of “lingering” Macondo oil to the deep-sea after the *Deepwater Horizon* oil spill. *Marine Chemistry*, 218, 103733. doi: <https://doi.org/10.1016/j.marchem.2019.103733>
- Pecoraino, G., D’Alessandro, W., & Inguaggiato, S. (2015). The other side of the coin: geochemistry of alkaline lakes in volcanic areas. In D. Rouwet, B. Christenson, F. Tassi, & J. Vandemeulebrouck (Eds.), *Volcanic Lakes* (pp. 219-237): Springer-Verlag Berlin Heidelberg, Germany. doi: https://doi.org/10.1007/978-3-642-36833-2_9
- Ping, H., Li, Z., Zhi-Song, C., Xiu-Chun, G., & Li, T. (2009). Isolation, identification and diversity analysis of petroleum-degrading bacteria in Shengli Oil Field wetland soil. *Yingyong Shengtai Xuebao*, 20(5).
- Pirnik, M., Atlas, R., & Bartha, R. (1974). Hydrocarbon metabolism by *Brevibacterium erythrogenes*: normal and branched alkanes. *Journal of Bacteriology*, 119(3), 868-878. doi: <https://doi.org/10.1128/jb.119.3.868-878.1974>
- Piubeli, F., Grossman, M. J., Fantinatti-Garboggini, F., & Durrant, L. R. (2012). Enhanced reduction of COD and aromatics in petroleum-produced water using indigenous microorganisms and nutrient addition. *International Biodeterioration & Biodegradation*, 68, 78-84. doi: <https://doi.org/10.1016/j.ibiod.2011.11.012>
- Plotnikova, E., Yastrebova, O., Anan’ina, L., Dorofeeva, L., Lysanskaya, V. Y., & Demakov, V. (2011). Halotolerant bacteria of the genus *Arthrobacter* degrading polycyclic aromatic hydrocarbons. *Russian Journal of Ecology*, 42(6), 502. doi: <https://doi.org/10.1134/S1067413611060130>
- Pontes, J., Mucha, A. P., Santos, H., Reis, I., Bordalo, A., Basto, M. C., Bernabeu, A., & Almeida, C. M. R. (2013). Potential of bioremediation for buried oil removal in beaches after an oil spill. *Marine Pollution Bulletin*, 76(1-2), 258-265. doi: <https://doi.org/10.1016/j.marpolbul.2013.08.029>
- Powelson, D. K., & Mills, A. L. (1996). Bacterial enrichment at the gas-water interface of a laboratory apparatus. *Applied and Environmental Microbiology*, 62(7), 2593-2597. doi: <https://doi.org/10.1128/aem.62.7.2593-2597.1996>
- Prince, R., Kelley, B., & Butler, J. (2016a). Three widely-available dispersants substantially increase the biodegradation of otherwise undispersed oil. *Journal of Marine Science: Research & Development*, 6(2). doi: <http://dx.doi.org/10.4172/2155-9910.1000183>
- Prince, R. C. (1993). Petroleum spill bioremediation in marine environments. *Critical Reviews in Microbiology*, 19(4), 217-240. doi: <https://doi.org/10.3109/10408419309113530>
- Prince, R. C. (2015). Oil spill dispersants: boon or bane? *Environmental Science & Technology*, 49(11), 6376-6384. doi: <https://doi.org/10.1021/acs.est.5b00961>

- Prince, R. C., Bare, R. E., Garrett, R. M., Grossman, M. J., Haith, C. E., Keim, L. G., Lee, K., Holtom, G. J., Lambert, P., & Sergy, G. A. (2003). Bioremediation of stranded oil on an Arctic shoreline. *Spill Science & Technology Bulletin*, 8(3), 303-312. doi: [https://doi.org/10.1016/S1353-2561\(03\)00036-7](https://doi.org/10.1016/S1353-2561(03)00036-7)
- Prince, R. C., & Bragg, J. R. (1997). Shoreline bioremediation following the Exxon Valdez oil spill in Alaska. *Bioremediation Journal*, 1(2), 97-104. doi: <https://doi.org/10.1080/10889869709351324>
- Prince, R. C., & Butler, J. D. (2014). A protocol for assessing the effectiveness of oil spill dispersants in stimulating the biodegradation of oil. *Environmental Science and Pollution Research*, 21(16), 9506-9510. doi:<https://doi.org/10.1007/s11356-013-2053-7>
- Prince, R. C., Butler, J. D., & Redman, A. D. (2017). The rate of crude oil biodegradation in the sea. *Environmental Science & Technology*, 51(3), 1278-1284. doi: <https://doi.org/10.1021/acs.est.6b03207>
- Prince, R. C., Clark, J. R., & Lindstrom, J. E. (2015). Field studies demonstrating the efficacy of bioremediation in marine environments. In *Hydrocarbon and Lipid Microbiology Protocols (pp. 81-93)*: Springer, Cham, Switzerland. doi: https://doi.org/10.1007/8623_2015_172
- Prince, R. C., Elmendorf, D. L., Lute, J. R., Hsu, C. S., Haith, C. E., Senius, J. D., Dechert, G. J., Douglas, G. S., & Butler, E. L. (1994). 17. alpha.(H)-21. beta.(H)-hopane as a conserved internal marker for estimating the biodegradation of crude oil. *Environmental Science & Technology*, 28(1), 142-145. doi: <https://doi.org/10.1021/es00050a019>
- Prince, R. C., McFarlin, K. M., Butler, J. D., Febbo, E. J., Wang, F. C., & Nedwed, T. J. (2013). The primary biodegradation of dispersed crude oil in the sea. *Chemosphere*, 90(2), 521-526. doi: <https://doi.org/10.1016/j.chemosphere.2012.08.020>
- Prince, R. C., Nash, G. W., & Hill, S. J. (2016b). The biodegradation of crude oil in the deep ocean. *Marine Pollution Bulletin*, 111(1-2), 354-357. doi: <https://doi.org/10.1016/j.marpolbul.2016.06.087>
- Prince, R. C., Parkerton, T. F., & Lee, C. (2007). The primary aerobic biodegradation of gasoline hydrocarbons. *Environmental Science & Technology*, 41(9), 3316-3321. doi: <https://doi.org/10.1021/es062884d>
- Prince, R. C., & Prince, V. L. (2022). Hydrocarbon Biodegradation in Utah's Great Salt Lake. *Water*, 14(17), 2661. doi: <https://doi.org/10.3390/w14172661>

- Prince, R. C., & Walters, C. C. (2016). Biodegradation of oil hydrocarbons and its implications for source identification. In *Standard Handbook Oil Spill Environmental Forensics* (pp. 869-916): Elsevier. doi: <https://doi.org/10.1016/B978-0-12-803832-1.00019-2>
- Qiao, N., & Shao, Z. (2010). Isolation and characterization of a novel biosurfactant produced by hydrocarbon-degrading bacterium *Alcanivorax dieselolei* B-5. *Journal of Applied Microbiology*, 108(4), 1207-1216. doi: <https://doi.org/10.1111/j.1365-2672.2009.04513.x>
- Qu, L., Zhu, F., Zhang, J., Gao, C., & Sun, X. (2011). *Marinobacter daqiaonensis* sp. nov., a moderate halophile isolated from a Yellow Sea salt pond. *International Journal of Systematic and Evolutionary Microbiology*, 61(12), 3003-3008. doi: <https://doi.org/10.1099/ijs.0.028993-0>
- Quijada, M. F., & Stewart, R. R. (2008). Petrophysical and seismic signature of a heavy oil sand reservoir: Manitou Lake, Saskatchewan. *Canadian Society of Exploration Geophysics, Consortium for Research in Elastic Wave Exploration Seismology*, 20, 1-17.
- Quinlan, A. R., & Hall, I. M. (2010). BEDTools: a flexible suite of utilities for comparing genomic features. *Bioinformatics*, 26(6), 841-842. doi: <https://doi.org/10.1093/bioinformatics/btq033>
- Rabus, R., Boll, M., Heider, J., Meckenstock, R. U., Buckel, W., Einsle, O., Ermler, U., Golding, B. T., Gunsalus, R. P., & Kroneck, P. M. (2016). Anaerobic microbial degradation of hydrocarbons: from enzymatic reactions to the environment. *Microbial Physiology*, 26(1-3), 5-28. doi: <https://doi.org/10.1159/000443997>
- Raczkowski, J., Turkiewicz, A., & Kapusta, P. (2004). Elimination of biogenic hydrogen sulfide in underground gas storage. A case study. In proceedings of the *SPE Annual Technical Conference and Exhibition*. doi: <https://doi.org/10.2118/89906-MS>
- Radović, J. R., Romero, I. C., Oldenburg, T. B., Larter, S. R., & Tunnell, J. W. (2020). 40 Years of weathering of coastal oil residues in the southern Gulf of Mexico. In *Deep Oil Spills* (pp. 328-340): Springer, Cham, Switzerland. doi: https://doi.org/10.1007/978-3-030-11605-7_20
- Ribicic, D., McFarlin, K. M., Netzer, R., Brakstad, O. G., Winkler, A., Throne-Holst, M., & Størseth, T. R. (2018). Oil type and temperature dependent biodegradation dynamics-Combining chemical and microbial community data through multivariate analysis. *BMC Microbiology*, 18(1), 1-15. doi: <https://doi.org/10.1186/s12866-018-1221-9>

- Rietz, D., & Haynes, R. (2003). Effects of irrigation-induced salinity and sodicity on soil microbial activity. *Soil Biology and Biochemistry*, 35(6), 845-854. doi: [https://doi.org/10.1016/S0038-0717\(03\)00125-1](https://doi.org/10.1016/S0038-0717(03)00125-1)
- Riis, V., Kleinstaub, S., & Babel, W. (2003). Influence of high salinities on the degradation of diesel fuel by bacterial consortia. *Canadian Journal of Microbiology*, 49(11), 713-721. doi: <https://doi.org/10.1139/w03-083>
- Rijnaarts, H. H., Norde, W., Lyklema, J., & Zehnder, A. J. (1995). The isoelectric point of bacteria as an indicator for the presence of cell surface polymers that inhibit adhesion. *Colloids and Surfaces B: Biointerfaces*, 4(4), 191-197. doi: [https://doi.org/10.1016/0927-7765\(94\)01164-Z](https://doi.org/10.1016/0927-7765(94)01164-Z)
- Rizzo, C., Conte, A., Azzaro, M., Papale, M., Rappazzo, A. C., Battistel, D., Roman, M., Lo Giudice, A., & Guglielmin, M. (2020). Cultivable Bacterial Communities in Brines from Perennially Ice-Covered and Pristine Antarctic Lakes: Ecological and Biotechnological Implications. *Microorganisms*, 8(6), 819. doi: <https://doi.org/10.3390/microorganisms8060819>
- Robinson, M. D., McCarthy, D. J., & Smyth, G. K. (2010). edgeR: a Bioconductor package for differential expression analysis of digital gene expression data. *Bioinformatics*, 26(1), 139-140. doi: <https://doi.org/10.1093/bioinformatics/btp616>
- Rodriguez-Valera, F., Juez, G., & Kushner, D. (1983). *Halobacterium mediterranei spec. nov.*, a new carbohydrate-utilizing extreme halophile. *Systematic and Applied Microbiology*, 4(3), 369-381. doi: [https://doi.org/10.1016/S0723-2020\(83\)80021-6](https://doi.org/10.1016/S0723-2020(83)80021-6)
- Roffey, R. (1989). Microbial problems during long-term storage of petroleum products underground in rock caverns. *International Biodeterioration*, 25(1-3), 219-236. doi: [https://doi.org/10.1016/0265-3036\(89\)90048-1](https://doi.org/10.1016/0265-3036(89)90048-1)
- Röling, W. F., De Brito, I. R. C., Swannell, R. P., & Head, I. M. (2004). Response of archaeal communities in beach sediments to spilled oil and bioremediation. *Applied and Environmental Microbiology*, 70(5), 2614-2620. doi: <https://doi.org/10.1128/AEM.70.5.2614-2620.2004>
- Röling, W. F., Head, I. M., & Larter, S. R. (2003). The microbiology of hydrocarbon degradation in subsurface petroleum reservoirs: perspectives and prospects. *Research in Microbiology*, 154(5), 321-328. doi: [https://doi.org/10.1016/S0923-2508\(03\)00086-X](https://doi.org/10.1016/S0923-2508(03)00086-X)
- Rullkötter, J., Spiro, B., & Nissenbaum, A. (1985). Biological marker characteristics of oils and asphalts from carbonate source rocks in a rapidly subsiding graben, Dead Sea, Israel. *Geochimica et Cosmochimica Acta*, 49(6), 1357-1370. doi: [https://doi.org/10.1016/0016-7037\(85\)90286-8](https://doi.org/10.1016/0016-7037(85)90286-8)

- SadrAzodi, S. M., Shavandi, M., Amoozegar, M. A., & Mehrnia, M. R. (2019). Biodegradation of long chain alkanes in halophilic conditions by *Alcanivorax sp.* strain Est-02 isolated from saline soil. *3 Biotech*, *9*(4), 1-10. doi: <https://doi.org/10.1007/s13205-019-1670-3>
- Samarkin, V. A., Madigan, M. T., Bowles, M. W., Casciotti, K. L., Priscu, J. C., McKay, C. P., & Joye, S. B. (2010). Abiotic nitrous oxide emission from the hypersaline Don Juan Pond in Antarctica. *Nature Geoscience*, *3*(5), 341-344. doi: <https://doi.org/10.1038/ngeo847>
- Sassen, R., Joye, S., Sweet, S. T., DeFreitas, D. A., Milkov, A. V., & MacDonald, I. R. (1999). Thermogenic gas hydrates and hydrocarbon gases in complex chemosynthetic communities, Gulf of Mexico continental slope. *Organic Geochemistry*, *30*(7), 485-497. doi: [https://doi.org/10.1016/S0146-6380\(99\)00050-9](https://doi.org/10.1016/S0146-6380(99)00050-9)
- Schafer, A. N., Snape, I., & Siciliano, S. D. (2009). Influence of liquid water and soil temperature on petroleum hydrocarbon toxicity in Antarctic soil. *Environmental Toxicology and Chemistry: An International Journal*, *28*(7), 1409-1415. doi: <https://doi.org/10.1897/08-434.1>
- Schmidt, M., Al-Farawati, R., & Botz, R. (2015). Geochemical classification of brine-filled Red Sea deeps. In *The Red Sea (pp. 219-233)*: Springer, Cham, Switzerland. doi: https://doi.org/10.1007/978-3-662-45201-1_13
- Schneider, W. R., & Doetsch, R. (1974). Effect of viscosity on bacterial motility. *Journal of Bacteriology*, *117*(2), 696-701. doi: <https://doi.org/10.1128/jb.117.2.696-701.1974>
- Sei, A., & Fathepure, B. (2009). Biodegradation of BTEX at high salinity by an enrichment culture from hypersaline sediments of Rozel Point at Great Salt Lake. *Journal of Applied Microbiology*, *107*(6), 2001-2008. doi: <https://doi.org/10.1111/j.1365-2672.2009.04385.x>
- Sharma, V. K., Rhudy, K., Brooks, R., Hollyfield, S., & Vazquez, F. G. (1997). Petroleum hydrocarbons in sediments of Upper Laguna Madre. *Marine Pollution Bulletin*, *34*(4), 229-234. doi: [https://doi.org/10.1016/S0025-326X\(96\)00109-9](https://doi.org/10.1016/S0025-326X(96)00109-9)
- Sims, W., & Frailing, W. (1950). Lakeview Pool, Midway-Sunset Field. *Journal of Petroleum Technology*, *2*(01), 7-18. doi: <https://doi.org/10.2118/950007-G>
- Sinninghe Damsté, J. S., De Leeuw, J. W., Kock-van Dalen, A., De Zeeuw, M. A., De Lange, F., Irene, W., Rijpstra, C., & Schenck, P. (1987). The occurrence and identification of series of organic sulphur compounds in oils and sediment extracts. I. A study of Rozel Point Oil (USA). *Geochimica et Cosmochimica Acta*, *51*(9), 2369-2391. doi: [https://doi.org/10.1016/0016-7037\(89\)90066-5](https://doi.org/10.1016/0016-7037(89)90066-5)

- Smith, V. H., Graham, D. W., & Cleland, D. D. (1998). Application of resource-ratio theory to hydrocarbon biodegradation. *Environmental Science & Technology*, 32(21), 3386-3395. doi: <https://doi.org/10.1021/es9805019>
- Sokol, E., Kozmenko, O., Smirnov, S., Sokol, I., Novikova, S., Tomilenko, A., Kokh, S., Ryazanova, T., Reutsky, V., & Bul'bak, T. (2014). Geochemical assessment of hydrocarbon migration phenomena: Case studies from the south-western margin of the Dead Sea Basin. *Journal of Asian Earth Sciences*, 93, 211-228. doi: <https://doi.org/10.1016/j.jseae.2014.07.023>
- Sokolov, A., & Trotsenko, Y. (1995). Methane consumption in (hyper) saline habitats of Crimea (Ukraine). *FEMS Microbiology Ecology*, 18(4), 299-303. doi: <https://doi.org/10.1111/j.1574-6941.1995.tb00186.x>
- Sørensen, S. J., Bailey, M., Hansen, L. H., Kroer, N., & Wuertz, S. (2005). Studying plasmid horizontal transfer in situ: a critical review. *Nature Reviews Microbiology*, 3(9), 700-710. doi: <https://doi.org/10.1038/nrmicro1232>
- Sorokin, D. Y., Janssen, A. J., & Muyzer, G. (2012). Biodegradation potential of halo (alkali) philic prokaryotes. *Critical Reviews in Environmental Science and Technology*, 42(8), 811-856. doi: <https://doi.org/10.1080/10643389.2010.534037>
- Stock, J. B., & Baker, M. (2009). Chemotaxis. In *Encyclopedia of Microbiology* (pp. 71-78): Elsevier Inc. doi: <https://doi.org/10.1016/B978-012373944-5.00068-7>
- Stout, S. A., & Payne, J. R. (2016). Macondo oil in deep-sea sediments: Part 1—sub-sea weathering of oil deposited on the seafloor. *Marine Pollution Bulletin*, 111(1-2), 365-380. doi:<https://doi.org/10.1016/j.marpolbul.2016.07.036>
- Sublette, K. L., Tapp, J. B., Fisher, J. B., Jennings, E., Duncan, K., Thoma, G., Brokaw, J., & Todd, T. (2007). Lessons learned in remediation and restoration in the Oklahoma prairie: A review. *Applied Geochemistry*, 22(10), 2225-2239. doi: <https://doi.org/10.1016/j.apgeochem.2007.04.011>
- Sun, S., Su, Y., Chen, S., Cui, W., Zhao, C., & Liu, Q. (2022). Bioremediation of oil-contaminated soil: Exploring the potential of endogenous hydrocarbon degrader *Enterobacter sp.* SAVR S-1. *Applied Soil Ecology*, 173, 104387. doi: <https://doi.org/10.1016/j.apsoil.2022.104387>
- Takagishi, H., Masuda, T., Shimoda, T., Maezono, R., & Hongo, K. (2019). Method for the calculation of the hamaker constants of organic materials by the lifshitz macroscopic approach with density functional theory. *The Journal of Physical Chemistry A*, 123(40), 8726-8733. doi: <https://doi.org/10.1021/acs.jpca.9b06433>
- Tapilatu, Y. H., Grossi, V., Acquaviva, M., Militon, C., Bertrand, J.-C., & Cuny, P. (2010). Isolation of hydrocarbon-degrading extremely halophilic archaea from an uncontaminated hypersaline pond (Camargue, France). *Extremophiles*, 14(2), 225-231. doi: <http://doi.org/10.1007/s00792-010-0301-z>

- Taylor, E., & Reimer, D. (2008). Oil persistence on beaches in Prince William Sound—A review of SCAT surveys conducted from 1989 to 2002. *Marine Pollution Bulletin*, 56(3), 458-474. doi: <https://doi.org/10.1016/j.marpolbul.2007.11.008>
- Tazi, L., Breakwell, D. P., Harker, A. R., & Crandall, K. A. (2014). Life in extreme environments: microbial diversity in Great Salt Lake, Utah. *Extremophiles*, 18(3), 525-535. doi: <http://doi.org/10.1007/s00792-014-0637-x>
- Tecon, R., Ebrahimi, A., Kleyer, H., Levi, S. E., & Or, D. (2018). Cell-to-cell bacterial interactions promoted by drier conditions on soil surfaces. In proceedings of the *National Academy of Sciences*, 115(39), 9791-9796. doi: <https://doi.org/10.1073/pnas.1808274115>
- Timmis, K. N., McGenity, T., Van Der Meer, J. R., & de Lorenzo, V. (2010). *Handbook of Hydrocarbon and Lipid Microbiology*: Springer-Verlag Berlin Heidelberg, Germany.
- Tissot, B. P., & Welte, D. H. (1984). *Petroleum Formation and Occurrence (Second Revised and Enlarged ed.)*: Springer-Verlag Berlin Heidelberg, Germany.
- Tolosa, I., de Mora, S., Sheikholeslami, M. R., Villeneuve, J.-P., Bartocci, J., & Cattini, C. (2004). Aliphatic and aromatic hydrocarbons in coastal Caspian Sea sediments. *Marine Pollution Bulletin*, 48(1-2), 44-60. doi: [https://doi.org/10.1016/S0025-326X\(03\)00255-8](https://doi.org/10.1016/S0025-326X(03)00255-8)
- Torsvik, V., Øvreås, L., & Thingstad, T. F. (2002). Prokaryotic diversity--magnitude, dynamics, and controlling factors. *Science*, 296(5570), 1064-1066. doi: <https://doi.org/10.1126/science.1071698>
- Tremblay, J., & Yergeau, E. (2019). Systematic processing of ribosomal RNA gene amplicon sequencing data. *GigaScience*, 8(12), giz146. doi: <https://doi.org/10.1093/gigascience/giz146>
- Tronczyński, J., Munsch, C., Héas-Moisan, K., Guiot, N., Truquet, I., Olivier, N., Men, S., & Furaut, A. (2004). Contamination of the Bay of Biscay by polycyclic aromatic hydrocarbons (PAHs) following the T/V “Erika” oil spill. *Aquatic Living Resources*, 17(3), 243-259. doi: <https://doi.org/10.1051/alr:2004042>
- Tsao, Y. H., Evans, D. F., & Wennerstroem, H. (1993). Long-range attraction between a hydrophobic surface and a polar surface is stronger than that between two hydrophobic surfaces. *Langmuir*, 9(3), 779-785.
- Tuller, M., Or, D., & Dudley, L. M. (1999). Adsorption and capillary condensation in porous media: Liquid retention and interfacial configurations in angular pores. *Water Resources Research*, 35(7), 1949-1964. doi: <https://doi.org/10.1029/1999WR900098>

- USEIA (2019). Global Liquid Fuels. Retrieved from https://www.eia.gov/outlooks/steo/report/global_oil.php (Accessed on 19 July, 2020).
- Van Trappen, S., Vandecandelaere, I., Mergaert, J., & Swings, J. (2004). *Gillisia limnaea* gen. nov., sp. nov., a new member of the family Flavobacteriaceae isolated from a microbial mat in Lake Fryxell, Antarctica. *International Journal of Systematic and Evolutionary Microbiology*, 54(2), 445-448. doi: <https://doi.org/10.1099/ijs.0.02922-0>
- Vauclare, P., Natali, F., Kleman, J.-P., Zaccai, G., & Franzetti, B. (2020). Surviving salt fluctuations: stress and recovery in *Halobacterium salinarum*, an extreme halophilic Archaeon. *Scientific Reports*, 10(1), 1-10. doi: <https://doi.org/10.1038/s41598-020-59681-1>
- Venosa, A. D., Suidan, M. T., Wrenn, B. A., Strohmeier, K. L., Haines, J. R., Eberhart, B. L., King, D., & Holder, E. (1996). Bioremediation of an experimental oil spill on the shoreline of Delaware Bay. *Environmental Science & Technology*, 30(5), 1764-1775. doi: <https://doi.org/10.1021/es950754r>
- Verwey, E. J. W., Overbeek, J. T. G., & Van Nes, K. (1948). Theory of the stability of lyophobic colloids: the interaction of sol particles having an electric double layer: Elsevier Publishing Company.
- Vieth, A., & Wilkes, H. (2006). Deciphering biodegradation effects on light hydrocarbons in crude oils using their stable carbon isotopic composition: A case study from the Gullfaks oil field, offshore Norway. *Geochimica et Cosmochimica Acta*, 70(3), 651-665. doi: <https://doi.org/10.1016/j.gca.2005.08.022>
- Vreeland, R. H. (2015). *Halomonas*. *Bergey's Manual of Systematics of Archaea and Bacteria*, 1-19. doi: <https://doi.org/10.1002/9781118960608.gbm01190>
- von Meijenfeldt, F. A., Arkhipova, K., Cambuy, D. D., Coutinho, F. H., & Dutilh, B. E. (2019). Robust taxonomic classification of uncharted microbial sequences and bins with CAT and BAT. *Genome Biology*, 20(1), 1-14. doi: <https://doi.org/10.1186/s13059-019-1817-x>
- Wan, J., & Tokunaga, T. K. (1997). Film straining of colloids in unsaturated porous media: Conceptual model and experimental testing. *Environmental Science & Technology*, 31(8), 2413-2420. doi: <https://doi.org/10.1021/es970017q>
- Wan, J., Wilson, J. L., & Kieft, T. L. (1994). Influence of the gas-water interface on transport of microorganisms through unsaturated porous media. *Applied and Environmental Microbiology*, 60(2), 509-516. doi: <https://doi.org/10.1128/aem.60.2.509-516.1994>

- Wang, C., Huang, Y., Zhang, Z., & Wang, H. (2018). Salinity effect on the metabolic pathway and microbial function in phenanthrene degradation by a halophilic consortium. *AMB Express*, 8(1), 1-13. doi: <https://doi.org/10.1186/s13568-018-0594-3>
- Wang, J., Sandoval, K., Ding, Y., Stoeckel, D., Minard-Smith, A., Andersen, G., Dubinsky, E. A., Atlas, R., & Gardinali, P. (2016). Biodegradation of dispersed Macondo crude oil by indigenous Gulf of Mexico microbial communities. *Science of The Total Environment*, 557, 453-468. doi: <https://doi.org/10.1016/j.scitotenv.2016.03.015>
- Wang, L., Gao, C.-X., Mbadanga, S. M., Zhou, L., Liu, J.-F., Gu, J.-D., & Mu, B.-Z. (2011). Characterization of an alkane-degrading methanogenic enrichment culture from production water of an oil reservoir after 274 days of incubation. *International Biodeterioration and Biodegradation*, 65(3), 444-450. doi: <https://doi.org/10.1016/j.ibiod.2010.12.010>
- Wang, Q., Garrity, G. M., Tiedje, J. M., & Cole, J. R. (2007). Naive Bayesian classifier for rapid assignment of rRNA sequences into the new bacterial taxonomy. *Applied and Environmental Microbiology*, 73(16), 5261-5267. doi: <https://doi.org/10.1128/AEM.00062-07>
- Wang, W., & Shao, Z. (2014). The long-chain alkane metabolism network of *Alcanivorax dieselolei*. *Nature Communications*, 5(1), 1-11. doi: <https://doi.org/10.1038/ncomms6755>
- Wang, Y., Wang, J., Leng, F., & Chen, J. (2020). Effects of oil pollution on indigenous bacterial diversity and community structure of soil in fushun, Liaoning province, China. *Geomicrobiology Journal*, 1-12. doi: <https://doi.org/10.1080/01490451.2020.1817196>
- Wang, Z., Yang, C., Parrott, J., Frank, R., Yang, Z., Brown, C., Hollebhone, B., Landriault, M., Fieldhouse, B., Liu, Y., Zhang, G., & Hewitt, L. (2014). Forensic source differentiation of petrogenic, pyrogenic, and biogenic hydrocarbons in Canadian oil sands environmental samples. *Journal of Hazardous Materials*, 271, 166-177. doi: <https://doi.org/10.1016/j.jhazmat.2014.02.021>
- Wankel, S. D., Joye, S. B., Samarkin, V. A., Shah, S. R., Friederich, G., Melas-Kyriazi, J., & Girguis, P. R. (2010). New constraints on methane fluxes and rates of anaerobic methane oxidation in a Gulf of Mexico brine pool via in situ mass spectrometry. *Deep Sea Research Part II: Topical Studies in Oceanography*, 57(21-23), 2022-2029. doi: <https://doi.org/10.1016/j.dsr2.2010.05.009>
- Ward, D. M., & Brock, T. (1978). Hydrocarbon biodegradation in hypersaline environments. *Applied Environmental Microbiology*, 35(2), 353-359. doi: <https://doi.org/10.1128/aem.35.2.353-359.1978>

- Whyte, L. G., Bourbonnière, L., Bellerose, C., & Greer, C. W. (1999). Bioremediation assessment of hydrocarbon-contaminated soils from the high Arctic. *Bioremediation Journal*, 3(1), 69-80. doi: <https://doi.org/10.1080/10889869991219217>
- Wiesenburg, D. A., Brooks, J. M., & Bernard, B. B. (1985). Biogenic hydrocarbon gases and sulfate reduction in the Orca Basin brine. *Geochimica et Cosmochimica acta*, 49(10), 2069-2080. doi: [https://doi.org/10.1016/0016-7037\(85\)90064-X](https://doi.org/10.1016/0016-7037(85)90064-X)
- Wilhelms, A., Larter, S., Head, I., Farrimond, P., di-Primio, R., & Zwach, C. (2001). Biodegradation of oil in uplifted basins prevented by deep-burial sterilization. *Nature*, 414(6859), 85-85. doi: <https://doi.org/10.1038/35082535>
- Xue, J., Zhang, Y., Liu, Y., & El-Din, M. G. (2016). Treatment of oil sands process-affected water (OSPW) using a membrane bioreactor with a submerged flat-sheet ceramic microfiltration membrane. *Water Research*, 88, 1-11. doi: <https://doi.org/10.1016/j.watres.2015.09.051>
- Yin, F., John, G. F., Hayworth, J. S., & Clement, T. P. (2015). Long-term monitoring data to describe the fate of polycyclic aromatic hydrocarbons in *Deepwater Horizon* oil submerged off Alabama's beaches. *Science of The Total Environment*, 508, 46-56. doi: <https://doi.org/10.1016/j.scitotenv.2014.10.105>
- Yoo, Y., Lee, H., Kwon, B.-O., Khim, J. S., Baek, S., Pathiraja, D., Park, B., Choi, I.-G., Kim, G.-H., & Kim, B. S. (2020). *Marinobacter halodurans* sp. nov., a halophilic bacterium isolated from sediment of a salt flat. *International Journal of Systematic and Evolutionary Microbiology*, 70(12), 6294-6300. doi: <https://doi.org/10.1099/ijsem.0.004530>
- Yoon, B. (2016). The Great Salt Lake enigma: science shows anomalies – evidence of a global flood? Retrieved from <https://www.ancient-origins.net/ancient-places-america/great-salt-lake-enigma-science-shows-anomalies-evidence-global-flood-007082> (Accessed on 20 July, 2020).
- Yoshida, N., Yagi, K., Sato, D., Watanabe, N., Kuroishi, T., Nishimoto, K., Yanagida, A., Katsuragi, T., Kanagawa, T., & Kurane, R. (2005). Bacterial communities in petroleum oil in stockpiles. *Journal of Bioscience and Bioengineering*, 99(2), 143-149. doi: <https://doi.org/10.1263/jbb.99.143>
- Young, I. M., & Crawford, J. W. (2004). Interactions and self-organization in the soil-microbe complex. *Science*, 304(5677), 1634-1637. doi: <https://doi.org/10.1126/science.1097394>
- Young, I. M., Crawford, J. W., Nunan, N., Otten, W., & Spiers, A. (2008). Microbial distribution in soils: physics and scaling. *Advances in Agronomy*, 100, 81-121. doi: [https://doi.org/10.1016/S0065-2113\(08\)00604-4](https://doi.org/10.1016/S0065-2113(08)00604-4)

- Zaghden, H., Kallel, M., Elleuch, B., Oudot, J., & Saliot, A. (2007). Sources and distribution of aliphatic and polyaromatic hydrocarbons in sediments of Sfax, Tunisia, Mediterranean Sea. *Marine Chemistry*, 105(1-2), 70-89. doi: <https://doi.org/10.1016/j.marchem.2006.12.016>
- Zaghden, H., Kallel, M., Elleuch, B., Oudot, J., Saliot, A., & Sayadi, S. (2014). Evaluation of hydrocarbon pollution in marine sediments of Sfax coastal areas from the Gabes Gulf of Tunisia, Mediterranean Sea. *Environmental Earth Sciences*, 72(4), 1073-1082. doi: <https://doi.org/10.1007/s12665-013-3023-6>
- Zahed, M. A., Aziz, H. A., Isa, M. H., & Mohajeri, L. (2010). Effect of initial oil concentration and dispersant on crude oil biodegradation in contaminated seawater. *Bulletin of Environmental Contamination and Toxicology*, 84(4), 438-442. doi: <https://doi.org/10.1007/s00128-010-9954-7>
- Zhou, H., Wang, H., Huang, Y., & Fang, T. (2016). Characterization of pyrene degradation by halophilic *Thalassospira sp.* strain TSL5-1 isolated from the coastal soil of Yellow Sea, China. *International Biodeterioration and Biodegradation*, 107, 62-69. doi: <https://doi.org/10.1016/j.ibiod.2015.10.022>
- Zhuang, M., Abulikemu, G., Campo, P., Platten III, W. E., Suidan, M. T., Venosa, A. D., & Conmy, R. N. (2016). Effect of dispersants on the biodegradation of South Louisiana crude oil at 5 and 25°C. *Chemosphere*, 144, 767-774. doi: <https://doi.org/10.1016/j.chemosphere.2015.08.040>